2011

Development and characterization of ternary solid dispersion granules of poorly water soluble drugs : diflunisal and mefenamic acid

Niraja Patel
The University of Toledo

A Thesis

Entitled

Development and Characterization of Ternary Solid Dispersion Granules of Poorly Water Soluble Drugs: Diflunisal and Mefenamic acid

by

Niraja Patel

Submitted as partial fulfillment of the requirements for
The Master of Science degree in
Pharmaceutical Sciences with Industrial Pharmacy option

_____
Dr. Kenneth S. Alexander, Committee Chair

_____
Dr. Curt D. Black, Committee Member

_____
Dr. Frederick E. Williams, Committee Member

_____
Dr. Patricia R. Komuniecki, Dean
College of Graduate Studies

The University of Toledo

August 2011

An Abstract of

Development and Characterization of Ternary solid dispersion granules of poorly water soluble drugs: Diflunisal and Mefenamic acid

by

Niraja Patel

Submitted as partial fulfillment of the requirements for The Master of Science degree in Pharmaceutical Sciences with Industrial Pharmacy option

The University of Toledo

August 2011

The objective of this study was to increase the solubility of two poorly water soluble drugs, namely Diflunisal USP and Mefenamic Acid USP, by the formation of ternary solid dispersion granules with a dispersion carrier and an adsorbent. The study also includes characterization of the ternary solid dispersion granules for their physicochemical properties initially and after storage for 3 months. The dispersion carrier used for this study was Gelucire 50/13® and the adsorbent was Neusilin US2®. The fusion (hot melt) granulation method was used to prepare the ternary solid dispersion granules. Various characterization techniques were used to characterize the solid dispersion including Differential Scanning Calorimetry (DSC), X-Ray Powder Diffraction (XRPD), Fourier Transform Infrared Spectroscopy (FTIR), Scanning Electron Microscopy (SEM) and in vitro dissolution studies.

The DSC data represents the ternary mixture of the drug (diflunisal or mefenamic acid), dispersion carrier (Gelucire50/13®) and adsorbent (Neusilin US2®), which formed the solid dispersion. The XRPD results confirmed the highly crystalline nature of the pure drug (diflunisal or mefenamic acid) and the conversion of the drug to the amorphous state in the solid dispersions. The FTIR study reveals hydrogen bonding which leads to solid dispersion formation. No other chemical interaction was observed between the components of the ternary solid dispersion granule. The SEM study provided evidence of the highly crystalline nature for the pure drug and the amorphous nature for the ternary solid phase dispersion. In vitro dissolution data reveals a significant increase in drug solubility from the ternary solid dispersion granule as compared to the solubility for the pure drug. The ternary solid dispersion granule formed for diflunisal and mefenamic acid were highly amorphous and able to significantly increase the solubility of each drug.

Stability studies were performed for the solid dispersion of both the drugs (diflunisal and mefenamic acid) by subjecting them to different isothermal temperatures (25ºC, 30ºC, 35ºC and 40ºC) and relative humidity conditions (22.5% RH, 52.89% RH, 75.29% RH and 100% RH) for three months. The solid dispersion for both drugs (diflunisal and mefenamic acid) remained unaffected by the temperature and humidity conditions to which they were exposed throughout the three months period. Thus, in this study, the ternary solid dispersion granules for the two poorly water soluble drugs (diflunisal and mefenamic acid) were formulated which showed an increased dissolution as well as rate. The solid dispersion granules were extremely stable for three month under accelerated temperature and humidity conditions.

ACKNOWLEDGEMENTS

I would to like to thank Dr. Kenneth Alexander, my instructer and advisor for giving me the opportunity to work in his laboratory and to pursue the Master's degree in the College of Pharmacy at The University of Toledo. I would like to express my deepest gratitude for his guidance and encouragement which he provided me during the past two years. I am also thankful to Dr Alan Riga, my co-advisor for his advice, encouragement and support.

I am thankful to Dr. Curt Black and Dr. Frederick E. Williams, my thesis committee members, for their priceless advice. I would also like to express my gratitude to Dr. Pannee Burckel for her support and help in using the PXRD, FTIR and SEM instruments. I also owe thanks to my labmates Arpana, Shikha, Girish, Bivash, Ranajoy, Ermias, Carrie and all my juniors.

I do not have enough words to express my gratitude towards my parents and brother for their endless love, care and support. Their confidence and faith in me always provided motivation to work hard and achieve my goals. I owe a special thanks to Alok, my best friend and my fiancée, for his support, care, encouragement and love throughout my stay in Toledo. Above all, I would like to thank the Almighty for blessing me with such a wonderful life.

Table of Contents

List of Figures

List of Tables

Chapter One

Introduction

Poor aqueous solubility and bioavailability of drugs into the body after administration are two prime issues which are faced by the pharmaceutical industry at the present time. This problem has been the major problem hampering the release of new chemical entities into the market. Every year more than 50% of the potentially active pharmaceutical ingredients get rejected due to the above stated problems[1]. During the last decade, more than 40% of the new chemical entities launched in the U.S. pharmaceutical market faced the problem of adequate aqueous solubility[2]. Therefore, pharmaceutical companies are focusing on finding a method or technology by which they can enhance the aqueous solubility and bioavailability of the drug. To date, various methods for modification of active pharmaceutical ingredients have included physical, chemical and controlled solid state methods[3]. Each of the methods given above has their own drawbacks which restrain their use to modify the active pharmaceutical ingredient to improve its aqueous solubility and bioavailability[3]. Some other conventional methods used to improve aqueous solubility and bioavailability include: the use of surfactants[4]; pH modification [5, 6]; solid dispersion technique[7, 8]; cosolvent and hydrotrop formation[9]; co-crystallization techniques[5, 10]; and many more.

Solid dispersions are defined by Chio and Riegelmann[7] as "a dispersion of one or more active ingredients in an inert carrier or matrix at solid state prepared by melting (fusion), solvent or melting-solvent method." Chiou and Riegelmann[7] classified solid dispersions into six major categories which includes; simple eutectic mixtures; solid solutions; glass

solutions of suspensions; compound or complex formation between the drug and the carrier; amorphous precipitations of a drug in a crystalline carrier; and any combinations among the above groups.

The formulation of solid dispersions of a poorly water soluble drug has several advantages which include the enhancement of aqueous solubility which may lead to increased bioavailability[11, 12]. Along with this advantage, solid dispersion techniques also have a few disadvantages which hamper their extensive use in the improvement of the pharmaceutical formulation[7]. These disadvantages include poor flowability, poor compressibility, and most importantly is reversable for the drug form in solid dispersion from the amorphous to crystalline state [13, 14]. All the above listed disadvantages limit the use of solid dispersions in the pharmaceutical industry. This limitation can be overcome by adsorbing the melt, which is made up of the drug and dispersion carrier, to an inert core material which is compressible and has good flowability. Various adsorbents such as talc, fumed silicon dioxide, Neusilin® and many more can be used[13, 14]. Neusilin US2® seems to be promising for formulating dosage forms successfully as it is inert, amorphous material made up of magnesium aluminosilicate with good flowability, compressibility (21%), high specific area (~300 m^2/g) and a high adsorption capacity (~3.2 mL/g) [15, 16]. Due to the highly amorphous nature of Neusilin US2®, it can prevent to certain extent the reversion of a drug from its amorphous state to the crystalline state when subjected to stability studies[16].

The solid dispersion technique as well as the surface adsorption technique were used together in the present study to enhance the aqueous solubility and bioavailability of two poorly water soluble drugs, Mefenamic Acid USP and Diflunisal USP by forming ternary

phase solid dispersions of the drugs with a carrier (Gelucire 50/13) and an adsorbent (Neusilin US2®). The ternary phase solid dispersion is than subjected to characterization by various analytical techniques such as Differential Scanning Calorimetry (DSC), X-ray Powder diffraction (XRPD), Fourier Transform Infrared (FTIR), Scanning Electron Microscopy (SEM) and invitro dissolution studies. Stability studies were performed on this formulation by subjecting them to different temperatures and different relative humidity conditions over a period of three months.

Chapter Two

Pharmaceutical Solid Dispersions

2.1 Introduction

The absorption of drugs from a solid dosage form, when taken orally, can be divided into two steps - (1) the process of dissolution of the drug in vivo which leads to a solution; and (2) the transport of the dissolved drug from the solution across the gastrointestinal membrane. Each step involved in the process of absorption of the drug is very crucial. The overall absorption and bioavailability of the drug may be affected by the poor performance of either step mentioned above[1]. From among the many new active pharmaceutical ingredients introduced into the market, almost all the active pharmaceutical ingredients face the problem enumerated above. Either step one or two may lead to a decrease in overall bioavailability of the active pharmaceutical ingredient. Biopharmaceutical Classification (BCS) system[2] classifies these active pharmaceutical ingredients into four classes as given below:

Class I – High permeability, High Solubility. Compounds of this class are well absorbed and the absorption rate for these compounds is greater than the rate of excretion.

Class II – High Permeability, Low Solubility. Compounds of this class have poor bioavailability because their rate of solvation is very low.

Class III – Low Permeability, High Solubility. Compounds of this class have poor bioavailability because their permeation rate is very low.

Class IV – Low Permeability, Low Solubility. Compounds of this class have poor bioavailability because of both low solubility and absorption which limits its permeation rate.

Fincher extensively studied the relationship between the particle size of drugs, their dissolution rates and their bioavailability[3]. According to Fincher, the majority of the poorly water-soluble drugs show poor bioavailability due to the poor rate of dissolution, which is further dependent on the surface area of the drug particle available for dissolution [3]. Therefore, the dissolution rate can be enhanced by increasing the surface area. This can be achieved by the process of particle size reduction.

Particle size reduction of the active pharmaceutical agent can be achieved by: (1) trituration and grinding; (2) ball milling; (3) fluid energy micronization; (4) precipitation under controlled condition which is achieved by changing solvents or temperature, by using ultrasonic waves[4] or spray drying[5]; and (5) using gastric fluid to precipitate the drug in the form of fine particles[6]. The above mentioned methods are able to easily achieve the reduction in particle size. However, the dissolution rate and absorption may not be increased due to the formation of aggregates and/or agglomerates among the fine particles which can be caused by increased surface energy and stronger Van der waals' interactions. Moreover, the fine drug particles may also have a wettability problem in water, which may lead to a poor dissolution rate[7].

A unique technique known as solid dispersion was introduced by Sekiguchi and Obi[8] in 1961 to reduce the particle size of the drug and increase the dissolution rate and rate of absorption. The first solid dispersion was developed using sulfathiazole (a poorly water

soluble drug) and urea (water soluble and physiologically inert) as a carrier to increase the dissolution rate and rate of absorption by reduction in particle size. The technique used in the preparation of the solid dispersion of sulfathiazole with urea as a carrier included melting the physical mixture to a high temperature followed by rapid solidification. The drug in solid dispersion form was considered to be released as fine and dispersed particles when they come in contact with aqueous fluid. Levy[6] and Kanig[9], who worked with a number of drugs using mannitol as a carrier introduced the term solid-solid solution. Chiou and Niazi[10] performed the experiment with sulfathiazole and urea and reported that the fused mixture of sulfathiazole and urea showed an increase in dissolution rates by forming an "amorphous precipitate" or "solid solution". In solid solutions the drug is considered to be dispersed in a soluble carrier. Tachibana and Nakamura[12] first introduced a new method of preparing a solid dispersion known as the solvent evaporation method. In this method they first dispersed β-carotene in a water-soluble polymer (polyvinylpyrollidone). They then dissolved both chemicals in a common solvent and finally completely evaporated the solvent.

According to Chiou and Riegelman[11] a solid dispersion is defined as "the dispersion of one or more active ingredients in an inert carrier or matrix in solid state prepared by melting (fusion), using a solvent or a melting-solvent method." The modern definition has broadened the concept to include certain terms such as co-precipitates, nano-particles, microcapsules, microspheres and other dispersions of drugs in polymers (carrier) prepared by using the above mentioned methods. Although the main goal of most solid dispersions is to increase the dissolution rate, this new broadened concept of a solid dispersion also has the aim of achieving goals such as altered solid-state properties,

sustained release of drugs, enhanced release of drugs from ointment and suppository bases and improved stability[13].

The process of dissolution of a drug from solid dispersion includes three steps : (1) interaction of a co-precipitate with water in its vicinity; (2) the finely dispersed drug particle in the matrix structure is released; and (3) supersaturation of the solubilized drug in the diffusion layer[14].

2.2 Carriers Used in Solid Dispersions

Initially, in order to increase the dissolution rate of a drug, hydrophilic or water-soluble polymers are used in solid dispersions. Some of the common carriers that have been used to make solid dispersions are Polyethylene Glycols (PEGs), Polyvinylpyrrolidone (PVP), and urea. Recently, water insoluble or hydrophobic carriers such as Gelucire®, Eudragit®, etc are also used to make solid dispersions. Other carriers used to make solid dispersions include polyvinyl alcohol (PVA), polyvinylpyrrolidone-polyvinylacetate copolymer (PVP-PVA), crospovidone (PVP-CL), hydroxypropyl cellulose (HPC), hydroxypropyl-methylcellulose (HPMC), hydroxypropyl methylcellulose phthalate (HPMCP), polyacrylates, polymethacrylates, polyols, emulsifiers, sugars and organic acids and their derivatives [15].

2.3 Classification of Solid dispersions

In 1971, Chiou and Riegelmann[11] classified solid dispersions into six major categories as given below –

(1) Simple eutectic mixtures

(2) Solid solutions

(3) Glass solutions and glass suspensions

(4) Amorphous precipitations of a drug in a crystalline matrix

(5) Compound or complex formation between the drug and the carrier

(6) Any combinations of the above groups

2.3.1 Simple eutectic mixtures

A simple eutectic mixture is a mixture of two or more compounds in such proportions that the melting point of the mixture is lower than the melting point of the individual constituents[11]. The eutectic mixture is observed to be immiscible in the solid state and miscible in the liquid state[11]. All the constituents present in the eutectic mixture crystallize simultaneously. This process of simultaneous crystallization of a eutectic mixture is known as a eutectic reaction. In a eutectic mixture, when the components in a liquid mixture crystallize, they are assumed to crystallize in very small particulate sizes. This decrease in particle size leads to an increase in specific surface area which results in an enhanced rate of dissolution and improved bioavailability of the drug[8, 16].

Apart from the decrease in particle size of the drug, the rate of dissolution may also increase due to the following reasons –

1) In the beginning of the dissolution process, when the carrier dissolves in a short period of time, a solubilization effect is exerted by the carrier and may take place in the diffusion layer immediately surrounding the drug particle[18].

2) The absence of any aggregates or agglomerates between the fine crystallites of the drug[11, 17].
3) The majority of the solid crystallites being exceptionally small[18].
4) The effect of wettability and dispersibility of the drug in the eutectic mixture[11, 17].

Figure 2.1 represents a phase diagram for a eutectic mixture. Both solids A and B in Figure 2.1 exhibit two endotherms in the Differential Scaning Calorimetry (DSC) study, but a binary eutectic mixture usually exhibits a single major endotherm in the Differential Scaning Calorimetry (DSC) study. It can be seen in the diagram that when a mixture of A and B having a composition E is cooled, A and B crystallize out simultaneously. Subsequently when a mixture with composition E consisting of a slightly soluble drug and an inert, highly water soluble carrier, is dissolved in an aqueous medium, the carrier dissolves rapidly, which then releases very fine crystals of the drug[8, 16].

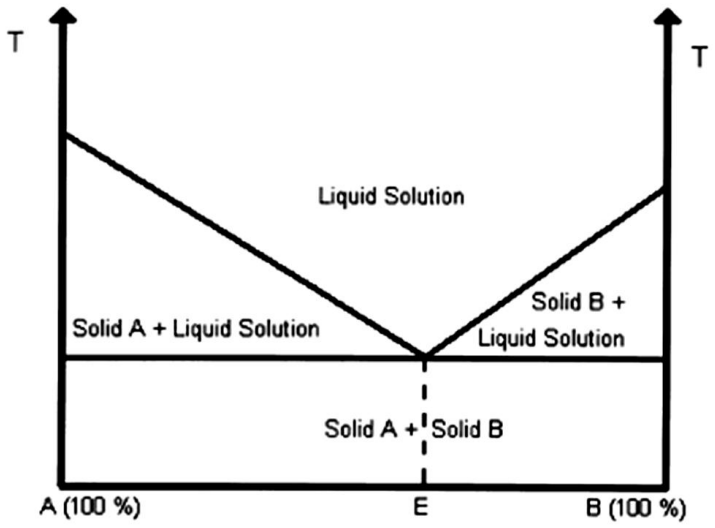

Figure 2.1: Phase diagram representing a eutectic mixture[15]

Chiou and Niazi[10] utilizing x-ray diffraction and DTA confirmed the fusion mixture for griseofulvin - succinic acid solid dispersion to be a eutectic. Studies on eutectic mixtures by other workers resulted in an increase in the dissolution rate and bioavailability of the following systems: acetaminophen – urea[16]; sulfathiazole – urea[8]; and phenacetin – phenobarbital[19].

2.3.2 Solid Solutions

A solid solution can be explained as a solid solute dissolved in a solid solvent. Levy, Kanig and Goldberg et al [16, 20] were the first to report that "a solid solution of a poorly water-soluble drug in a water-soluble carrier achieves a faster dissolution rate than a eutectic because the particle size of the drug is reduced down to its molecular level". Before a solid solution comes in contact with water, the drug molecule is dissolved in the solid state and therefore the characteristics of the carrier molecule plays an important role in determining the overall dissolution rate in water[9, 16 ,20].

Solid solutions can be classified based on the following:

1) Their miscibility with continuous or discontinuous solid solution phases.
2) The pattern in which the solvate is distributed in the solvent (substitutional, interstitial or amorphous).

2.3.2.1 Continuous Solid Solutions

In continuous solid solutions both components are completely miscible with each other in all proportions in the solid as well as liquid state. Theoretically, this means that the bonding strength between the two components is stronger than the bonding strength

between the molecules of individual components. This phenomenon has been expained theoretically, but no pharmaceutical solid solution of this type has been reported in the literature to date[15, 21]. Figure 2.2 represents the phase diagram for a continuous solid solution.

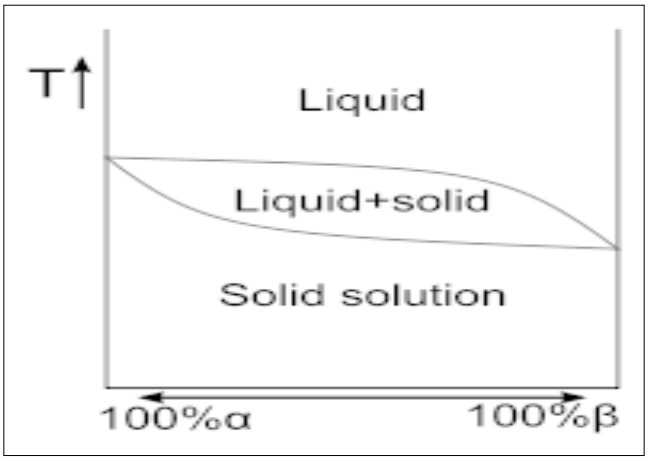

Figure 2.2: Phase diagram representing continuous solid solution[21]

2.3.2.2 Discontinuous Solid Solutions

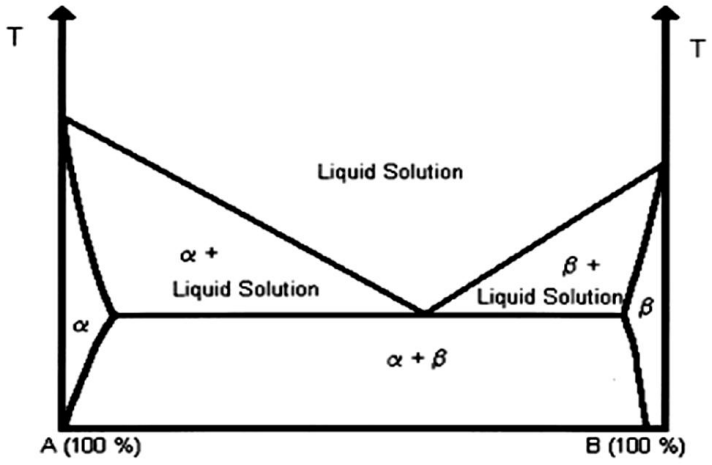

Figure 2.3: Phase diagram representing discontinuous solid solution[22]

In a discontinuous solid solution, the solubility of each component within the other component is limited. Figure 2.3 represents the phase diagram for a discontinuous solid solution. The region of true solid solution is represented by α and β in Figure 2.3, where above the eutectic temperature one of the solid components is completely dissolved in the other solid component. The region of solid solution becomes smaller as the temperature decreases and therefore the overall solubility decreases[21, 22].

2.3.2.3 Substitutional Solid Solutions

In the substitutional solid solution the solvent molecules are substituted by the solute molecule in the interstitial space of the crystal lattice of the solid solvent. Figure 2.4 represents the substitutional solid solution. In the figure, solute molecules are represented by dark circles and the solvent molecules by open circles.

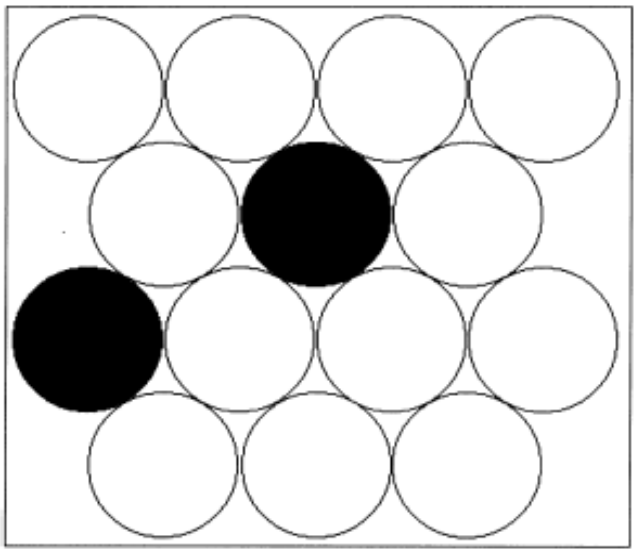

Figure 2.4: Substitutional solid solutions[21]

Based on the type of material used for the formation of a solid solution, they can be categorized as either continuous or discontinuous solid solutions. This type of solid solution can be formed only if the molecular size of the two components (solute and solvent) does not differ by more than 15%[21].

For example – Ammonium, anthracene-acenapthene, potassium thiocyanate, p-dibromobenzene and p-chlorobromobenzene tend to form solid solutions and therefore are able to increase their dissolution rate[23].

2.3.2.4 Interstitial Solid Solutions

In interstitial solid solutions, the solute molecule occupies the interstitial space between the solvent molecules in the crystal lattice.

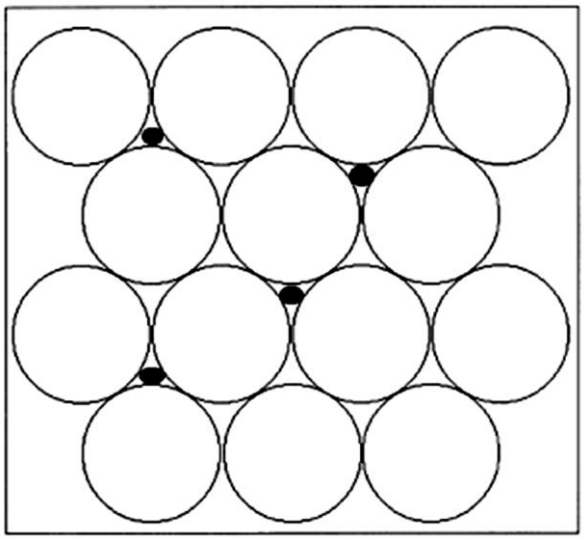

Figure 2.5: Interstitial solid solution[21]

Figure 2.5 represents the interstitial solid solution. In the figure solute molecules are represented by dark circles and the solvent molecules by open circles.

In order for interstitial solid solutions to form, the following factors must be present: (1) the diameter of the solute molecule should be less than 59% of the solvent molecule diameter; (2) the volume of the solute molecule should be less than 20% of the solvent molecule; and (3) the pattern in which the solute and solvent molecule are arranged should favor the formation of an interstitial solid solution[15, 21].

2.3.2.5 Amorphous Solid Solutions

In amorphous solid solutions the solute molecules are dispersed molecularly but irregularly within the amorphous solvent. Figure 2.6 represents the amorphous solid solution. Polymer carriers are more likely to form amorphous solid solutions since the polymer itself is often present in the form of an amorphous polymer chain network.

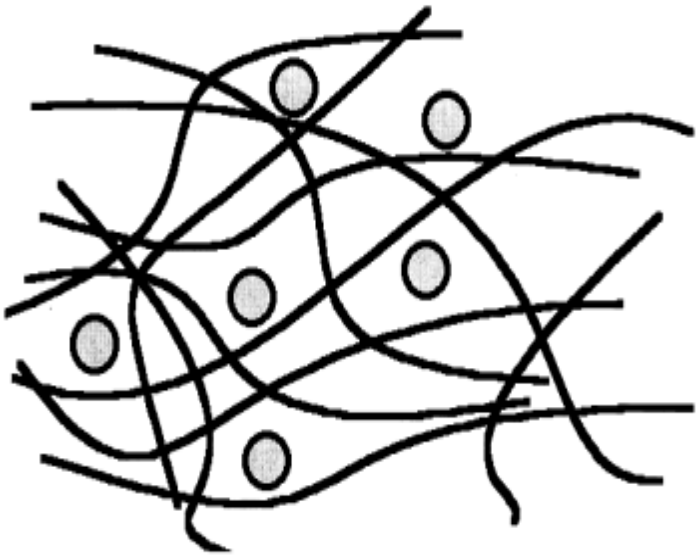

Figure 2.6: Amorphous solid solution[21]

In addition, the solute molecules may serve to plasticize the polymer, leading to a reduction in its glass transition temperature.

Chiou and Riegelman[24] were the first to report the formation of an amorphous solid solution to improve a drug's dissolution properties by using griseofulvin in citric acid.

2.3.3 Glass Solutions and Glass Suspensions

Chiou and Riegelman[24] first introduced the concept of the formation of a glass solution as another potential modification of a dosage form which can increase drug dissolution and absorption. A glass solution is "a homogenous system in which the glassy or vitreous form of the carrier solubilizes the drug molecule in its matrix"[13]. The term glass is used to describe a pure chemical or a mixture of chemicals in a glassy state. The glassy state or vitreous state is achieved by rapid quenching of the melt[25]. This glassy state or vitreous state is characterized by transparency and brittleness below the glass transition temperature (T_g). It continuously softens upon heating and gives a broad melting point. Heating the glassy state of pure compounds can transform it into a crystalline state. Various physicochemical properties such as viscosity, refractive index, thermal conductivity, compressibility, etc. change within the glass transition region when a substance is heated or cooled[26].

2.3.4 Amorphous Precipitations in a Crystalline Matrix

"Amorphous precipitations occur when a drug precipitates as an amorphous form in an inert crystalline carrier"[13]. The amorphous form of a drug is expected to produce a higher dissolution rate and increased bioavailability since the amorphous form of a drug

molecule has higher energy than its crystalline form. Moreover, the molecules in the amorphous form are arranged randomly, whereas the molecules in the crystalline form are arranged three dimensionally[27]. Thus, amorphous precipitates of the drug molecule are able to increase the dissolution rate and bioavailability.

Some examples of amorphous precipitations in a crystalline matrix, which were able to increase their dissolution rates, include chloramphenicol-PVP or hydroxypropyl cellulose[28], and sulfamethiazole-PVP coprecipitate systems[29].

2.3.5 Complex Formation

Complex formation can be characterized by the complexation of two components (drug and carrier) in a binary system during the preparation of a solid dispersion. The availability of the drug from the complex formed depends on stability, dissociation constant, solubility and intrinsic absorption rate of the complex. The type of carrier molecule used plays a vital role in determining the dissolution rate and bioavailability of the drug[13].

2.3.6 Combinations of these groups

In certain cases, the solid dispersion formed is able to increase the dissolution rate but it does not fall under any of the above mentioned groups. In this case, the solid dispersion formed is considered to be produced by a mechanism which is a combination of any of the above groups.

2.4 Methods of preparation of solid dispersions

2.4.1 Fusion method (Hot-melt method)

In the fusion method, the carrier is heated to a temperature slightly above its melting point and the drug is incorporated into the matrix. To ensure a homogenous dispersion of the drug in the matrix, the mixture is cooled with constant stirring. The dispersion may be cooled slowly to room temperature or rapidly in an ice bath. The fusion method is also known as the hot-melt method. This term can be used only when the starting material used in the process is crystalline in nature. After the dispersion is cooled, the resultant product is pulverized and sieved in order to process it into a dosage form. In this method, if the mixing of components is performed by an extrusion process, then the method is known as the hot melt extrusion method. The fusion method was first used by Sekiguchi and Obi[8] in 1961 to melt a eutectic mixture of sulfathiazole and urea above its eutectic temperature. This eutectic mixture exhibited an increased dissolution rate and increased bioavailability.

If the solubility of drug in a carrier is very high, then drug therein is dissolved in the carrier in the solid state, it results in a solid solution. In the solid solution molecular dispersion of drug is achieved due to particle size reduction. This may help to enhance the dissolution rate. If the solubility of the drug is poor in the carrier, then the crystallites of drug becomes dispersed in the carrier matrix which may lead to a moderate enhancement in the dissolution rate. In addition to the above mechanism, the drug can also be converted to the amorphous form in the carrier matrix which exhibits different dissolution rates[30].

The fusion method has some important advantages and disadvantages associated with it which are given below.

Advantages[30] –

1) The fusion method is preferably used for drugs and carriers that are miscible with each other in the molten state.
2) This method is less time consuming and is easy to perform.

Disadvantages –

1) There is risk of exposure of the drug to high temperatures, particularly if the carrier is a high melting solid and the drug is heat sensitive[30].
2) Drug and carrier miscibility with each other in the solid state is important for method utilization. Immiscibility within their phase diagram may lead to irregular crystallization and instability[9, 30].
3) Other potential problems that may appear include thermal degradation, sublimation and polymorphic transformations[16].
4) The solidification temperature affects the crystallite size and hardness of the dispersion[31].
5) The solidified melt may be tacky, difficult to handle and novel formulation techniques may become necessary to get an elegant dosage form for the product[32, 33, 34].
6) Tacky or glassy dispersions or their comminution may induce crystallization and modify their dissolution characteristics[35].

7) Decomposition or thermal degradation is often composition dependant and is usually affected by melting time and the rate of cooling[10, 36, 37].

2.4.2 Solvent method

In the solvent method, both the carrier and drug are dissolved in a suitable common organic solvent. The solvent is then evaporated to dryness by exposing the system to elevated temperatures or under vacuum[38]. This may result in supersaturation which leads to simultaneous precipitation of the constituents and solid residue formation. These types of solid dispersions are often termed coprecipitates[39] or coevaporates[40]. The residue thus obtained is then milled and sieved for further use. Various other methods can also be used for solvent evaporation such as spray drying or freeze drying[41]. Solvent removal is very crucial in this method since the solid dispersion formed may unintentionally trap some solvent in its crystal lattice structure. Since most of the solvents used in this method are non-aqueous and toxic in nature, the problem may arise with respect to pharmaceutical acceptance. Therefore, complete removal of the solvent from the solid dispersion becomes necessary. Various thermal analytical techniques such as DSC, DTA and TGA can be used to ensure that the complete removal of the solvent has been achieved[38].

The solvent method has some important advantages and disadvantages associated with it which are given below.

Advantages[42] –

1) This method may be used for thermolabile drugs since the solvent may be evaporated using reduced pressure and lower temperature.
2) In this method polymers with high melting points are also considered as carriers.
3) To enhance the integrity of the drug, freeze drying may be used to evaporate the solvent in aqueous systems.

Disadvantages[42] –

1) Selection of a suitable common solvent for both the drug and carrier is difficult. This problem becomes more complicated when the drug shows polymorphic changes with different solvents.
2) The complete removal of the solvent from the solid dispersion is often difficult and time consuming. Certain solvents may plasticize polymeric carriers, such as PVP, making their complete removal even more difficult[43].
3) Reproducibility of the crystalline form may be difficult.
4) An economic limitation also arises since a large amount of solvent may be needed in this method.
5) The temperature and rate of solvent removal is also important and should be controlled since they may affect the particle size, stability and dissolution characteristics of the drug.

2.4.3 Fusion-Solvent Method

The fusion-solvent method is a combination of the above two methods. In this method the drug to be incorporated into the carrier melt is solubilized in a suitable solvent and then is added to the carrier melt with continuous stirring followed by cooling. The carrier used in this method should have a capability to hold a certain proportion of liquid, maintaining its solid state, and the liquid used should be innocuous in nature[11, 12].

The fusion-solvent method has some important advantages and disadvantages associated with it which are given below.

Advantages –

1) This method is useul for drugs having a high melting point or drugs that are thermolabile in nature.

Disadvantages –

1) This method requires complete evaporation of the solvent because it may cause toxicity.
2) The selected solvent or dissolved drug may not be miscible with the carrier melt.
3) This method is generally limited to drugs with low therapeutic doses since low drug loading is obtained by this method.

2.5 Characterization of solid dispersions

Characterizations of solid dispersions utilizing various methods have been described in the literature[7, 8, 10, 12]. In order to characterize the solid dispersions prepared in the present research the following methods were used: Differential Scanning Calorimetry

(DSC); X-Ray Powder Diffraction (XRPD); Fourier Transform Infrared Radiation (FTIR); Scanning Electron Microscopy (SEM); dissolution studies using USP Apparatus II; and UV-Visible spectrophotometery.

Chapter Three

Differential Scanning Calorimetry

3.1 Introduction

Differential Scanning Calorimetry (DSC) is one of the most widely used thermal analytical method of analysis[1]. There are a number of thermal analysis techniques which can be employed including: Differential Scanning Calorimetry (DSC), Differential Thermal Analysis (DTA), Thermo Gravimetric Analysis (TGA), Derivative Thermogravimetry (DTG) and Evolved Gas Detection (EGD)[2]. These techniques are based on the principle of measuring the changes in physical properties of a substance as a function of temperature when that substance is subjected to a controlled temperature program[3]. Differential scanning calorimetry is now the most widely used method for the characterization of a solid dispersion[4].

Differential Scanning Calorimetry (DSC) is defined as "A technique in which a difference in the heat flow (power) to the sample (pan) and reference (pan) is monitored against time or temperature while the temperature of the sample, in a specified atmosphere, is programmed[5]." The plot obtained from the DSC instrument is seen as a differential heating rate versus temperature or time (Joules/second or Calories/second)[6].

Differential Scanning Calorimetry (DSC) has evolved from the technique of Differential Thermal Analysis (DTA) but does not account for the fundamental change in the working principle. It only includes some changes in thermocouple sensor's position and keeping the heat flux to the sample constant[7]. Differential Scanning Calorimetry (DSC) can be

used to obtain details about the physical and chemical properties of the sample. Heat is either absorbed or liberated when a substance is heated. This occurs because the sample undergoes a chemical reaction or a change in the physical state. Heat absorbed corresponds to endothermic changes and heat liberated corresponds to exothermic changes[8]. Glass transition, crystallization, melting, chemical reaction (oxidation, decomposition) can be determined by the curve obtained from Differential Scanning Calorimetry (DSC)[9].

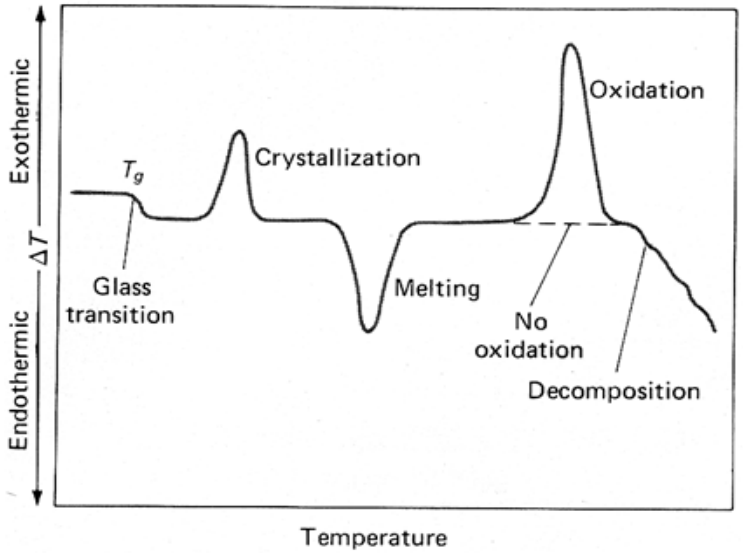

Figure 3.1 : A typical DSC Scan[10].

3.2 Types of DSC

In accordance with the basic principle of the instrument used for DSC measurements, DSC can be divided into two types – 1) Heat Flux DSC and 2) Power Compensated DSC[11].

3.2.1 Heat Flux DSC

In heat flux DSC (Figure 3.2), the sample and reference gets heated by the same source which is an electrically heated constantan thermoelectric disk and the temperature difference (ΔT) is measured. This signal is then converted to a power difference (ΔP) with the help of calorimetric sensitivity. The difference in the sample temperature from the reference temperature is due to the heat changes in the sample material[10, 11]. Figure 3.2 represents a schematic diagram of the heat flux DSC unit.

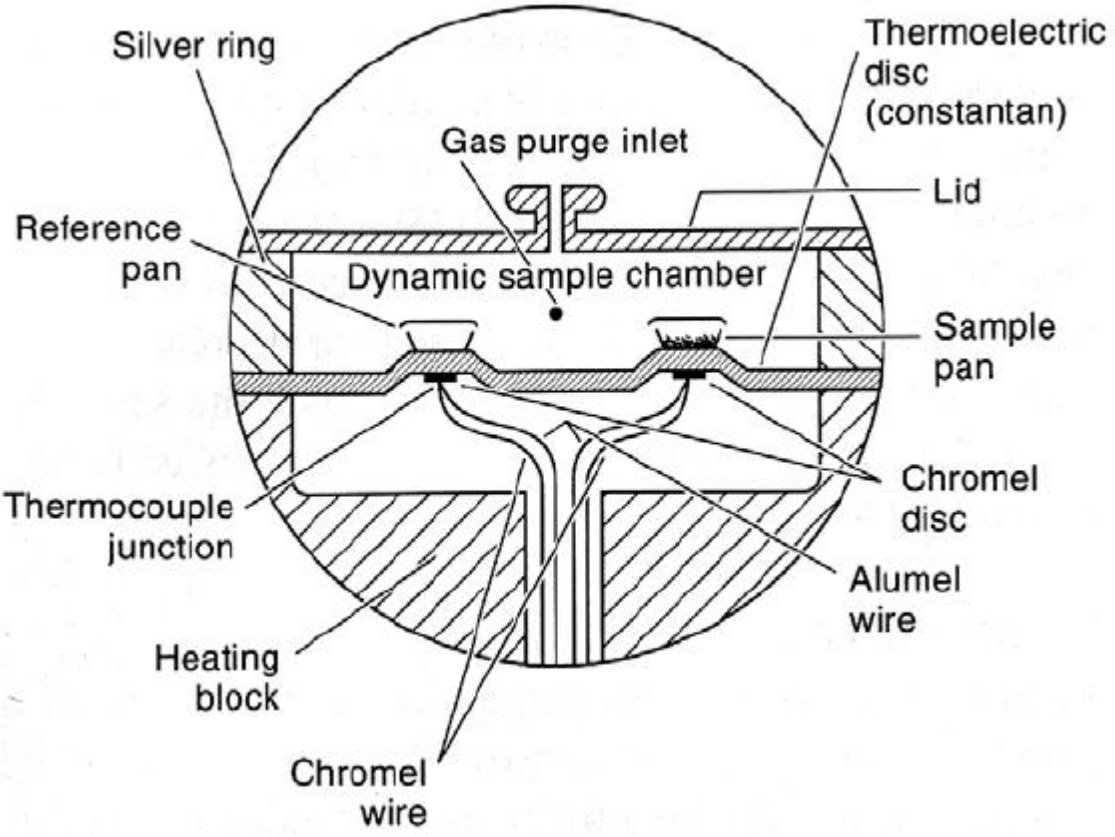

Figure 3.2: Schematic diagram of a heat flux DSC unit[12]

In a heat flux DSC unit, the platform has a constantan disc on which the sample pan and reference pan are placed while enclosed in a single furnace. Heat coming from the source is then passed to the sample and reference pans via a contantan disc. The differential heat flow between the reference and sample is monitored by chrome-constantan area thermocouples (produced by the junction between the constantan disc and a chromel disk) which are arranged back to back[9, 10]. Alumel wires are attached to the chromel discs which provide the chromel-alumel junctions. It has the function of independently measuring the temperature of the sample and reference. A separate thermocouple, which is enclosed in the silver block, serves as a function of temperature controller for the programmed heating cycle. An inert gas is allowed to pass through the cell at a constant flow rate[10]. The baseline obtained by the heat flux DSC is stable. Sensitivity of the heat flux DSC instrument is very high since it produces very little (negligible) noise[9].

3.2.2 Power Compensated DSC

In power compensated DSC (Figure 3.3), the sample and reference pan are heated independently by individual (identical) heaters. The difference in temperature between the sample and reference pan is maintained at nearly zero. The difference in electrical power needed to maintain equal temperatures of the sample and reference pan are measured. It is a measure of the heat capacity changes in the sample relative to the reference ($\Delta P = d(\Delta Q)/dt$)[11]. Figure 3.3 represents a schematic diagram of the power compensated DSC unit.

The large temperature controlled heated sink encloses the furnace. The sample and reference pan are placed above the furnaces which consists of platinum resistance thermometers attached to them. Platinum resistance thermometers measure the temperature of the sample pan and the reference pan continuously[10]. A rapid rate of heating, cooling and equilibration is achieved due to the small furnace used. Moreover, due to the small heat resistance from the heater to sample pan, the peaks obtained are sharp and with good resolution[13].

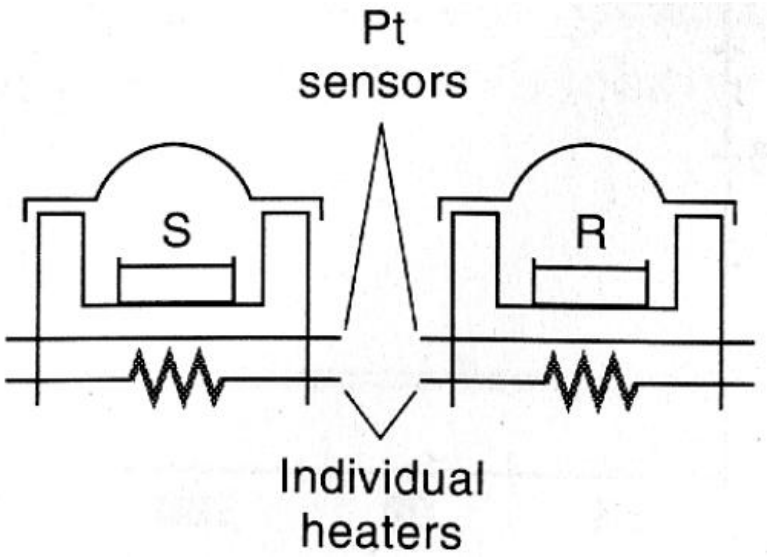

Figure 3.3: Schematic diagram of a power compensation DSC[12].

3.3 Parameters affecting experimental data obtained from DSC

3.3.1 Sample Pans

The sample pans used for Differential Scanning Calorimetry (DSC) are made from metals such as aluminum, stainless steel, silver, gold or platinum. Aluminum pans and lids are the most common and are widely used in the laboratory for performing experiments

because of the following properties. Most aluminum pans do not have a tendency to react with the sample materials. The melting point of aluminum is around 600°C. The DSC run can be conducted in the temperature range of -150 to 600°C using aluminum pans. In certain cases the sample reacts with aluminum. When this occurs, another type of material such as silver, gold or platinum should be used. Depending on the requirement of the sample to be ran, the pan can be sealed, pin holed or left open. For volatile samples sealed pans are used to avoid evaporation of the sample. Thermal conductivity characteristics of the type of crucible used may affect the curve obtained by DSC[11, 14, 15].

3.3.2 Sample Size

A thermal gradient across the sample decreases as the sample becomes smaller and increases with an increase in sample[16]. However, in certain cases, where the sample consists of a number of materials, it becomes very difficult to obtain a small, representative sample. In such cases a weak transition is observed. To avoid this possibility it would be appropriate to increase the sample size[11, 16]. Therefore, in order to obtain reasonable results the sample size should be within the range of 3-5 mg[17].

3.3.3 Sampling

Generally, a 3-5 mg sample is placed into the sample pan for the DSC experiment. During this process it is important to make sure that the sample is distributed widely and evenly on the bottom of the sample pan. It is important that the pan used for the DSC experiment to have a flat bottom. During the experiment contact between the sample and

cell, cell and detector should be optimized for the best condition to obtain reasonably good data[18].

While sampling powder materials, the sample used should be of small and uniform size. In the case of a liquid sample, pin hole pans are used to allow the vapor formed during heating to escape. For fiberous and film material the sample should be properly cut using scissors or other sharp instruments before placing it into the sample pan[19,20].

3.3.4 Purge Gas

Corrosive gases which are produced during the heating of the sample in a DSC run are removed by passing a purge gas continuously throughout the experimental time. Purge gases generally used are nitrogen or argon but for some cases oxygen or air can be used as a purge gas depending on the experiment and sample under study. The usual flow rate for the purge gas is within the range of 50 to 80 ml/min[14].

3.3.5 Starting Temperature and Heating rate

For any DSC experiment it is desirable to start with a temperature which is at least 3 degrees below the temperature of transition[16]. Heating rate used for most of the sample is in the range of 10 to 20°C/min. The heating rate is reduced to the range of 1 to 5°C/min for certain experiments where a small change in phase transition has to be studied[14].

3.3.6 Calibration

It is very important to calibrate the DSC instrument on a temperature scale as well as to determine its calorimetric sensitivity in order to obtain accurate and reproducible results[11].

3.3.6.1 Temperature Calibration

For DSC temperature calibration, it is considered appropriate that the temperature plotted on the abscissa of a DSC graph is directly proportional to the electromotive force (emf) which is generated at the thermocouple located under the sample pan[21]. Standard calibration charts are used to convert the emf values which are previously obtained to temperature units. A standard substance such as Indium (melting point: 156.6 °C) and Zinc (melting point: 419.4 °C) with known melting points are used for calibration of the temperature scale. EMF values obtained from the above are thus compared with the standard calibration charts[10, 11]. A list of some other materials which can be used for DSC temperature calibration are given in Table 3.1[12].

Table 3.1: Melting points and EMF value for common DSC standard materials

Material	T_m (°C)	H_f (J/g)
Mercury	-38.8344	11.469
Gallium	29.7646	79.88
Indium	156.5985	28.62
Tin	231.298	7.170
Bismuth	271.40	53.83
Lead	327.462	23.00
Zinc	419.527	108.6
Aluminum	660.323	398.1

3.3.6.2 Calorimetric Calibration

For DSC calorimetric calibration, the difference in values for specific heats or the enthalpy content of the samples from those values previously obtained is determined and compared with the calculated values[10].

For the heat flux DSC system the heat balance equation can be presented as follows[10]:

$$\frac{dH'}{dt} = \frac{T_{SP} - T_{RP}}{R_D} + (C_S - C_R)H + C_S \frac{R_D + R_S}{R_D} \frac{d(T_{SP} - T_{RP})}{dt} \qquad \text{Eqn 3.1}$$

Where, (dH'/dt) refers to the heat evolution which denotes exothermic peak. The first term on the right hand side of Equation 3.1 refers to the area under the DSC peak, after baseline correction. The second term on the right hand side of Equation 3.1 refers to the actual baseline and is the one which is used in the determination of specific heat. The last term on the right hand side of Equation 3.1 takes into account the fact that some of the heat which is evolved during the process will be taken up by the sample itself to increase its temperature. This may result in a distorted peak shape but does not affect the area under the DSC peak.

This calorimetric calibration method involves a comparison of the thermal lag between the sample and the reference. The system is first calibrated with a sapphire specimen, so that[10,21]

$$C_{sapphire} = E_q Y / HM \qquad \text{Eqn 3.2}$$

Where, ($C_{sapphire}$) is the specific heat capacity of the sapphire, (E) is a calibration constant, (q) is the Y-axis range ($Jsmm^{-1}$), (Y) the difference in Y-axis deflection between sample (or sapphire) and blank curves at the temperature of interest, (H) is the imposed heating rate and (M) is the mass of the specimen.

The area under the peak of the DSC thermogram can be used to determine the enthalpy changes, where the DSC thermogram is a plot of (ΔT) versus time. Equation 3.1 can be used only when the instrument is in the calibrated mode[10,21].

3.4 Applications

The most widely used instrumental methods in the pharmaceutical industry for the characterization of a given sample include: Differential Scanning Caloriemetry (DSC) and Differential Thermal Analysis (DTA). Applications of DSC for the evaluation of substances are numerous and can be roughly generalized into two groups as follows[11]:

- The first group includes various types of chemical reactions which include decomposition, dehydration, oxidative attack and polymer curing.
- The second group includes various types of physical changes and measurements which include melting, changes in liquid, changes in liquid crystalline states, changes in polymers, crystalline phase changes, heat capacity, glass transitions, emissivity, thermal conductivity and diffusivity.

Chapter Four

X-Ray Diffractometry

4.1 Introduction

X-ray diffraction is a non-destructive technique[1]. It is presently an important analytical tool in the pharmaceutical industry for providing both qualitative and quantitative information about the structure of a molecule. The qualitative application is supported by the fact that all crystalline samples have a unique x-ray diffraction pattern. This method can also be used for the quantitative measurement of a crystalline compound in a mixture[2]. It is a predominantly powerful tool, commonly used for the characterization of crystalline materials and other pharmaceutical solids. A clear understanding and basic information about the physical, chemical and structural properties of polymeric materials, metals and other solids can be obtained with the x-ray diffraction technique[2].

The x-ray diffractometer follows the principle of scattering[1]. Fundamental information about the structure of a crystalline sample can be easily obtained with an x-ray diffractometer[1]. The incident beams are scattered in all directions by the plane of the crystalline solid sample, due to interaction with electrons present in the sample as it passes through[3]. When the scattered beams of radiation interferes with one another in both a constructive (Figure 4.1 a) and destructive (Figure 4.1 b) manner, it leads to the phenomenon of x-ray diffraction[4, 5, 6].

A crystal lattice in a crystal has unit cells which are arranged periodically with each unit cell having systematically arranged atoms within it[8].

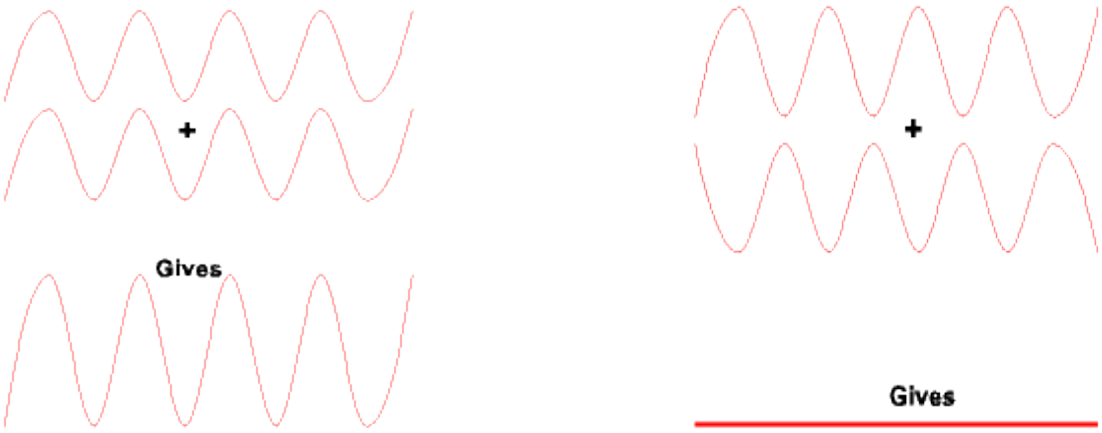

(a) (b)

Figure 4.1 – Figure showing (a) constructive interference and (b) destructive interference[7]

When an x-ray beam is incident to a crystal surface at an angle (θ), a fraction of the x-ray beam is diffracted by atoms present at the surface of the crystal and the remaining unscattered fraction penetrates the second layer of atoms. A fraction of the x-ray beams are diffracted and the remaining fraction penetrates the third layer (Figure 4.2). The diffracted x-rays are detected and analyzed by the detector of the x-ray diffractometer. The two major prerequisites for the application of x-ray diffraction phenomenon are: 1) all the crystal substances under study should have their scattering centers which are spatially distributed in a regular pattern and 2) spacing between the layers of atoms in a crystal lattice should be in accordance with the wavelength of the radiation[3].

4.2 Bragg's law

Bragg's law provides a relationship between the angle of incidence, incident x-ray wavelength and spacing between the layer of atoms in a crystal lattice[12]. Bragg's law

assumes a model where the atoms in a crystal lattice are arranged in a periodic pattern in parallel sheets which is separated by a fixed distance (d), to explains the phenomenon of diffraction of x-rays by crystals[9]. According to Bragg, in a crystal with interplaner spacing (lattice constant) d, which consists of large number of planes, the reflected beam is detectable only at a particular incident angle. As the difference between the distance travelled by the beam of rays is of the same magnitude as the wavelength, the reflected beam then interferes. A requirement for x-ray diffraction studies is a constructive interference of the wave formed and not the destructive interference[10, 11]. The detectable maxima can be obtained from the reflected beams of rays only when the difference between the distance covered equals the integral multiple of the wavelength (λ)[11].

Bragg's law is represented as follows:

$$n\lambda = 2d \sin\theta \qquad \text{(Eqn 4.1)}$$

where, (n) is the order of reflection, (λ) is the wavelength of the x-ray beam incident on a crystal at angle (θ), (d) is the inter-planar distance (in angstrom units) and (θ) is the angle between the incident ray and the scattering planes[9].

The angle (θ) of the scattering x-ray is measured by keeping the sample at a fixed position, in order to maintain a constant angle between the sample, the source of radiation and moving the detector[14]. If the wavelength of the incident beam is known, the use of Bragg's law will enable one to determine the spacing between the planes (d)[14]. Since the interplaner spacing (d) is unique for each crystalline compound, the value of (d) obtained by Bragg's law can be used to identify compounds[15].

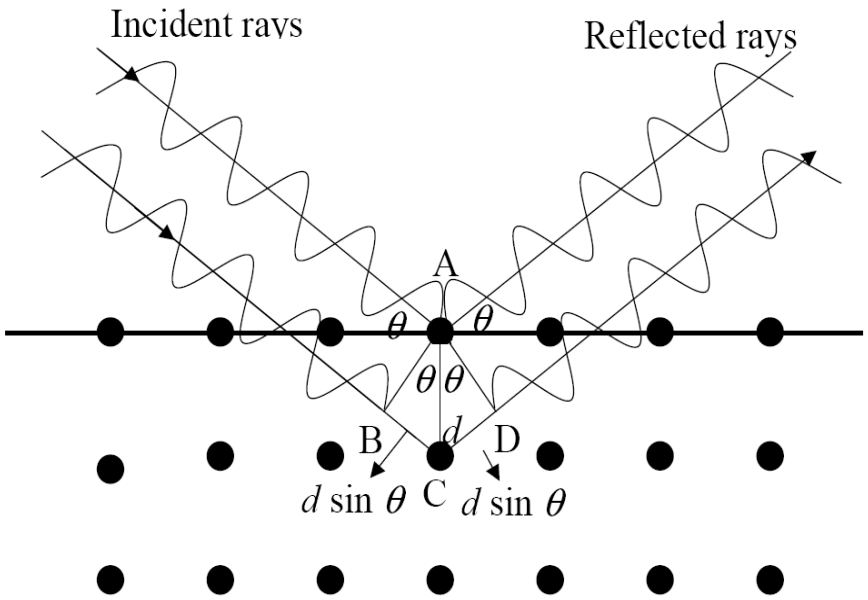

Figure 4.2 - X-rays diffraction by a crystal[13]

4.3 Instrumentation

The measuring system of the X-ray diffractometer includes an X-ray generator, X-ray tube, filter, sample holder and X-ray detector[16].

The X-ray generator has the function of holding the X-ray tube and other equipment which stabilizes and regulates the beam intensity[16].

The X-ray tube produces radiation by heating a filament in the cathode ray tube[17]. Material of the anode is the deciding factor which governs the voltage of the tube[16]. Thus, by applying an appropriate voltage, electrons are accelerated towards the target sample[17].

Monochromatic x-rays are needed for diffraction measurement by the sample. This can be achieved by using an absorption edge filter, a single crystal monochromator which is

placed before and after the sample and energy discrimination. A metal foil whose absorption edge lies between K_α and K_β is introduced into the path of the beam. This will lead to a decrease in the intensity of the continuous radiation and K_β lines. A monochromator has the function of decreasing the intensity of disturbing radiation and decreasing divergence[16].

Samples under evaluation are placed onto the sample holder which is usually made up of glass, plastic or light metals (tungsten, aluminium, copper, chromium, cobalt, iron or silver)[16, 18].

The detectors used for X-ray diffraction are separated in two groups depending on the requirement of the polycrystalline sample under study. 1) Sensitive photographic film is used to record the reflected beams at the same time in the whole angle range. Special different chambers are used for this purpose including Debye-Scherrer and Guinier. 2) At a given dispersion angle, detectors such as the Geiger-Muller, proportional, semiconductor and scintillation counting tube are used to detect different reflections. These detectors are frequently used in the field of powder diffractometry[16]. All types of detectors have the function of recording, converting and processing the data from signals in order to obtain results seen on a computer screen[18].

Basic and essential components of an X-ray Diffractometer are seen in Figure 4.3. The crystalline sample is placed on a goniometer which has the capability of rotating in order to determine the angle (θ) between the collimated incident beam and crystalline sample face. The detector should be mounted on a second table which can rotate at a speed twice

as fast as compared to the speed of the sample rotation. If the crystalline sample rotates through an angle (θ), the detector should move through an angle (2θ)[3].

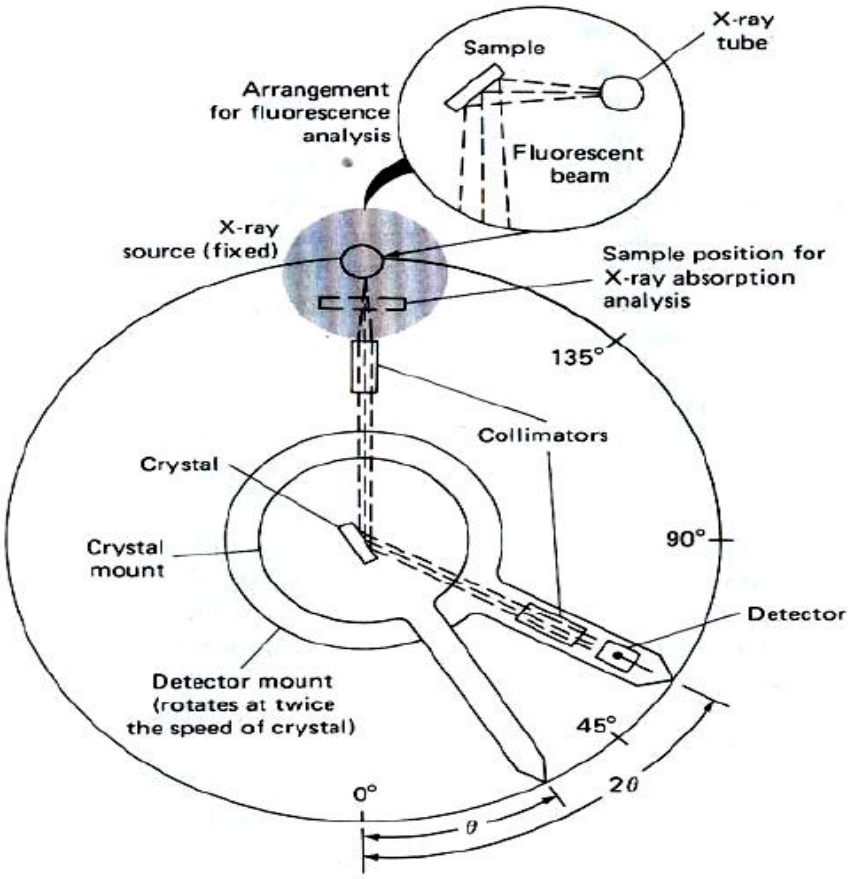

Figure 4.3 – Schematic diagram of an X-ray Diffractometer[3]

4.4 Sample Preparation

There are many different methods by which the sample can be prepared in order to undergo a diffraction study depending on nature and type of compound being analyzed[19]. The most common method used is to triturate the sample to a homogenous fine powder[2]. Such a sample may have a large number of small crystallites which are

oriented in all possible directions. Therefore, a significant number of crystallites are oriented when an x-ray beam is passed through the material so as to fulfill the Bragg's condition of deflection which requires deflection of x-ray radiation from all possible interplanar spacing[2].

Some of the important issues in which care must be taken during sample preparation include: the size of the crystallite; the orientation of the powder sample in the sample holder; the co-planarity of the surface of the sample; the holder; and the method of filling the powdered sample in the sample holder[20]. Sieves and size reduction equipment should be used in order to obtain the desired crystallite size range. Preparation of sample slurry with different organic solvents and the use of software called Rietveld can help to avoid preferred orientation problems. Preferred orientation problems are common with samples which contain rod or plate like crystals. These types of crystals have the tendency to avoid certain x-ray beam deflection which may be important for analysis of the sample by lying flat on the sample holder[20, 21].

Sample holders used to load samples for diffraction studies are usually rectangular plates. These plates have a small rectangular opening into which the powdered sample is filled[20]. A sample holder is commonly composed of aluminum, glass, quartz, silica or any possible material which creates very low background noise[22]. Preferred orientation can be minimized to a certain extent by filling the sample from the side of the sample holder. It has been proven by a few studies[1, 23].

4.5 Interpretation of X-ray diffraction patterns

In the identification of a given compound, the X-ray diffraction study plays an important role in determining its morphology. Moreover, each pure sample has a unique pattern of diffraction which can be useful in the identification of the compound. An amorphous sample has a disordered lattice which gives it a broad peak when subjected to the diffraction study[24]. The position of the lines, in terms of θ and 2θ, and the relative intensities of the lines are used for identification purposes. Spacing between two particular sets of planes is used for the determination of the diffraction angle (2θ). The Bragg equation can be used to calculate the distance between two planes (d) from the wavelength of the source and the measured angle[25]. Identification of the components of the sample requires a large number of sophisticated software (such as – JCPDS data base, X'pert Pro, Fityk 0.0.4 fit software (www.fityk.sf.net), Scintag program DMSNT (Diffraction Management System for NT), Rietveld refinement technique, etc.) are available which provides information about the percent of crystalline character and the compounds identity[24, 26].

4.6 Applications

The X-ray powder diffraction technique is a non-destructive technique which is widely used and can be applied in various scientific fields. Other than normal XRPD, we also have variable-temperature XRPD in which the sample can be heated or cooled to any desired temperature. This method is very useful when the study of thermally induced changes in sample morphology is desired. This method can be a complement to thermal methods of analysis[1, 27]. Various applications for XRPD are as follows:

- Phase identity of materials - The intensity ratio and the d-spacing are used for the comparison[28].
- It is mostly used in the determination of the polymorphic character of a sample[14].
- It is extensively used to determine the degree of crystallinity of the sample[14].
- It is very useful for stability studies of powdered drug samples in which we examine the crystalline content of the drug[29].
- For the determination of crystalline phases and orientation of the sample[14].
- For the measurement of single and multiple layer thicknesses[25].

Chapter Five

Fourier Transform Infrared Spectroscopy

5.1 Introduction

"Fourier spectroscopy" can be described as the analysis of signal variation into its constituent frequency components[1]. Fourier transform of an optical interferogram providing a spectrum of absorption, emission, reflection, or photoacoustics constitutes FT-IR spectroscopy. Because of its speed, accuracy and sensitivity FT-IR spectrometers are gaining popularity over wavelength dispersive spectrometers[1]. The principles of FT-IR spectroscopy are different than the principles seen with dispersive spectroscopy techniques. Instead of being exposed to a varying energy of electromagnetic radiation, the sample in FTIR is subjected to a single pulse of radiation which consists of frequencies in a particular range[2].

For the identification of an organic compound, infrared (IR) absorption spectroscopy can provide preliminary data[3]. The infrared (IR) absorption spectroscopy provides a spectrum which is a plot of the percentage of infrared radiation that passes through the sample (% transmission) vs. the wavelength (or wave number) of the radiation[4]. Radiations which has wavenumbers in the range of 4000 cm^{-1} to 400 cm^{-1} under normal circumstances falls within the infrared region of the spectrum. The infrared spectrum can be further divided into 3 regions including far-IR (100-400 cm^{-1}), mid IR (400-4000 cm^{-1}) and near-IR (400-1400 cm^{-1})[4]. Samples with molecular species which possess small energy differences between various rotational states and vibrational states are capable of infrared radiation absorption. These types of molecules experience a net change in dipole

moment due to the rotational and vibrational motions produced[3]. Values for the estimation of the characteristic absorption frequency for specific functional groups are summarized in Table 5.1 and 5.2 based on the approximation of Hooke's law.

Regions of the Infrared Spectrum for Preliminary Analysis

Region	*Group*	*Possible Compounds Present (or Absent)*
3700–3100	—OH	Alcohols, aldehydes, carboxylic acids
	—NH	Amides, amines
	≡C—H	Alkynes
3100–3000	=CH	Aromatic compounds
—	$-CH_2$ or —CH=CH—	Alkenes or unsaturated rings
3000–2800	$-CH$, $-CH_2-$, $-CH_3$	Aliphatic groups
2800–2600	—CHO	Aldehydes (Fermi doublet)
2700–2400	—POH	Phosphorus compounds
	—SH	Mercaptans and thiols
	—PH	Phosphines
2400–2000	—C≡N	Nitriles
	$-N=\overset{+}{N}=\overset{-}{N}$	Azides
	—C≡C—	Alkynes*
1870–1650	C=O	Acid halides, aldehydes, amides, amino acids, anhydrides, carboxylic acids, esters, ketones, lactams, lactones, quinones
1650–1550	C=C, C=N, NH	Unsaturated aliphatics,* aromatics, unsaturated heterocycles, amides, amines, amino acids
1550–1300	NO_2	Nitro compounds
	CH_3 and CH_2	Alkanes, alkenes, etc.
1300–1000	C—O—C and C—OH	Ethers, alcohols, sugars
	S=O, P=O, C—F	Sulfur, phosphorus, and fluorine compounds
1100–800	Si—O and P—O	Organosilicon and phosphorus compounds
1000–650	=C—H	Alkenes and aromatic compounds
	—NH	Aliphatic amines
800–400	C—halogen	Halogen compounds
	Aromatic rings	Aromatic compounds

Table 5.1 - Regions of the IR spectrum used for detail chemical analysis of compound[3].

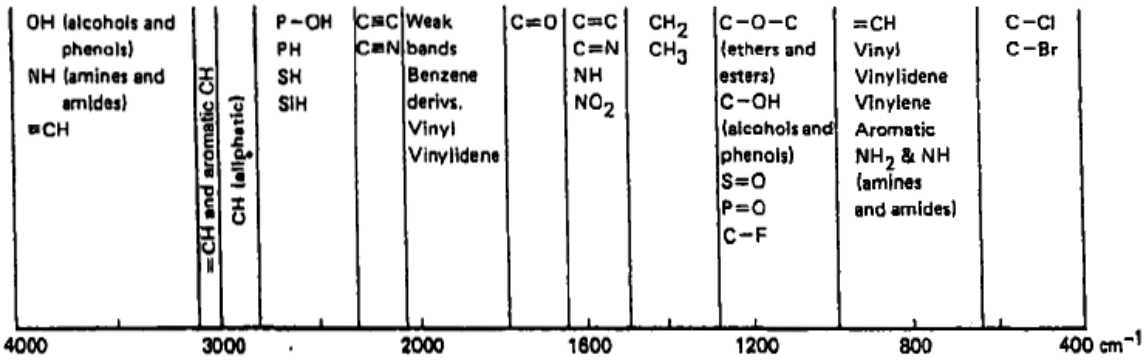

Table 5.2 - Regions of the IR spectrum used for preliminary analysis of a compound[3].

5.2 Instrumentation

A Fourier transform spectrometer cannot measure the desired spectrum directly. The FTIR instrument is non dispersive and uses an interferometer to encode data from the whole spectral range at the same time[5]. Figure 5.1 represents the basic components of a single beam FTIR spectrophotometer.

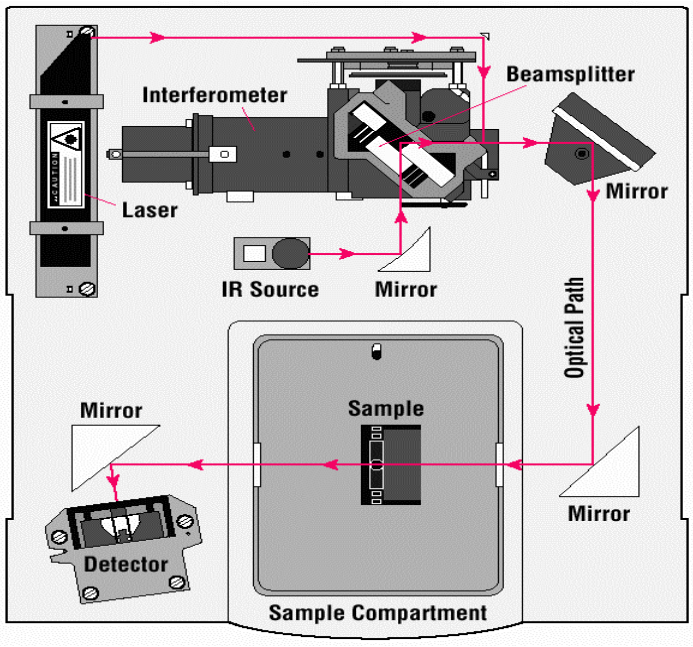

Figure 5.1 – Schematic of single beam FTIR spectrophotometer[6].

In the single beam FTIR spectrophotometer, the radiation emerging from the source first enters the interferometer before passing through the sample. After radiation passes through the sample, the data are collected by the detector. An analog to digital converter is used to convert the data obtained into digital form which is further treated by Fourier transform software installed on the computer[7].

Fourier transform spectrometers most commonly use a Michelson interferometer[8]. Based on the design and the manner in which the FT-IR spectrometer, utilizing a Michelson interferometer are operated, it can be differentiated into several types. It can be operated as follows: (1) rapidly without chopping of the infrared beam; (2) a slow continuous manner with chopping of the infrared beam (slow scanning); or (3) scanning in a discontinuous stepwise manner (step-scan interferometer)[8]. As seen in Figure 5.2, a Michelson Interferometer consists of two plane mirrors which are set perpendicular to each other. It has a beam splitter which bisects the planes of the two mirrors[9].

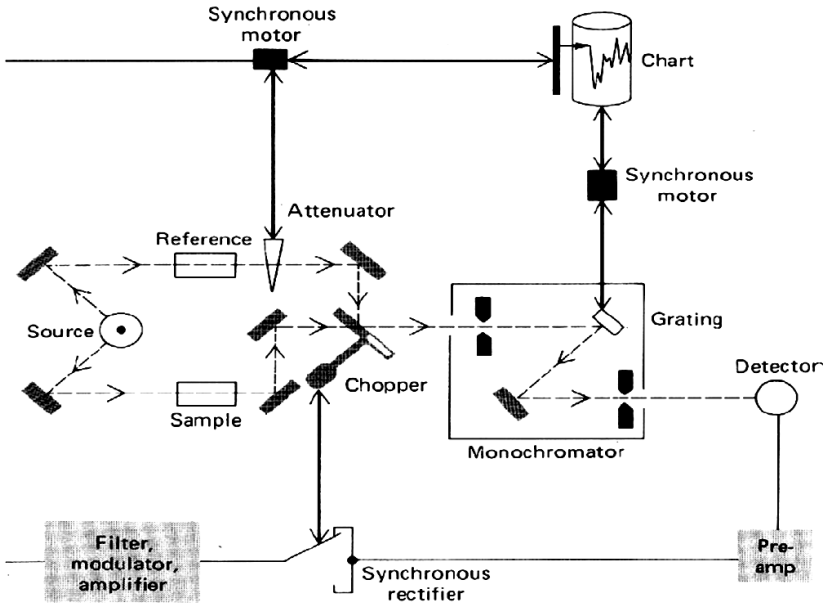

Figure 5.2 - Schematic of a double beam FTIR spectrophotometer[9].

Depending upon the region to be examined, the material of the beam splitter is selected. To make a beam splitter for the mid infrared region or near infrared regions materials such as iron-oxide or germanium are coated onto an „infrared-transparent' substrate. To make a beam splitter for the far-infrared region a thin organic film of polyethylene terphthalate is used[9]. The thickness and coatings of the beam splitter are very crucial[8]. The beam splitter has the function of dividing the amplitude of the monochromatic beam of radiation, in which one part (50%) goes to the moving mirror and other part (50%) goes to the fixed mirror. The reflected returning beams from these mirrors recombine again at the beam splitter and undergo interference. Fifty percent of the beam reflected from the fixed mirror is transmitted through the beam splitter. The remaining 50% is reflected back in the direction of the source. The reconstructed beam is then passed through the sample and focused onto the FTIR detector[9, 10].

The source most commonly used for the near infrared region is a tungsten halogen lamp. The source used for the mid infrared region is a Globar source or a Nernst glower. The source used for the far infrared region is a high pressure mercury lamp. Detectors used for the near infrared region include lead sulfide photoconductors. Those for the mid infrared region use a pyroelectric device incorporating deuterium tryglycine sulfate (DTGS). Those for the far infrared region use germanium or indium-antimony detectors[9, 11].

There are many advantages for using FTIR spectrometers over conventional spectrometers. This often leads to the frequent use of FTIR spectrometers. The most

important advantages for FTIR spectrometers over conventional spectrophotometers include: higher accuracy in frequency measurement for the spectra; high resolution (<0.1 cm^{-1}); highly reproducible frequency determination; and higher signal-to-noise ratios for spectra recorded for the same measurement time[1, 9].

5.3 Application

The applications for FTIR spectrometers abound in almost every field. In the last few decades the importance of FTIR spectrophotometry has dramatically increased its potential in qualitative and quantitative analysis. Use of the FTIR spectroscopic technique along with suitable software for calculations make it possible to obtain a large amount of information contained in the IR spectra for organic substances and for the resolution of complex mixtures simultaneously[1].

Because of the ability of FTIR to provide crucial information in a timely manner frequent use of FTIR in industry has increased exponentially[1].This technique is economical since it provides more data at a lower cost for the same amount of materials; thin films or residues are identified with a sensitivity that is highly competitive with electron- or ionbased surface analysis techniques[1, 12]. It has a capability of analyzing areas as small as 10–15 microns. As shown by Markhan et al[12], "The technique has also been used to measure surface temperature, which is independent of the material emissivity, surrounding radiation sources, and instrument calibration."

Infrared absorption spectroscopy can also be used as a detector for gas chromatography where FTIR has the ability to identify the compound, while when coupled with a gas

chromatograph it has the ability to separate the components. It is also used for the analysis of atmospheric pollutants from industrial processes[13].

Fourier transform instruments have the advantage that their optics provides a much larger energy throughput as compared to dispersive instruments, which in themselves are limited in throughput because they have the necessity of requiring narrow slit widths. Because each IR frequency is in effect modulated at a different frequency, the interferometer is free from the problem of stray radiation[7, 13].

Chapter Six

Scanning Electron Microscopy

6.1 Introduction

The scanning electron microscope (SEM) is one of the most versatile analytical instruments. It is commonly used for the examination and analysis of the microstructure morphology and chemical composition characterizations of solid samples[1]. SEM analysis is a non-destructive method of analysis. Therefore, it is possible to analyze the same materials repeatedly[2]. A focused beam of high-energy electrons is utilized by the scanning electron microscope (SEM) in order to generate a variety of signals at the surface of solid specimens. The signals produced by the interaction of the solid sample with electrons provides information about the sample which includes external morphology (texture), crystalline structure, orientation of material and chemical composition[3]. The fundamental principle of scanning electron microscopy is based on a variety of phenomenon. In SEM the accelerated electrons carry a significant amount of kinetic energy. This kinetic energy is dissipated in the form of a variety of signals which are produced by the interaction between the sample and electrons when the incident electrons are decelerated in the solid sample. The signals which are produce by above interaction includes secondary electrons, backscattered electrons, diffracted backscattered electrons, photons, visible light and heat. Secondary electrons and backscattered electrons are frequently used for imaging samples. Secondary electrons are specifically used for obtaining morphology and topography of samples and backscattered electrons are specifically used for illustrating contrasts in composition in multiphase samples.

Diffracted backscattered electrons are used to determine crystal structures and the orientation of the sample. Photons are used for elemental analysis[4, 5].

The SEM is frequently used to produce high-resolution images of shapes of samples and to show spatial variations in chemical compositions of the sample by:

1) Acquiring elemental maps or spot chemical analyses using energy dispersive x-ray spectroscopy.
2) Discrimination of phases based on mean atomic number (which is mostly related to relative density) using back scattered electrons.
3) Compositional maps based on differences in a trace element called "activitors" using cathodoluminescence.

The SEM is also widely used to identify phases based on qualitative chemical analysis and/or crystalline structure. Precise measurement of very small features and objects down to 50 nm in size can also be accomplished using the SEM.

6.2 Instrumentation

The essential components of an SEM include - electron source (electron gun), electron lenses, detectors and image processing.

6.2.1 Electron source (Electron gun)

An electron gun in the SEM instrument serves as a stable beam of electrons of adjustable energy. The SEM instrument described previously consists of tungsten or LaB_6 thermionic emitters as the electron source. Recently, a cold, thermal or Schottky field emission source has been used because they provide enhanced reliability, performance and last a lifetime[6]. Figure 6.1 represents a configuration of a typical electron gun[7].

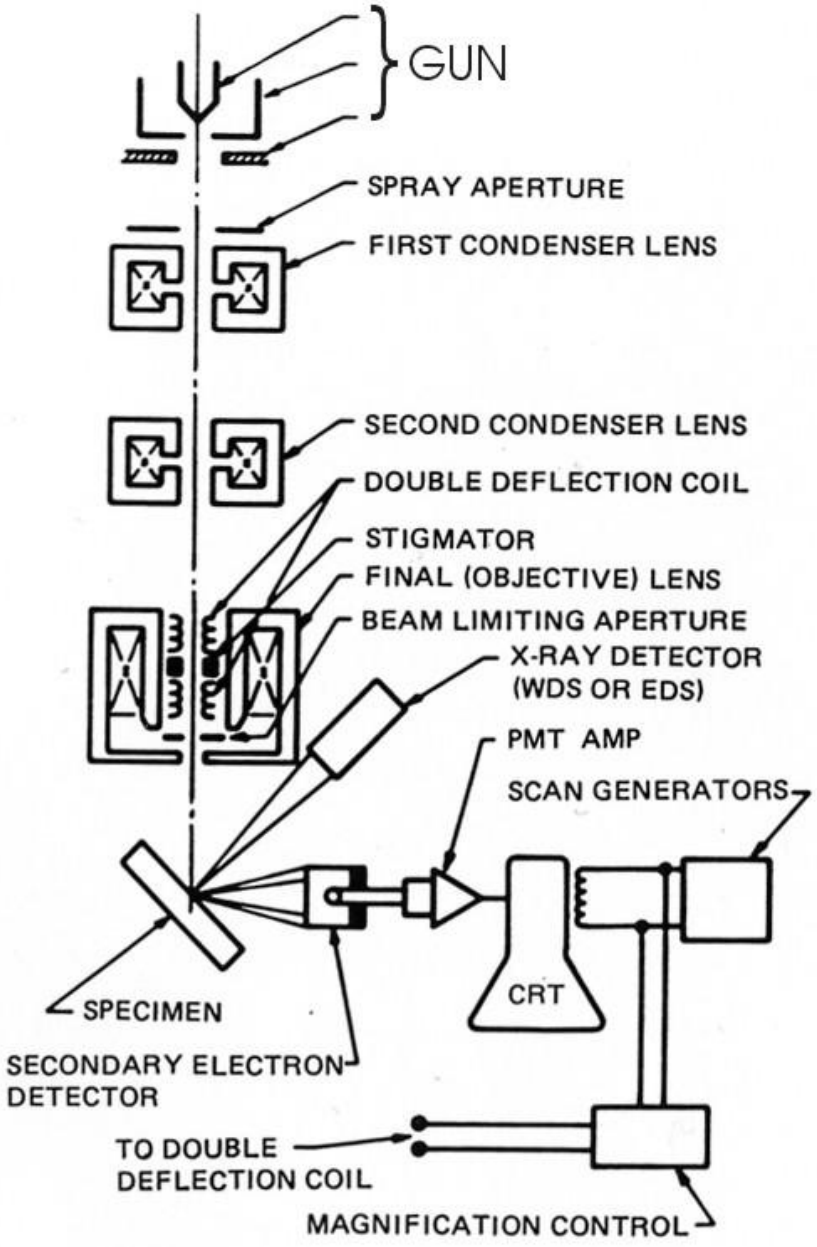

Figure 6.1 – Schematic diagram of a typical electron gun[7]

The most frequently used electron gun consists either of a tungsten hairpin electron gun, Lanthanum hexaboride (LaB_6) electron gun or an Field emission electron gun. The

tungsten hairpin electron gun consists of a hairpin which serves as a cathode, a grid cap which serves as a control electrode and an anode. These components are maintained at different electrical voltages which can vary in the range of 0.1 to 30 kV. A grid cap is set at a little higher voltage then the filament which provides a focusing effect on the beam[6]. The lanthanum hexaboride (LaB_6) electron gun provides 5 to 10 times better brightness and a longer life time as compared to the tungsten hairpin electron gun because lanthanum hexaboride has a lower work function. Thus, more electrons are emitted by lanthanum hexaboride at the same heating temperature. The above two thermionic sources are relatively inexpensive but they have several disadvantages such as limited lifetime, large energy spread and low brightness. A field emission electron gun is a source of electrons which is free from these disadvantages mentioned above[6]. A field emission electron gun consists of a sharply pointed tungsten tip which is held at several kilovolts negative potential relative to a nearby electrode.

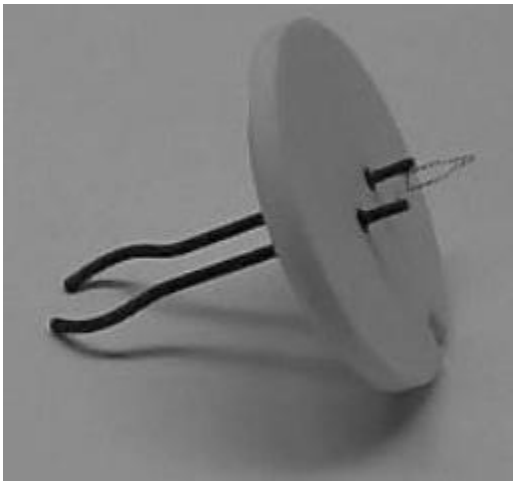

Figure 6.2 – Figure showing Tungsten hairpin type filament[9]

It can generate a very high potential gradient at the surface of the tungsten tip. Thus, the electrons at the metal surface are transported by the phenomenon of delocalization. This

process is called the tunneling effect which acts as a basic principle of electron emission from the field emission electron gun[8]. Figure 6.2 shows a typical tungsten hairpin type filament[9].

6.2.2 Electron Lenses

Electron lenses have a function of manipulating the configuration of the electron beam by acting as a magnet. The condenser lens is variable and controls the amount of demagnification for a particular imaging mode. A condenser lens system consists of one or more lenses which has the function of determining the current that impinges on the sample. The objective lens in the SEM has a function of establishing the final spot size[9, 10].

6.2.3 Detectors

Detectors frequently used in scanning electron microscopy are as follows[10]:

1) Catodoluminescence detector
2) Solid state detector
3) Scintillator Photomultiplier detector
4) Specimen current detector

The radiation coming from the sample is accepted by the detector. These signals are further converted into an electrical signal and amplified. Modulating the gray level intensities on the cathode ray produce the image[9,10].

6.2.4 Image Processing

Optimization of the image obtained from SEM is carried out to obtain the desired information. The three methods commonly used for this purpose are as follows[11]:

1) Digital image processing

2) Optical photographic methods

3) Electrical analog methods

6.3 Sample Preparation

Depending on the nature of the samples and the data required the process of sample preparation can be optimized. In order to obtain an image using SEM, the sample should be conductive in nature[12]. If the sample under SEM study is non conductive in nature then the sample becomes negatively charged by collecting the electrons from electron bombardment thus obscuring the image obtained[13]. Pharmaceutical samples commonly studied under SEM are non conductive in nature and require a coating with a conductive material[14]. Most electrically insulating samples are coated with a thin layer of conducting material such as carbon, gold, or some other metal or alloy. The choice of material for conductive coatings depends on the data to be acquired. Carbon is specifically used if elemental analysis is a priority, while metal coatings are effective for high resolution electron imaging applications. Alternatively, an electrically insulating sample can be examined without a conductive coating in an instrument capable of "low vacuum" operation[12, 15].

Coating the sample is carried out by the method called sputter coating. This process is carried out in an evacuated glass chamber. Argon is pumped into the chamber through a needle valve. The base plate in the instrument is used to hold the sample. A sputtering of atoms occurs when high voltage is applied across the electrodes which lead to a metal foil being bombarded with ions. Thus, the sample is coated by depositing atoms onto the surface. The discharge current and time are the two factors which are modulated in order to control the thickness of the coating on the sample[10, 16].

Chapter Seven

Ultraviolet-Visible Absorption Spectroscopy

7.1 Introduction

Ultraviolet-visible (UV-Vis) absorption spectroscopy involves photon spectroscopy which includes measurement of the wavelength and absorption intensity of a sample in the UV-visible region of the electromagnetic spectrum. In this spectroscopic method light in the visible, adjacent near ultraviolet and near infrared region of electromagnetic spectrum is used for excitation of electrons to a higher energy level. Upon absorption of radiation in this region of the electromagnetic spectrum, molecules undergo electronic transitions as seen in Figure 7.1[1, 2].

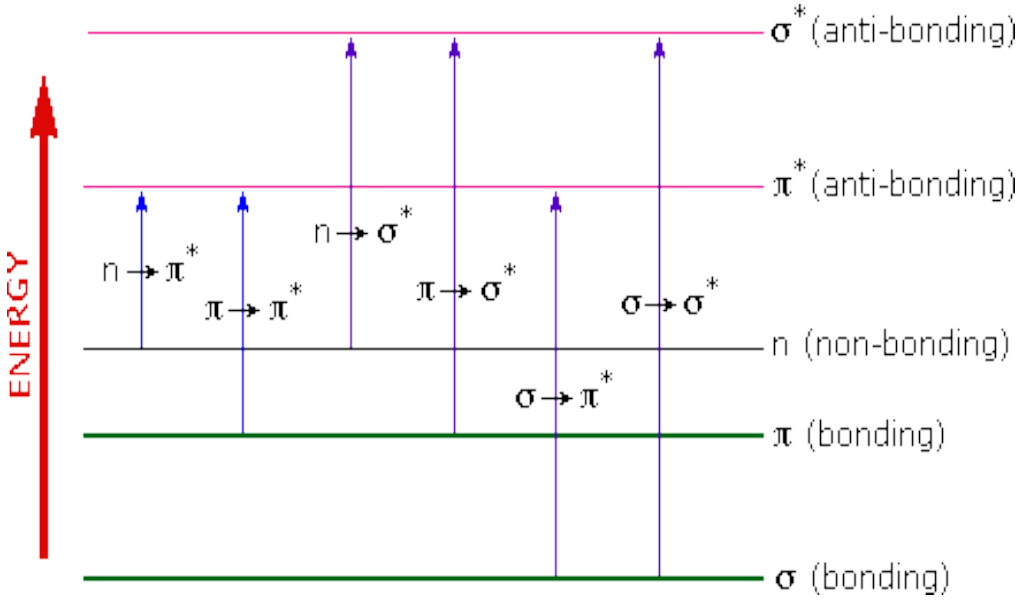

Figure 7.1 - Energy diagram depicting various electronic transitions[3]

Murrel[4] and Jaffe and Orchin[5] explained the theory of transition and gave six different types of transitions that can occur when a molecule absorbs energy. Some of the light energy is absorbed when a sample's molecules are exposed to light having an energy which is similar to the electronic transition within the molecule. As a consequence, the electron is promoted to a higher energy level. When the energetically favored electron transition takes place from the highest occupied molecular orbital (HOMO) to the lowest unoccupied molecular orbital (LUMO), the resulting state of the electron is called an excited state[3, 4, 5]. Transitions occurring between bonding and anti-bonding orbitals are termed as N→V transitions. It includes $\sigma \rightarrow \sigma^*$ and $\pi \rightarrow \pi^*$ transitions under this class. Transitions occurring between non-bonding and anti-bonding orbitals are termed as N→Q transitions. It includes $n \rightarrow \sigma^*$ and $n \rightarrow \pi^*$ transitions under this class. Transitions occurring between ground state and one in a higher energy orbital are termed as N→R transitions. It includes $\pi \rightarrow \sigma^*$ and $\sigma \rightarrow \pi^*$ transitions under this class. The most commonly found transitions in the UV-Visible region are $n \rightarrow \pi^*$ and $\pi \rightarrow \pi^*$[4,5]. The ultraviolet-visible (UV-Vis) absorption spectroscopy technique is complementary to fluorescence spectroscopy. Ultraviolet-visible (UV-Vis) absorption spectroscopy deals with transitions from ground state to the excited state, whereas fluorescence spectroscopy deals with transitions from the excited state to the ground state[1]. A UV-Vis spectrometer records the absorption wavelengths of sample molecules as well as the degree of absorption at each wavelength. Therefore, by applying the Beer-Lambert law the concentration of a sample molecule can be determined[4, 5].

7.2 Beer-Lambert Law

The Beer-Lambert law states that the light absorbance in a solution is directly proportional to the concentration of absorbing species when the length of the light path is fixed and directly proportional to the light path when the concentration is fixed[1]. A quantitative analysis which uses absorption of radiation, considers one or the other relationships given above[6]. The Beer-Lambert Law is given as:

$$A = - \log_{10}(I/I_0) = \varepsilon.c.l \qquad \text{Eqn. 7.1}$$

where (A) is the measured absorbance, (I) is the intensity of transmitted light, (I_0) is the intensity of the incident light at a given wavelength, (ε) is a molar absorptivity constant or extinction coefficient which is wavelength dependent, (c) the concentration of the analyte and (l) the pathlength through the sample[1].

The presence of an analyte in the solution being measured gives a response peak whose height corresponds to the analyte concentration in the solution. To obtain accurate results, the response to the analyte is compared with the response to a standard. Two absorption curves (one of the analyte and the other of the standard) can only be compared if the same solvent was used for both the experiments. UV-Vis spectroscopy can therefore be used for the determination of the concentration of an analyte in solution. Thus, UV-Vis spectroscopy is applicable to dissolution experiments[1, 4].

Beer's law also applies to a solution where more than one kind of absorbing species are involved. In order to apply Beer's law to such solutions there should be no interaction

between the various species[7]. For a multi-component system, the total absorbance is given by:

$$A_{total} = A_1 + A_2 + ……..+ A_n \quad \text{Eqn. 7.2}$$

$$A_{total} = \varepsilon_1 bc_1 + \varepsilon_2 bc_2 + ……..+ \varepsilon_n bc_n \quad \text{Eqn. 7.3}$$

Where the subscript 1, 2,……n refers to the absorbing species[7].

7.3 Instrumentation –

A UV-Vis spectrophotometer consists of four basic parts namely: (1) light source; (2) monochromator or diffraction grating; (3) absorption cell assembly and (4) detector[8]. A light source typically used for measurement in the UV region is the deuterium arc lamp (190-400 nm) or hydrogen discharge lamp. Whereas, for measurement in the visible and near IR region, A tungsten filament lamp (300-2500 nm) is used. A xenon arc lamp and light emitting diodes are used today for the measurement in the visible region. The detector commonly used in UV-Vis spectrophotometery is the photodiode array detector or a Charge Coupled Device (CCD)[9]. Spectrophotometers used are of two types, which are either a single beam spectrophotometer or a double beam spectrophotometer. In the single beam spectrophotometer, all the light from the source is allowed to pass through the sample cell. Here, the intensity of the incident light at a given wavelength is obtained by removing the sample. In the double-beam spectrophotometer, the light coming from the source is split into two separate beams before it reaches the sample. One of the beams is allowed to pass through the sample and the other is used as a reference[5, 8].

A schematic representing a double beam UV-Vis spectrophotometer is seen in Figure 7.2. At low pressure the light source bombards the radiation in the direction of the collimating mirror. The collimating mirror further transmits the radiation in a parallel path which then passes through the entrance slit. It is then separated into constituent wavelengths by a diffraction grating.

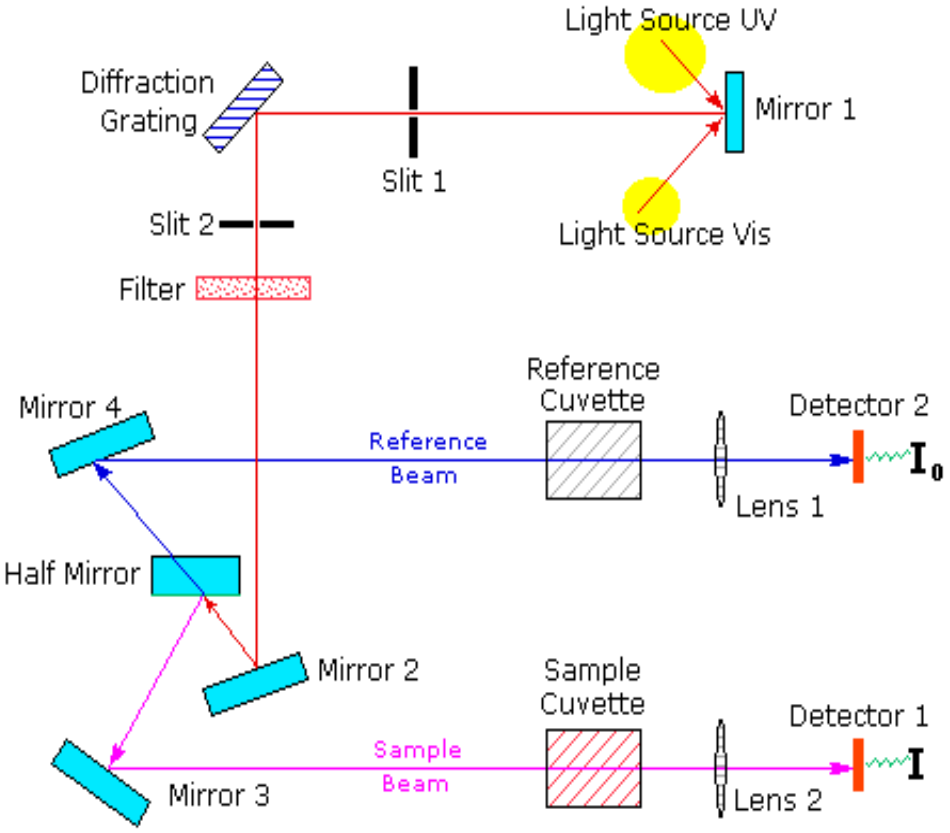

Figure 7.2 - Schematic of a double beam UV-Vis spectrophotometer[3]

The radiation of a particular wavelength then passes through another slit to limit the intensity and the spectral width. After passing through the filter, a beam then divides it into two separate beams by mirrors. One of the beams passes through the reference and

other beam passes through the sample. The relative intensity of the radiation transmitted by the sample is then measured by the detector[5, 7, 8].

Some double-beam spectrophotometers use two detectors, therefore the measurement of the sample and reference beam at the same time is possible. Some other spectrophotometers have two beams which pass through a beam chopper, which functions by blocking one beam at a time. Here the detector performs by alternating between the measurement of the sample beam and measurement of the reference beam[7, 8]. Samples used in the UV-Vis spectrophotometer are usually placed in a transparent unit, known as a cuvette. Fused silica and quartz glass, which are transparent through the UV, visible and near IR region, are used to make cuvettes. Glass and plastic cuvettes are also used, but they have a limitation. Glass and most plastics cannot absorb in the visible region. Liquid samples are mostly used for UV/Vis spectrophotometry measurement. Gases and solid samples can also be measured using UV/Vis spectrophotometry[10].

7.4 Application –

UV-Vis spectroscopy may not provide unambiguous identification of an organic compound and therefore possess a very limited application in the qualitative analysis of organic compounds. However, absorption measurement in the ultraviolet and visible regions by the UV-Vis spectrophotometer detects the presence of certain functional groups which acts as chromophores[11]. Solvent polarity and pH have the potential to affect the absorption spectrum of a compound and have been used for identification of functional groups[9]. Displacement of a weak absorption band in the region of 280-290 nm towards shorter wavelengths with increasing solvent polarity is indicative of the

presence of carbonyl groups. Confirmation of the presence of an aromatic amine or phenolic groups in the structure of a compound can be obtained by observing the effect on the spectra of solutions containing a sample with a change in pH[11].

UV-Vis spectroscopy has been used extensively for the quantitative determination of solutions containing highly conjugated organic compounds as well as transition metal ions. A number of inorganic, biochemical and organic species absorb in the ultraviolet and visible region and are susceptible for direct determination[9, 10, 12].

UV/Vis absorption spectroscopy is highly sensitive and is able to perform the analysis for concentrations in the range of 10^{-4} to 10^{-5} M. Spectrophotometric measurements are performed rapidly and easily with modern instruments[12]. The experiments are conducted with moderate to high selectivity and good accuracy with relatively minimaal error in the range of 1-3% which can be further reduce by applying special techniques[12].

Chapter Eight

Dissolution Testing

8.1 Introduction

Bioavailability of drugs and bioequivalence studies between two drugs is a topic of prime importance over the past few years. This led to the development of a process called dissolution testing. Dissolution testing is used for screening new product, monitoring the process of manufacturing as well as the formulation of products and to perform bioequivalence studies between different batches of product[1, 2]. Dissolution testing is also used to determine the physicochemical consistency of the product from batch to batch since it is an inexpensive indicator. In order to determine the bioequivalence of the product and its overall pharmacological action, data obtained from dissolution rate experiments are extensively used[3].

Dissolution rate is defined as, "The amount of drug substance that goes into solution per unit time under standardized conditions due to liquid/solid interface, temperature and media composition[4]." Dissolution is the process by which a solid or a liquid sample forms a homogenous mixture with the solvent (solution)[5, 6]. Dissolution is governed by the affinity between the solvent and the solid sample (drug)[4]. When a solid dosage form is administered into body, it enters the gastrointestinal tract where the intact solid dosage form disintegrates into granules which are then further converted to fine particles[7]. The drug in the form of fine particles begins to dissolve in the biological media. The dissolved drug is then absorbed into the systemic circulation. The process of disintegration,

deaggregation and dissolution may occur simultaneously with the release of the drug from its delivery form[4] as seen in Figure 8.1.

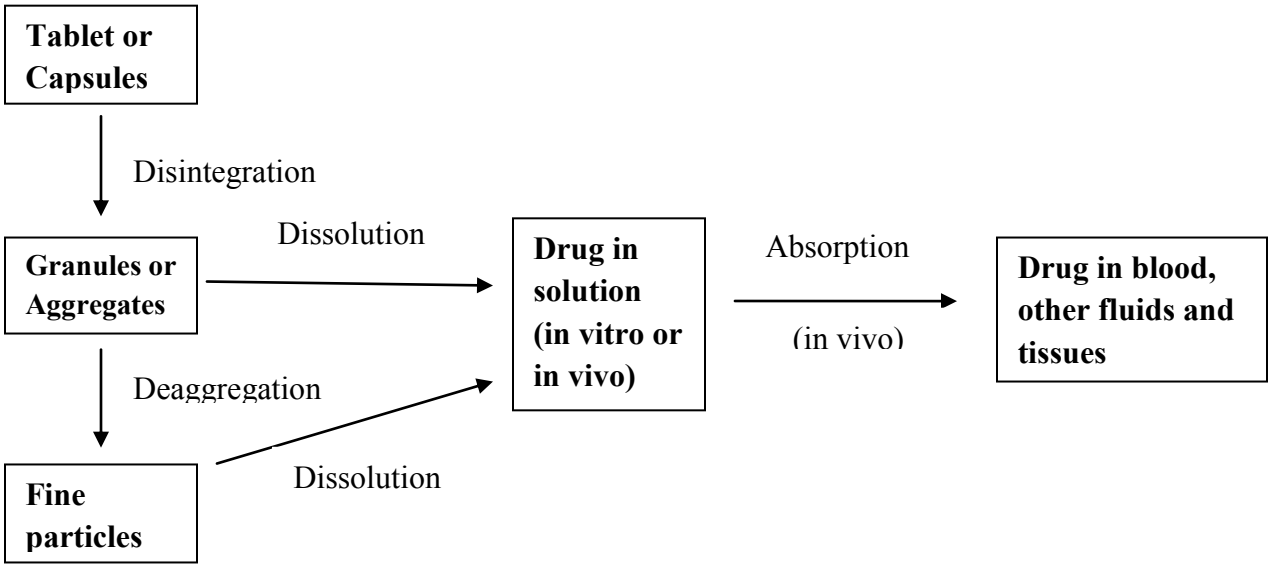

Figure 8.1 – Schematic for the Disintegration, Deaggregation and Dissolution stages as the drug leaves a tablet or a granular matrix[7]

Various physicochemical processes of the dosage form such as physical characteristics, wettability, disintegration and deaggregation, penetrability into the dissolution medium, and the swelling process among others governs the dissolution rate of the drug[4].

A scheme involving the following steps depict the release of the drug from the dosage form as proposed by Carstensen[3]:

1. Initial mechanical lag
2. Wetting of the dosage form
3. Penetration of the dissolution medium into the dosage form
4. Disintegration
5. Deaggregation of the dosage form and dislodgement of the granules

6. Dissolution
7. Occlusion of some particles of the drug

In order to obtain the pharmacological action from a drug, its dissolution rate of a drug becomes one of the most important governing parameters. The drug dissolution step is the rate limiting step for drugs with poor solubility for determining their absorption into the circulatory system[1].

Noyes-Whitney[8] proposed a mathematical expression for the dissolution rate which is given by the following equation:

$$dC/dt = K(C_s - C_t) \qquad \text{Eqn 8.1}$$

Nernst and Brunner[7] further modified this equation and is represented as:

$$\frac{dM}{dt} = \frac{D.A}{h}(C_s - C_t) \qquad \text{Eqn 8.2}$$

where K = dissolution constant; C_s = concentration of saturated solution; C_t = concentration of solution after time (t); M = mass of solid material at time (t); D = diffusion coefficient; A = area available for mass transfer and h = thickness of the diffusion layer.

8.2 Methods for dissolution testing

The USP XXX[9] and BP[10] provides for four types of dissolution apparatii which includes the rotating basket, paddle, reciprocating cylinder and flow through cell. The

most common dissolution methods used among these four dissolution apparatus are the rotating basket and the paddle.

8.2.1 USP Apparatus 1 (Rotating Basket Apparatus)

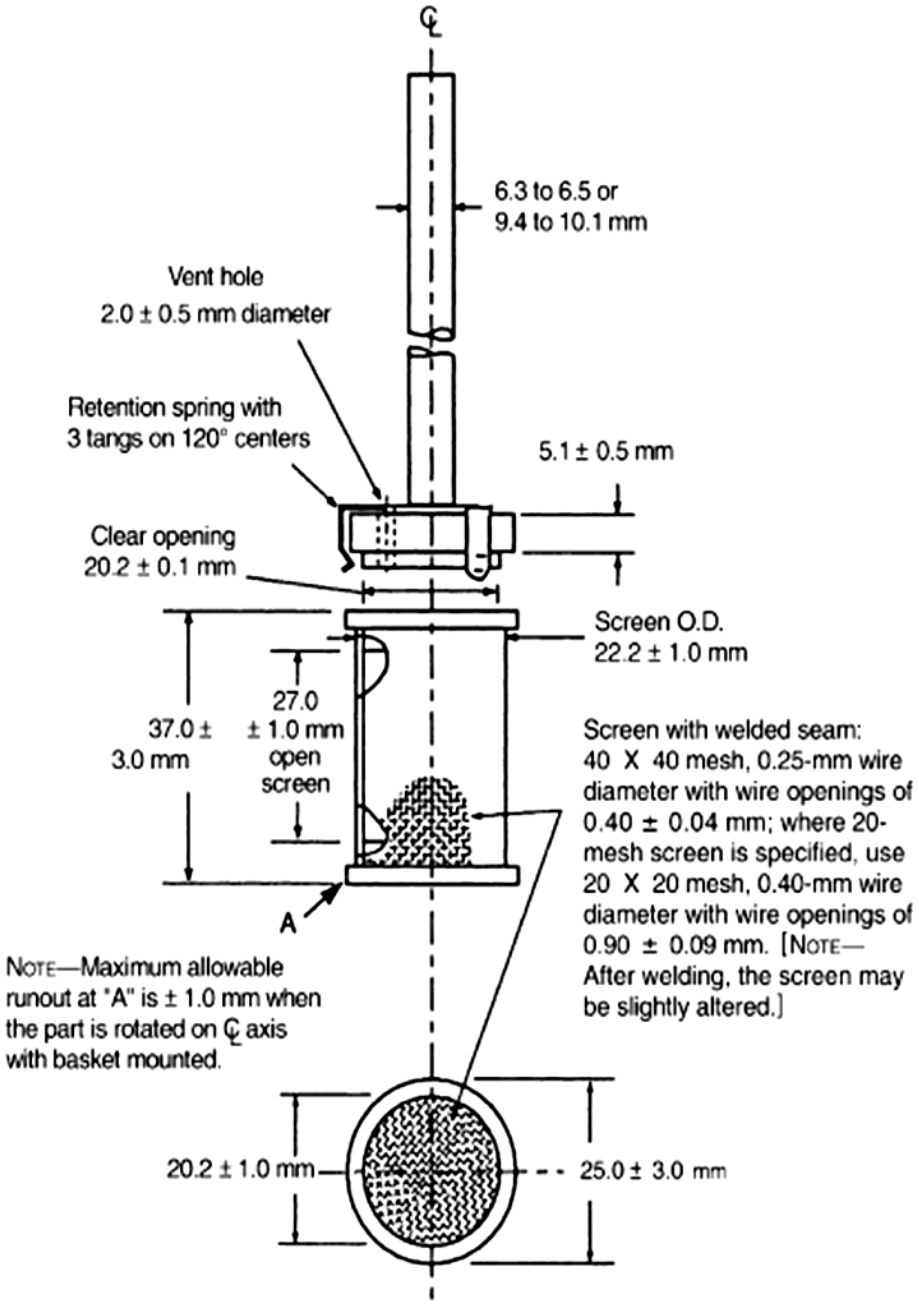

Figure 8.2 – USP Apparatus 1- Basket Stirring Element[9]

The assembly for Apparatus 1 (rotating basket) consists of a cylindrical basket, a covered vessel made of glass or other inert transparent material, a motor, a metallic drive shaft as seen in Figure 8.2. The vessel in Apparatus I is partially immersed in a water bath system of appropriate size. The water bath is heated with the help of a heater which has a capability to hold the temperature at 37 ± 0.5 ^{0}C inside the vessel. The apparatus is made of stainless steel, type 316 or other inert material. It is approximately one inch in diameter, 1-3/8 inch in height and the 40 mesh wire. The basket is rotated at a constant speed within a range of 25 to 250 rpm. The basket is then immersed in the dissolution media of about 900 ml in the vessel with the capacity of 1000 ml. During the experiment a distance of 25±2 mm is maintained between the bottom of the basket and the inside bottom of the vessel[9].

8.2.2 USP Apparatus 2 (Paddle Apparatus)

The assembly for Apparatus 2 (paddle) is similar to the assembly for Apparatus 1 (rotating basket) in several aspects, except that a paddle formed from a blade and a shaft replaces the basket[9]. Figure 8.3 provides the compendial specification for the USP Type II apparatus. The shaft in apparatus 2 is positioned in such a way that its axis is not more than 2 mm from the vertical axis of the vessel at any point. It should be able to rotate smoothly without creating any significant wobble which may affect the results. Before starting the apparatus for the experiment, the sample is allowed to settle to the bottom of the vessel[9].

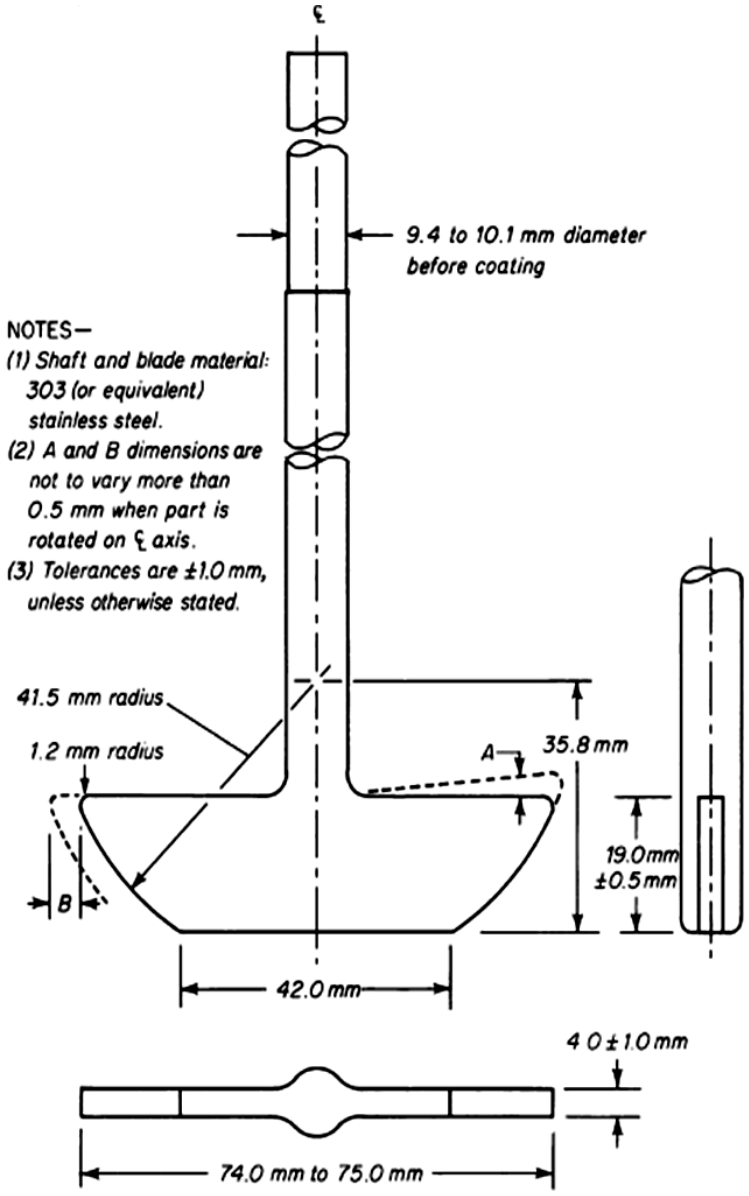

Figure 8.3 – USP Apparatus 2 - Paddle Stirring Element[9]

8.2.3 USP Apparatus 3 (Reciprocating Cylinder)

The assembly for Apparatus 3 (reciprocating cylinder) consists of a set of glass vessels which are cylindrical and flat-bottomed. It also consists of a set of reciprocating cylinders made up of glass and screens that are made of a suitable nonreactive material which are

designed to fit the tops and bottoms of the reciprocating cylinders. In addition, it consists of a motor and drive assembly which has the function of reciprocating the cylinders vertically as well as horizontally as per the assay[9]. Figure 8.4 provides all the specifications and details associated with USP Apparatus 3. The vessels in Apparatus 3 are partially immersed in a water bath system of convenient size. The water bath is heated with the heating system to hold the temperature at 37 ± 0.5 ^{0}C inside the vessel[9].

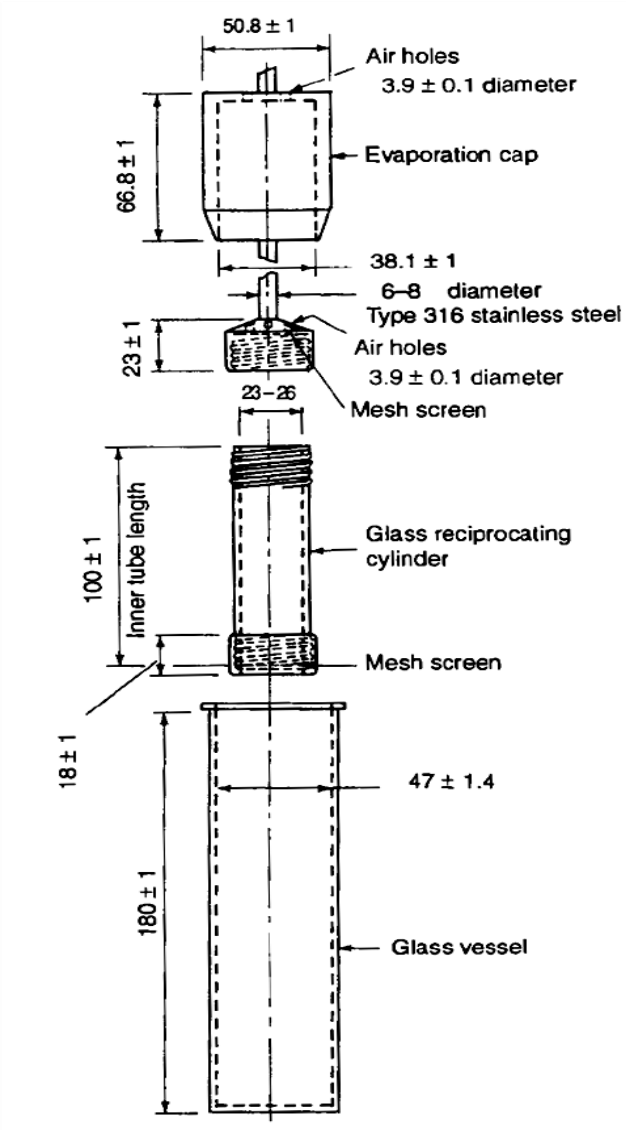

Figure 8.4 – USP Apparatus 3 - Reciprocating Cylinder[9]

8.2.4 USP Apparatus 4 (Flow-Through Cell)

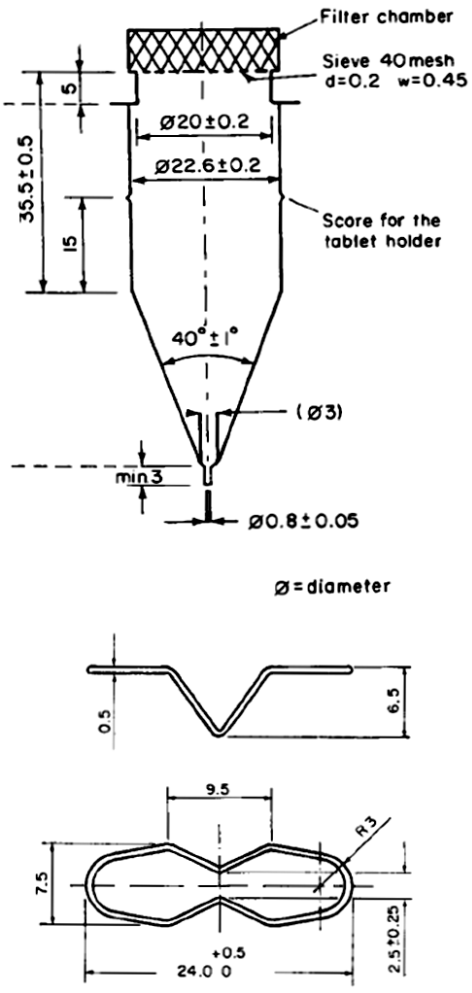

Figure 8.5 – USP Apparatus 4 - Large cell for tablets and capsules (top), Tablet holder has a large cell (bottom)[9]

The assembly for Apparatus 4 (flow-through cell) consists of a flow-through cell which is made up of an inert and transparent material which is mounted vertically with a filter system in order to prevent the escape of undissolved particles from the top of the cell. In addition, it has a reservoir and a pump for pumping the dissolution medium in an upward

direction in the cell at a rate of 240 ml to 960 ml per hour with standard flow rates of 4, 8 and 16 ml per minute. The flow profile obtained is sinusoidal in nature with a pulsation of 120 ± 10 pulses per minute. It also consists of a water bath system that maintains the temperature of the dissolution medium at 37 ± 5^0 C. The flow through cell is around 12 and 22.6 mm in diameter and has a cone which is filled with small glass beads of about 1 mm in diameter. In order to provide protection to the fluid entry tube, one bead of about 5 mm placed at the apex[9].

8.3 Factors Affecting Dissolution Rate

The rate of dissolution is governed by various factors including[11]:

1. Properties of the solute - chemical structure, solubility and crystallinity
2. Properties of the solvent - pH, viscosity, surface tension, buffering capacity, chemical structure and ionic strength.
3. Conditions for dissolution - temperature, ratio of liquid volume to solid volume, flowability of the liquid around the solid surfaces and the intensity of fluid mixing.

Chapter Nine

Materials and methods

9.1 Materials :

9.1.1 Mefenamic acid

9.1.1.a Introduction

Source: Spectrum Chemical Mfg Corp, Lot # SF1673, CAS no: 61-68-7

Chemical Name: Benzoic acid, 2-[(2,3-dimethylphenyl)amino]- ; N-(2,3-Xylyl) anthranilic acid[1]

Empirical Formula: $C_{15}H_{15}NO_2$[1]

Molecular Weight: 241.29[1]

Structural Formula:

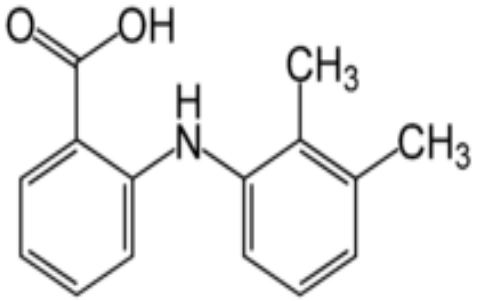

Figure 9.1 Structure of Mefenamic acid[2]

9.1.1.b Physical Properties

Appearance: White to off-white, crystalline powder that darkens on prolonged expose to light[1].

Odor and Taste: Odorless, initial taste is very mild but aftertaste is bitter[1].

Apparent pKa: 4.2[3].

Melting Point: 227 ºC – 232 ºC[1]

Solubility: Insoluble in water; sparingly soluble in chloroform and ether. 1 g in 220 ml alcohol is completely soluble[1].

9.1.1.c Pharmacodynamics

Mefenamic acid is a non-steroidal anti-inflammatory drug with anti-inflammatory, analgesic and anti-pyretic properties[4]. Chemically it belongs to the anthranilic acid derivatives class[5]. Mefenamic acid inhibits the enzyme cyclooxygenase (COX) to exert its anti-inflammatory effect and inhibits the synthesis of prostaglandin to produce analgesic action[4]. Mefenamic acid produces both central and peripheral analgesic action. It is a nonselective COX inhibitor, which inhibits both the COX-1 enzyme and COX-2 enzyme[5]. Its anti-inflammatory, analgesic and antipyretic activity are mainly considered to be obtained through COX-2 enzyme inhibition. On the other hand, unwanted effects on the GI mucosa are considered to be caused by COX-1 enzyme inhibition[6].

9.1.1.d Uses, Side effects and contraindication

Mefenamic acid is indicated for the treatment of mild to moderate pain, primary dysmenorrhea, dental extractions, menstrual cramps, muscle ache and athletic injuries[1, 7, 8]. Diarrhea is the most important dose related side effect and haemolytic anaemia is a rare but serious complication. Other untoward effects include thromobocytopenia purpura, bone-marrow hypoplasia, leucopenia, pancytopenia agranulocytosis, gastrointestinal discomfort, dizziness, headache, vomiting, urticaria, rashes and other CNS manifestations[1, 5, 8]. Mefenamic acid is contraindicated in children under the age of 14 years, patients suffering from upper or lowers intestinal tract ulcer, pregnant women and patients having hypersensitivity to the drug[1, 8].

9.1.1.e Available dosage forms and doses[1, 2, 9]

Marketed dosage forms include: Ponstel®, Ponstan®, Meftal® and Medol®.

Dosage form: Capsule, Suspension and Syrup.

Dose: For adults and children above 14 years of age, the usual dose is 500 mg initially and repeat using 250 mg every 6 hours, if needed.

9.1.2 Diflunisal

9.1.2.a Introduction

Source: Spectrum Chemical Mfg Corp, Lot # TE1230, CAS no:22494-42-4

Chemical Name: [1,1'-Biphenyl]-3-carboxylic acid, 2',4'-difluoro-4-hydroxy-, Dolobid® (MSD)[10].

Empirical Formula: $C_{13}H_8F_2O_3$[10]

Molecular Weight: 250.20[10]

Structural Formula:

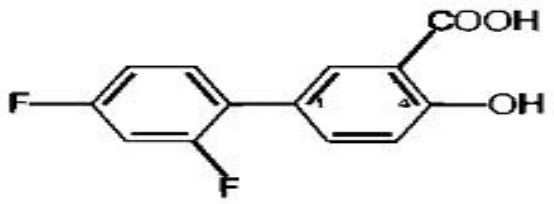

Figure 9.2 - Structure of Diflunisal[11]

9.1.2.b Physical Properties

Appearance: White crystalline powder[10]

Apparent pKa: 2.9[12]

Melting Point: 210 ºC[10]

Solubility: Sparingly soluble in water, soluble in dilute aqueous base and in most organic solvents[10].

9.1.2.c Pharmacodynamics

Diflunisal is a non-steroidal anti-inflammatory drug with anti-inflammatory, analgesic and anti-pyretic properties. Chemically it belongs to the salicylic acid derivatives class[13]. Diflunisal is a reversible inhibitor of enzyme cyclooxygenase-1

and 2 which leads to a decrease in production of prostaglandin precursor. Thus, diflunisal acts by inhibiting the production of prostaglandin , a hormone which is involved in inflammation and pain[13,14].

9.1.2.d Uses, Side effects and contraindication

Diflunisal is indicated for the management of mild to moderate pain[10]. It is commonly used to treat pain, swelling and stiffness associated with osteoarthritis[15]. It is also used for the treatment of acute pain following oral surgery, especially after the removal of wisdom teeth[16]. The most prominent side effects caused by diflunisal are gastrointestinal pain, diarrhea and dyspepsia. Other common side effects include headache, nausea, dizziness and rashes. Diflunisal is contraindicated in patients with a previous history of acute asthmatic attack, urticaria or rhinitis being precipitated by aspirin[10, 17, 18, 19].

9.1.2.e Available dosage forms and doses

Marketed dosage forms include: Dolobid®[20]

Dosage form: Tablets[10]

Dose: For the management of mild to moderate pain, the usual adult dose is 1000 mg followed by 500 mg every 12 hours. For the treatment of Osteoarthritis pain, the usual adult dose is 500 to 1000 mg daily in two divided doses. The dose should not exceed 1500 mg per day[10,16].

9.1.3 Gelucire 50/13®

9.1.3.a Introduction

Source: Gattefosse´ (France) Lot # 106058 Pastilles

Chemical Name: Stearoyl Macrogolglycerides EP, Stearoyl Polyoxylglycerides USP/NF[21].

Gelucire 50/13® is described as a well-defined mixture of mono- and di-fatty esters of polyethylene glycol and mono-, di- and triglycerides. It is manufactured from both vegetable and petrochemical origins[22].

9.1.3.b Physical Properties[22]

Appearance: Roughly white, waxy solid.

Odor: Faint

Melting Point: Melting initiate around 50^0C and complete melting is observed between 60-80^0C.

Solubility: Dispersible in water, soluble in chloroform and methylene chloride, insoluble in ethanol and mineral oils.

9.1.3.c Uses and Toxicity[22]

Gelucire 50/13® is used as an excipient for hard gelatin capsules. Gelucire 50/13® is also used as a controlled-release agent and bioavailability enhancer. Due to its high melting point it controls the rate of release of active pharmaceutical ingredients. It is

used to increase the solubility of poorly soluble drugs. A liquid can be formulated as a solid dosage form with Gelucire 50/13®. Gelucire 50/13® can be used to handle toxic drugs, low density products and low dose active drugs. It provides protection to drugs against hydrolysis and oxidation.

Acute toxicity was observed in rats when given by oral route where the Loading dose exceeded 20 g/kg.

9.1.4 Neusilin US2®

9.1.4.a Introduction

Source: Chemical Industry Co, Ltd Japan. Lot # 901001

Chemical Name: Magnesium aluminometasilicate[23].

Empirical Formula: $Al_2O_3.MgO.\ 7SiO_2.xH_2O$[23]

Neusilin® is a synthetic, amorphous form of Magnesium alumino metasilicate. Being a multi functional excepient, it can be used for wet granulation of solid dosage forms as well as for direct compression of solid dosage forms. In pharmaceutical preparations, Neusilin® is widely used to improve the quality of tablet, granules, suspensions, powders, capsules and ointment dosage forms[23].

9.1.4.b Physical Properties[24,25]

Appearance: White amorphous granule.

Solubility: Practically insoluble in water and ethanol.

Composition (%) on dried basis: Al_2O_3 (29.1-35.5), MgO (11.4-14.0), SiO_2 (29.2-35.6).

Loss on drying (%) 110 ºC for 7 hours: less than 7 %

True specific gravity: 2.0 -2.2

Specific surface area**:** 300 m^2/g

Particle size distribution**:** <75µ (less than 40%) 75-250µ (more than 60%)

Angle of repose **:** 30°

Water adsorbing capacity (ml/g)**:** 2.4-3.1

Oil adsorbing capacity (ml/g)[*2]**:** 2.7-3.4

Acid consuming capacity(ml/g)[*3]**:** > 210

Apparent specific volume**:** 6.5 ml/g

pH (4% slurry)[*4]**:** 6.0 – 8.0

Toxicity**:** very low toxicity

9.1.4.c Charecteristics

1. Neusilin® has excellent compressibility[26]. It makes hard tablets at low compression force[23].

2. Neusilin® increases the hardness synergy with other filler and binder excipients at low concentrations[23].

3. Neusilin® is stable against heat and has a long shelf life[23, 26].

4. Neusilin® has very good flow enhancing and anticaking properties[25]

5. Neusilin® is neutral, unlike other silicates which exist as either acidic or alkaline with respect to their surface properties[25].

6. Neusilin® is amorphous and possesses a very large specific surface area, high oil and water absorption capacity as well as excellent dispersibility[23, 26].

7. Neusilin® is available in different grades which differ in bulk density, water content, particle size, apparent specific volume and pH (4% Slurry). It is selected in accordance with its specific applications[23, 26].

9.1.4.d Uses[27]

1. Neusilin US2® is used as a diluent in solid dosage form.

2. Used as a binder to increase hardness and as a disintergration aid in tablet preparation.

3. Used as a solidifying agent for liquid Active Pharmaceutical Ingredients (API) (Solidifying oil to powder)

4. Used for the stabilization of deliquescent drugs (stabilization of unstable pharmaceutical agent/preparation to moisture).

5. Used as a compounding base as well as dispersing aid.

6. Used as an adsorbing agent.

9.1.5 Potassium Acetate

9.1.5.a Introduction[28]

Source: Fisher Scientific, Lot no:063249, CAS no:127-08-2

Empirical Formula: CH_3COOK

9.1.5.b Physical Properties[28]

Color: Colorless or white crystalline powder.

Taste: Saline and slightly alkaline taste.

Solubility: 1 gm dissolves in 0.5 ml water and 0.2 ml boiling water.

9.1.5.c Uses

It is used as an expectorant as well as a diuretic[28]. A saturated solution of potassium acetate can be prepared to produce a relative humidity of 22.5 ± 0.32% in a sealed chamber[29].

9.1.6 Magnesium Nitrate

9.1.6.a Introduction[30]

Source: Fisher Scientific, Lot no: 083827, CAS no: 13446-18-9

Empirical Formula: $Mg(NO_3)_2$

9.1.6.b Physical Properties[30]

Color: White crystalline powder.

Solubility: 1.25 gm dissolves in 1 ml water.

9.1.6.c Uses

A saturated solution of magnesium nitrate can be prepared to produce a relative humidity of 52.89 ± 0.22% in a sealed chamber[29].

9.1.7 Sodium Chloride

9.1.7.a Introduction[31]

Source: Mallinckrodt Chemical Works, St. Louis

Empirical Formula: NaCl

9.1.7.b Physical Properties[31]

Color: Colorless or white crystalline powder.

Odor: Odorless

Taste: Saline

Solubility: 1 gm dissolves in 2.8 ml water and in 10 ml of glycerine.

9.1.7.c Uses

Used for its electrolyte replenishment therapy[31]. A saturated solution of sodium chloride can be prepared to produce a relative humidity of 75.29 ± 0.12% in a sealed chamber[29].

9.1.8 Deionized Water

Deinized water can be used to produce a relative humidity of 100% in a sealed chamber[29]. It was obtained from University of Toledo sources.

9.2 Methods

9.2.1 Preparation of Solid Dispersion Granules

The hot melt granulation method was used to prepare ternary phase solid dispersion granules of the drugs. Gelucire 50/13® was used as the dispersion carrier and Neusilin US2® was used as the adsorbent along with the drug to prepare ternary phase solid dispersion granules. For the preparation of the solid dispersion, the drug, Gelucire 50/13® and Neusilin US2® were used in the ratio of 1:1:1.5. Gelucire 50/13® was first placed in a beaker and heated to a temperature just above the melting point of Gelucire 50/13®. The drug was then added to the molten Gelucire 50/13® and heated with continuous stirring to get a clear molten mixture. The above molten mixture was then added to Neusilin US2® (preheated to 80ºC) with continuous stirring in a dropwise manner over a period of one minute. It was followed by quench cooling by dropping the ternary phase solid dispersion into liquid nitrogen. The ternary phase solid dispersion of drug, mefenamic acid and diflunisal were prepared using Gelucire 50/13® (dispersions carriers) and Neusilin US2® (adsorbent). The granules were sieved through # 20 sieve and stored in a moisture resistant container for further use.

9.3 Instrumentation

9.3.1 Differential Scanning Calorimetry

DSC studies were performed using a Mettler Toledo DSC 822^e with a TS0801RO Sample Robot and a TS0800GCI Gas Controller from Mettler-Toledo. Inc., 1900 Polaris Parkway, Columbus, OH, 43240. It is operated using Star^e Software V8.10. A 3-5 mg sample was weighed on a Mettler MT 5 microbalance and placed into a 100 µL aluminium pan which is further crimped with a lid. The pan was then placed into

the DSC unit along with a similar pan as a reference. The sample was scanned at a heating rate of 10^0C/min from 0 ºC to 260 ºC and purged under nitrogen gas flow rate of 50 ml/min. The DSC was calibrated using indium (5-10 mg) with a melting onset of 156 ± 0.2 ºC as the standard.

9.3.2 X-Ray powder Diffraction (XRPD)

XRPD was performed to observe the physical state of the solid dispersion and to evaluate any interaction between the drug, carrier and adsorbent in solid dispersion. PAN analytical X-Pert Pro V1.6 with X-Pert Data Collector V2.1 software was used equipped with a $CuK_{\alpha 2}$ anode tube and diffractometer of radius 240mm. The XRD scan was performed using BB004 flatstage. The powdered sample was placed in a plastic sample holder of 1 inch square. Data were collected at 45 kV and 40 mA. Samples were scanned from 0-40 $^{\circ}$ 2θ at a step size of 0.0084 and scan rate of 1.00 º/min.

9.3.3 Fourier Transform Infrared Spectroscopy (FTIR)

FTIR spectra were obtained using a PerkinElmer FTIR System with Spectrum GX v 5.0.1 software. A KBr pellet of drug, carrier, adsorbent and the solid dispersion granules was prepared. The sample was dispersed in the KBr and ground using a mortar and pestle. The KBr pellet was prepared by the application of high pressure. Averages of 100 scans of each sample were collected at 4 cm^{-1} resolution over a wavenumber region of 4000-600 cm^{-1}.

9.3.4 Scanning Electron Microscopy (SEM)

The surface characteristics for the drug, carrier, adsorbent and solid dispersion were studied using a scanning electron microscope equipped with JSM 6100. Snappy 4® software was used in order to obtain the digital picture. Double-sided adhesive tape was used to fix the sample onto a brass stub, which was coated in a sputter coater (Denton Vacuum Desk II) under vacuum. The SEM pictures for all samples were taken under a magnification of 100X.

9.3.5 Dissolution Testing

Dissolution studies for the solid dispersion granules were carried out using USP Type II apparatus (Vanderkamp® 600 six spindle dissolution apparatus) at 37 ± 0.5 ºC with a paddle rotation speed adjusted to 50 rpm. A 900 ml portion of buffer at pH 9 (for Mefenamic acid) and pH 7.2 (for Diflunisal) was used as the dissolution medium (in accordance with USP 2002). Moreover, deionized water was also used as the dissolution medium. A sample of pure drug and solid dispersion equivalent to 50 mg were added to the dissolution medium. At each specific interval of time, a 5 ml of sample was withdrawn and filtered through a filter paper. In order to maintain a constant volume of dissolution medium, an equal amount of fresh dissolution medium was replaced immediately. The samples withdrawn were then analyzed using a spectrophotometer at a specific wavelength to determine the amount of drug dissolved.

9.3.6 Ultraviolet-Visible Absorption spectroscopy

A stock solution for each drug was prepared using the appropriate dissolution medium. A calibration curve for each drug was obtained using a serial dilution of stock solution and performing a scan using the UV-Visible Spectrophotometer to determine the maximum absorption wavelength for the drug. UV absorption studies were performed on a Genesys-6® UV Spectrophotometer from Thermo Scientific Inc. A plot of absorption versus concentration resulted in a straight line which was used as a standard curve to determine the solubility of the drug. At fixed wavelength, the samples from the dissolution of the solid dispersion were analyzed to determine the drug concentration from the absorbance values obtained and comparing it to the previously obtained Beer's curve for each drug.

9.3.7 Humidity and Temperature Studies

Solid dispersion granules were subjected to different humidity conditions and different temperature conditions. Solid dispersions were subjected to different temperature conditions namely 25 ºC, 30 ºC, 35 ºC and 40 ºC for 3 months as well as subjected to different humidity conditions namely 22.5% RH, 52.89% RH, 75.29% RH and 100% RH for 3 months. For the humidity study, various saturated salt solutions were prepared to obtain a particular relative humidity within a chamber for the entire time of storage. A saturated solution of potassium acetate was prepared to produce the relative humidity of 22.5 ± 0.32% in the chamber. A saturated solution of magnesium nitrate was prepared to produce the relative humidity of 52.89 ± 0.22% in the chamber. A saturated solution of sodium chloride was prepared to produce the

relative humidity of 75.29 ± 0.12% in the chamber. Pure water was used to produce a relative humidity of 100% in the chamber. The chambers were sealed with paraffin film after the samples were deposited in order to maintain constant relative humidity in the chamber. For the temperature study, samples in a beaker were placed in various ovens which were adjusted to a fixed temperature (i.e. 25 ºC, 30 ºC, 35 ºC and 40 ºC) for the entire time of storage.

Chapter Ten

Results and Discussion

10.1 Diflunisal solid dispersion granules

Ternary solid dispersion granules of Diflunisal were prepared by the hot melt granulation technique using Gelucire 50/13® as the dispersion carrier and Neusilin US2® as the adsorbent. Different ratios of drug (Diflunisal), dispersion carrier (Gelucire 50/13®) and adsorbent (Neusilin US2®) were tried to obtain ternary solid dispersion granules. The ratio of 1:1:1.5 of Diflunisal, Gelucire 50/13® and Neusilin US2® provided the best solid dispersion granules. Therefore, the solid dispersion granules thus obtained were analyzed and characterized by performing DSC, XRPD, FTIR, SEM and dissolution studies. The stability study was performed on the solid dispersion granules by subjecting them to different temperature conditions (25ºC, 30ºC, 35ºC and 40ºC) and different humidity conditions (22.5% RH, 52.89% RH, 75.29% RH and 100% RH) for a period of three months. The solid dispersion granules used in the stability study were characterized by performing XRPD, FTIR and dissolution studies after the first, second and third month.

10.1.1 DSC study

The DSC studies were performed in order to determine the melting point, to observe changes in crystallinity and to detect any possible interaction between the drug (Diflunisal), dispersion carrier (Gelucire 50/13®) and adsorbent (Neusilin US2®). The DSC runs for pure Diflunisal, Gelucire 50/13® (G), Neusilin US2® (N) and Ternary phase solid dispersion is seen in Figure 10.1.

The DSC curve for Diflunisal showed a sharp melting peak at 212.67ºC which corresponds to its melting point. This is indicative of the crystalline nature of the drug. The DSC curve for Neusilin US2® showed no melting peak which indicates the complete amorphous nature of Neusilin US2®. The DSC curve for Gelucire 50/13® showed a peak

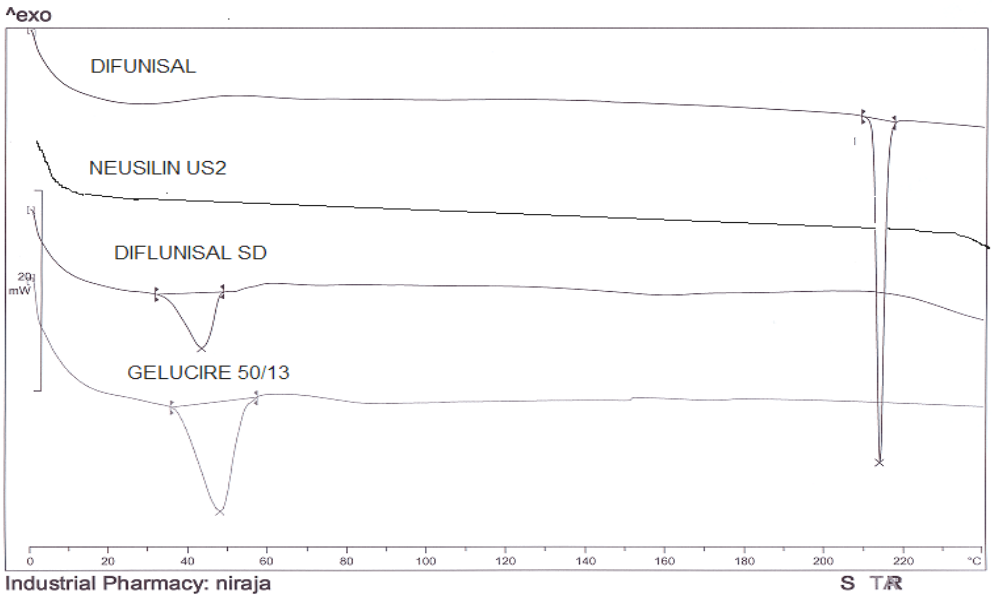

Figure 10.1 - Overlay of the DSC curves for Diflunisal, Neusilin US2®, 1:1:1.5 Dif/G/N Ternary phase Solid Dispersion and Gelucire 50/13®.

at 44.81ºC which corresponds to its melting point. The DSC curve for 1:1:1.5 Dif/G/N (Ternary solid dispersion granules) showed a peak at 42.87 ºC but did not show any peak at 212.67 ºC. The disappearance of the endothermic peak at 212.67 ºC indicates that the drug is dispersed in the carrier, Gelucire 50/13®. Thus the DSC studies indicate the formation of a solid dispersion for Dif/G/N in the ratio of 1:1:1.5 which is evident by the appearance of one peak in the DSC profile for the solid dispersion.

10.1.2 XRPD study

The X-ray powder diffraction studies were performed to determine the study phase analysis and crystalline properties for the drug (Diflunisal), dispersion carrier (Gelucire 50/13®) and adsorbent (Neusilin US2®). X-ray powder diffraction studies were performed to detect any changes in the crystallinity of drug (Diflunisal) in the ternary solid dispersion state. The x-ray diffraction pattern for pure Diflunisal, Gelucire 50/13® (G), Neusilin US2® (N) and Ternary phase solid dispersion (Dif/G/N) is seen in Figure 10.2.

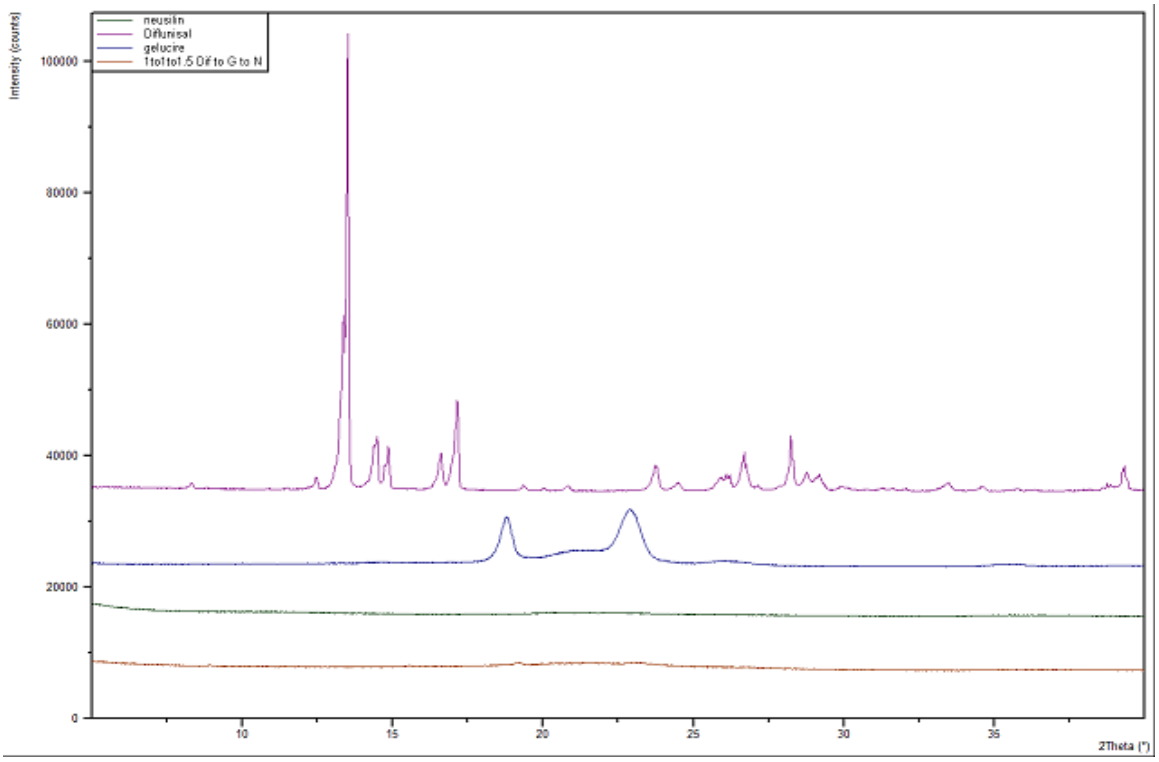

Figure 10.2 - Overlay of the XRPD pattern for Diflunisal, Gelucire 50/13®, Neusilin US2® and 1:1:1.5 Dif:G:N solid dispersion displayed from top to bottom.

Pure drug (Diflunisal) showed numerous peaks which demonstrate the crystalline nature of the drug, whereas Neusilin US2® showed diffused peaks which are indicative of its amorphous nature. Gelucire 50/13® shows few peaks which is indicative of some

crystalline characteristics. The ternary phase solid dispersion for Dif/G/N showed a diffused peak which indicates a significant conversion to the amorphous state on formation of the solid dispersion granules.

XRPD was performed on the solid dispersion granules after the first, second and third month to observe any change in the amorphous characteristic of the ternary phase solid dispersion (Dif/G/N) when subjected to different temperatures and relative humidity conditions. After the first, second and third month, the XRPD pattern for the ternary solid dispersion granules (Dif/G/N) exposed to different temperatures (25ºC, 30ºC, 35ºC and 40ºC) and relative humidity conditions (22.5% RH, 52.89% RH, 75.29% RH and 100% RH), showed no significant change with respect to their XRPD for the ternary solid dispersion granules at the initial stage.

Figures 10.3 and 10.4 represent the overlay of the XRPD profiles for Diflunisal, Gelucire 50/13®, Neusilin US2®, solid dispersion granules of Dif/G/N initially and after one month storage at different temperatures (25ºC, 30ºC, 35ºC and 40ºC) and relative humidity conditions (22.5% RH, 52.89% RH, 75.29% RH and 100% RH), respectively. Figures 10.5 and 10.6 represent the overlay for the XRPD profile for Diflunisal, Gelucire 50/13®, Neusilin US2®, solid dispersion granules of Dif/G/N initially and after two months storage at different temperatures (25ºC, 30ºC, 35ºC and 40ºC) and relative humidity conditions (22.5% RH, 52.89% RH, 75.29% RH and 100% RH), respectively. Figures 10.7 and 10.8 represent the overlay for the XRPD profiles for Diflunisal, Gelucire 50/13®, Neusilin US2®, solid dispersion granules of Dif/G/N initially and after three months storage at different temperatures (25ºC, 30ºC, 35ºC and 40ºC) and relative humidity conditions (22.5% RH, 52.89% RH, 75.29% RH and 100% RH), respectively.

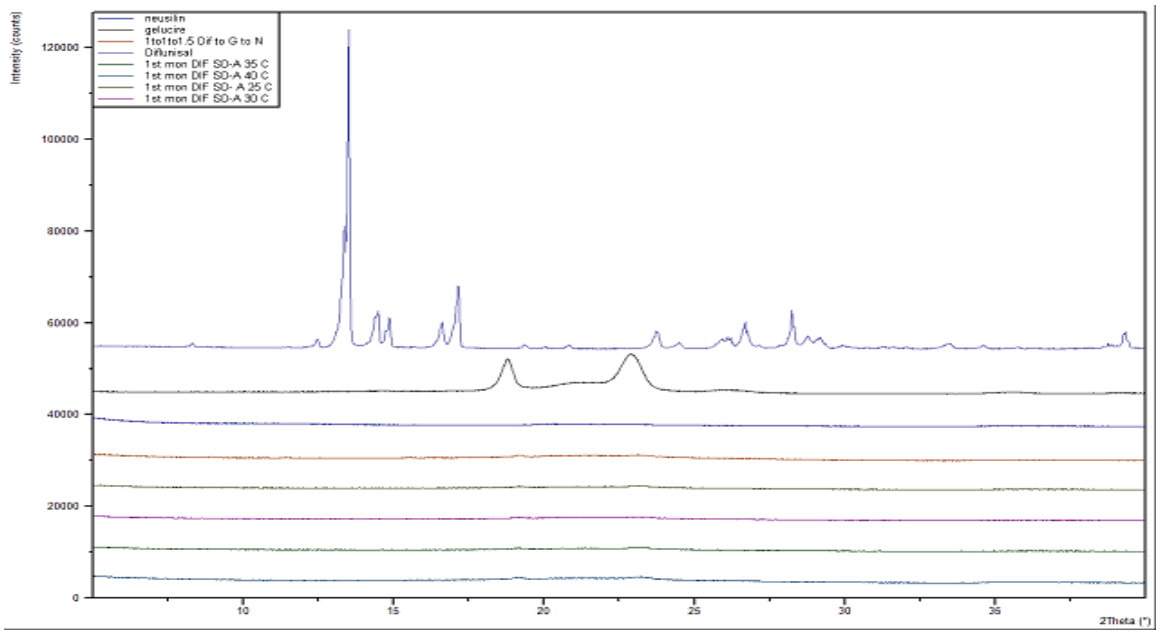

Figure 10.3 - Overlay of Diflunisal, Gelucire 50/13®, Neusilin US2®, 1:1:1.5 Dif:G:N solid dispersion granules initially, at 25ºC, 30ºC, 35ºC and 40ºC after one month, displayed from top to bottom.

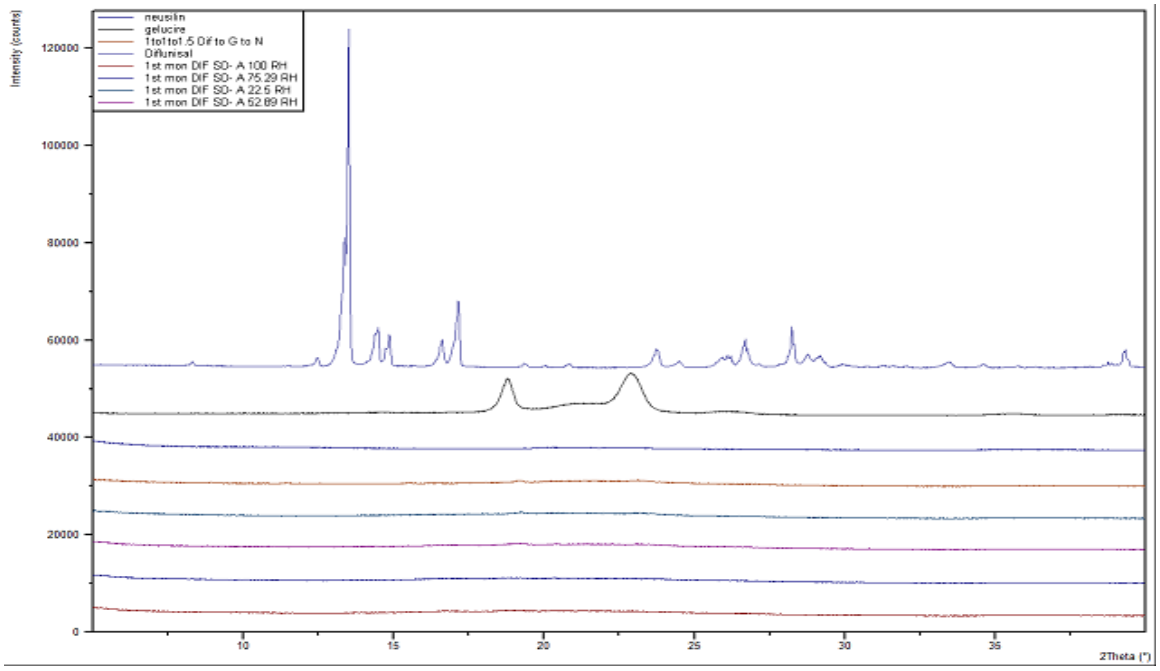

Figure 10.4 - Overlay of Diflunisal, Gelucire 50/13®, Neusilin US2®, 1:1:1.5 Dif:G:N solid dispersion granules initially, at 22.5% RH, 52.89% RH, 75.29% RH and 100% RH after one month, displayed from top to bottom.

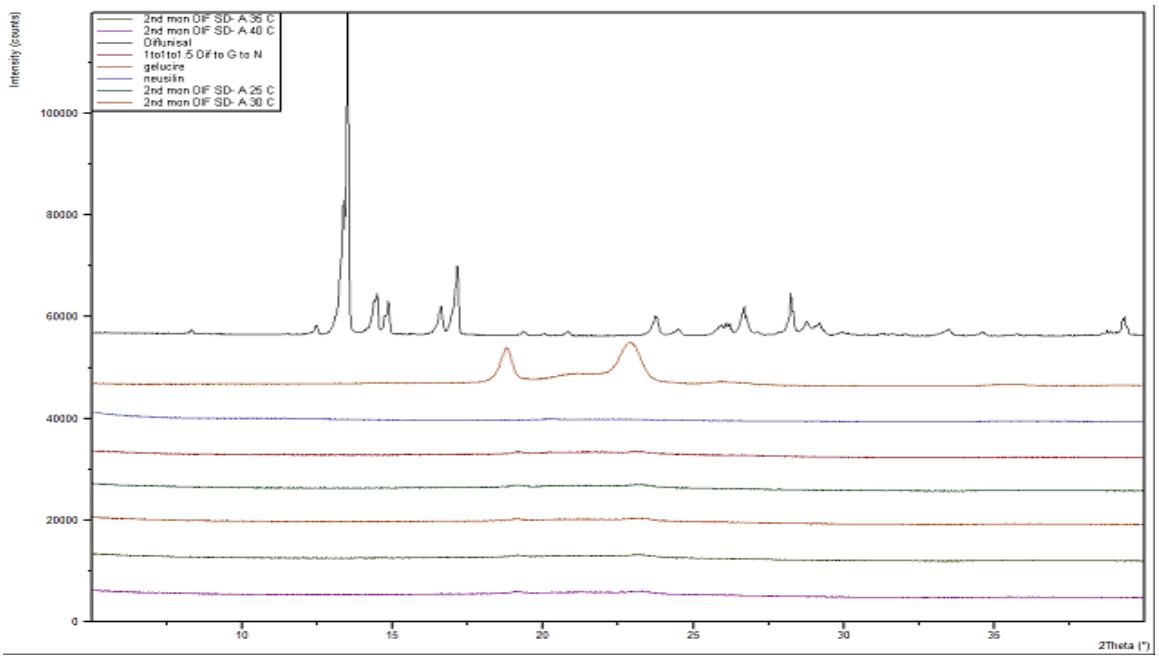

Figure 10.5 - Overlay of Diflunisal, Gelucire 50/13®, Neusilin US2®, 1:1:1.5 Dif:G:N solid dispersion granules initially, at 25ºC, 30ºC, 35ºC and 40ºC after two months, displayed from top to bottom.

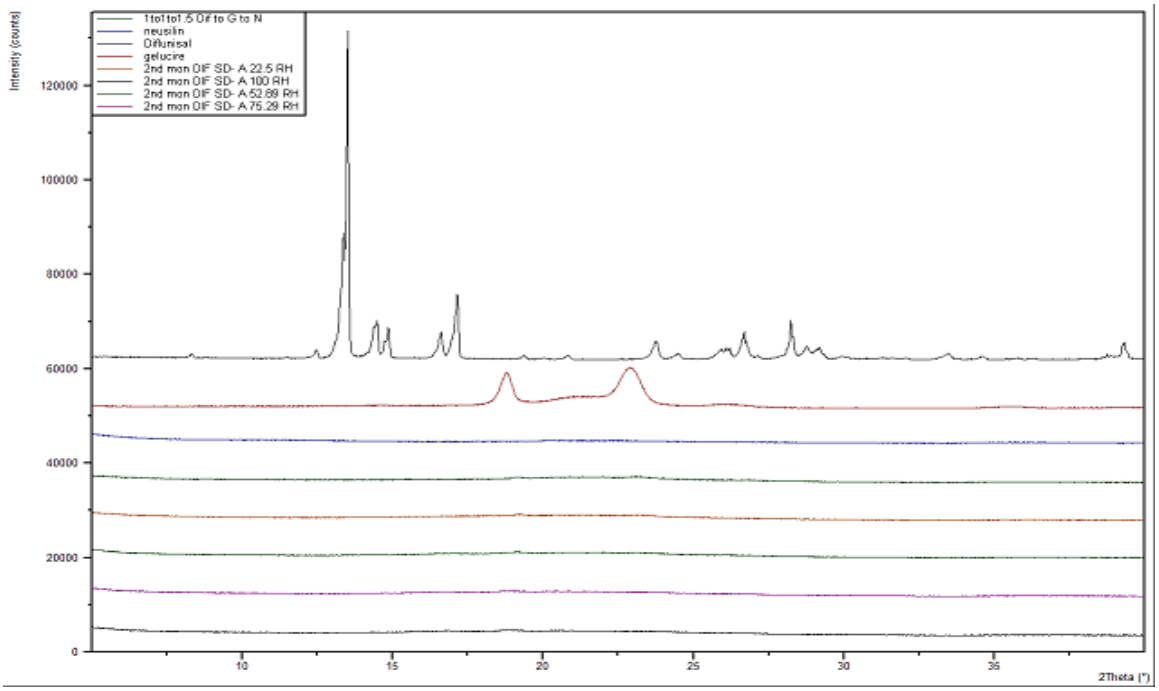

Figure 10.6 - Overlay of Diflunisal, Gelucire 50/13®, Neusilin US2®, 1:1:1.5 Dif:G:N solid dispersion granules initially, at 22.5% RH, 52.89% RH, 75.29% RH and 100% RH after two months, displayed from top to bottom.

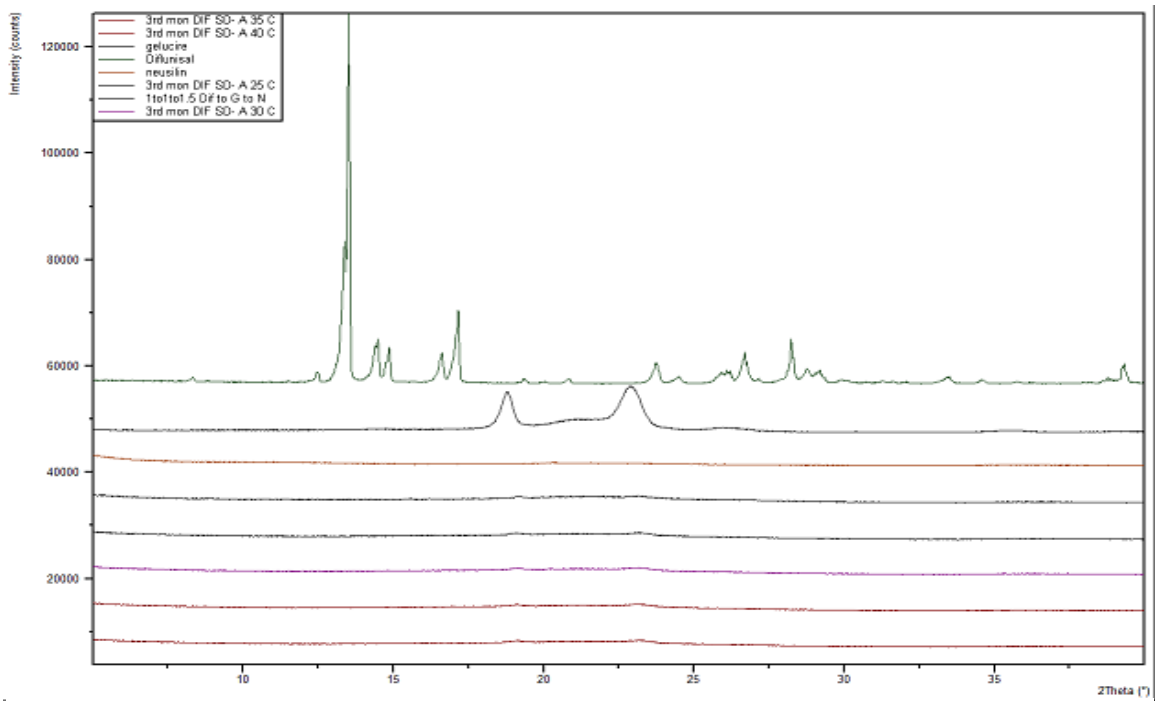

Figure 10.7 - Overlay of Diflunisal, Gelucire 50/13®, Neusilin US2®, 1:1:1.5 Dif:G:N solid dispersion granules initially, at 25ºC, 30ºC, 35ºC and 40ºC after three months displayed from top to bottom.

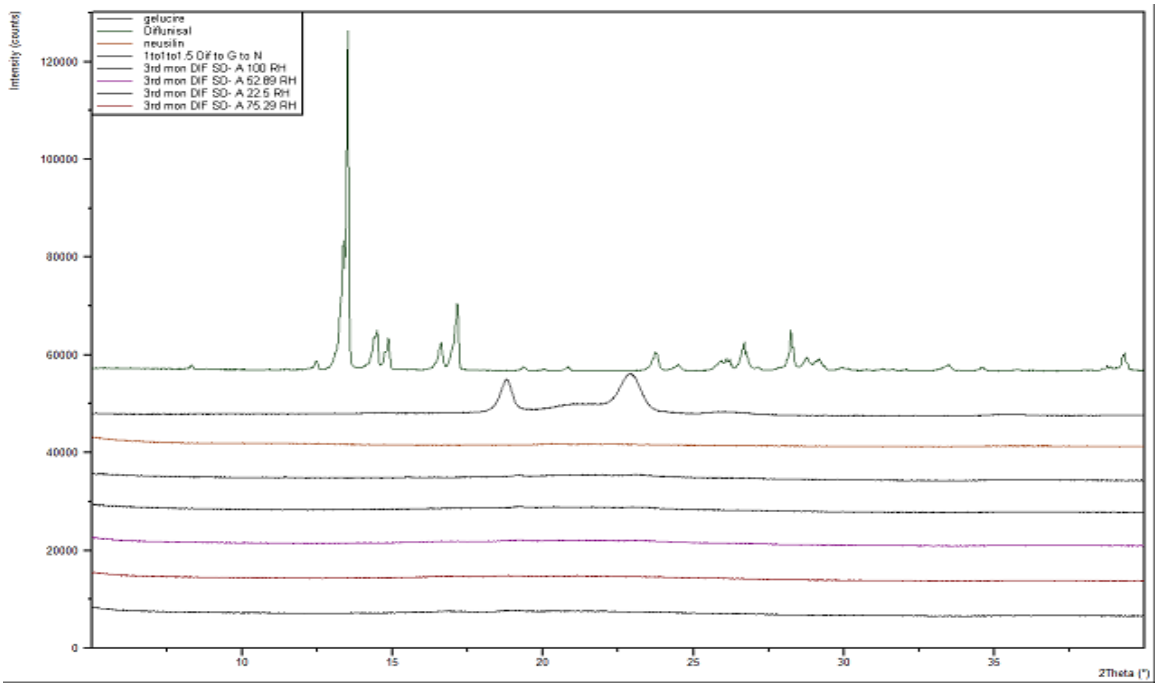

Figure 10.8 - Overlay of Diflunisal, Gelucire 50/13®, Neusilin US2®, 1:1:1.5 Dif:G:N solid dispersion granules initially, at 22.5% RH, 52.89% RH, 75.29% RH and 100% RH after three months, displayed from top to bottom.

10.1.3 FTIR study

FTIR studies were performed to aid the evaluation of any possible chemical interaction between the drug (Diflunisal), dispersion carrier (Gelucire 50/13®) and adsorbent (Neusilin US2®). Moreover, molecular level characterization of the solid dispersions can also be done by FTIR. The FTIR for pure Diflunisal, Gelucire 50/13® (G), Neusilin US2® (N) and Ternary phase solid dispersion (Dif/G/N) as seen in Figure 10.9.

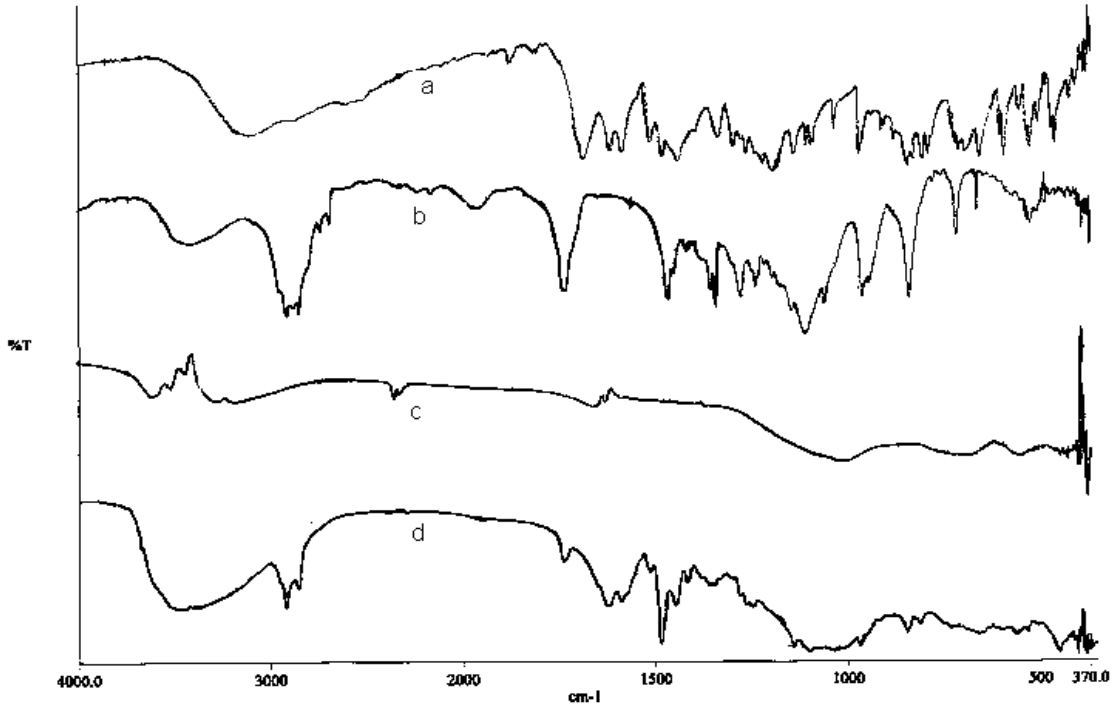

Figure 10.9 - Represents the FTIR spectrum for (a) Diflunisal (b) Gelucire 50/13® (c) Neusilin US2® (d) Ternary solid dispersion granules of Dif/G/N.

The FTIR spectrum for diflunisal shows a distinct broad peak at around 2500-3200 cm^{-1} which is due to the presence of a carboxylic acid moiety in the structure of diflunisal [1,2]. The same also represents the intra- and intermolecular hydrogen bonding due to the –OH groups. The peak at 1650-1750 cm^{-1} is due to the presence of the C=O group [1,2]. The

presence of a peak at 1000 cm $^{-1}$ indicates the presence of a phenyl group [1,2]. The FTIR spectrum for diflunisal shows a distinct peak around 650-700 cm^{-1} due the presence of two C-F groups [1,2].

The FTIR spectrum for Gelucire 50/13® shows a stretching band at 2800-3000 cm $^{-1}$ due to the presence of CH_3 groups. The peak at 1750 cm $^{-1}$ is due to the presence of a C=O group [1,2].

The FTIR spectrum for Neusilin US2® shows the broad stretch band at 3400-3000cm $^{-1}$ which is suggestive of the presence of a secondary amine [1,2].

The FTIR for the ternary phase solid dispersion of Dif/G/N shows a stronger broad peak at 3400 cm $^{-1}$ due to hydrogen bonding (-OH) which is suggestive of a formation of the solid dispersion. The stretch at 2900 cm^{-1} is observed due to the C-H stretching present. The peak at 1000 cm $^{-1}$ indicates the presence of a phenyl group [1,2].

FTIR was performed on the solid dispersion granules after the first, second and third months in order to observe any change in chemical interaction within the ternary phase solid dispersion (Dif/G/N) when subjected to different temperatures and relative humidity conditions. After the first, second and third months, the FTIR study for the ternary solid dispersion granules (Dif/G/N) which were exposed to different temperatures (25ºC, 30ºC, 35ºC and 40ºC) and relative humidity conditions (22.5% RH, 52.89% RH, 75.29% RH and 100% RH), showed no significant change with respect to their FTIR study for the ternary solid dispersion granules from their initial stage.

Figures 10.10 and 10.11 represent the overlay of the FTIR profiles for the solid dispersion granules of Dif/G/N initially and after one month storage at different temperatures (25ºC, 30ºC, 35ºC and 40ºC) and relative humidity conditions (22.5% RH, 52.89% RH, 75.29% RH and 100% RH), respectively. Figures 10.12 and 10.13 represent the overlay of the FTIR profile for the solid dispersion granules of Dif/G/N initially and after two month storage at different temperatures (25ºC, 30ºC, 35ºC and 40ºC) and relative humidity conditions (22.5% RH, 52.89% RH, 75.29% RH and 100% RH), respectively. Figures 10.14 and 10.15, represent the overlay of the FTIR profile for the solid dispersion granules of Dif/G/N initially and after three months storage at various temperatures (25ºC, 30ºC, 35ºC and 40ºC) and relative humidity conditions (22.5% RH, 52.89% RH, 75.29% RH and 100% RH), respectively.

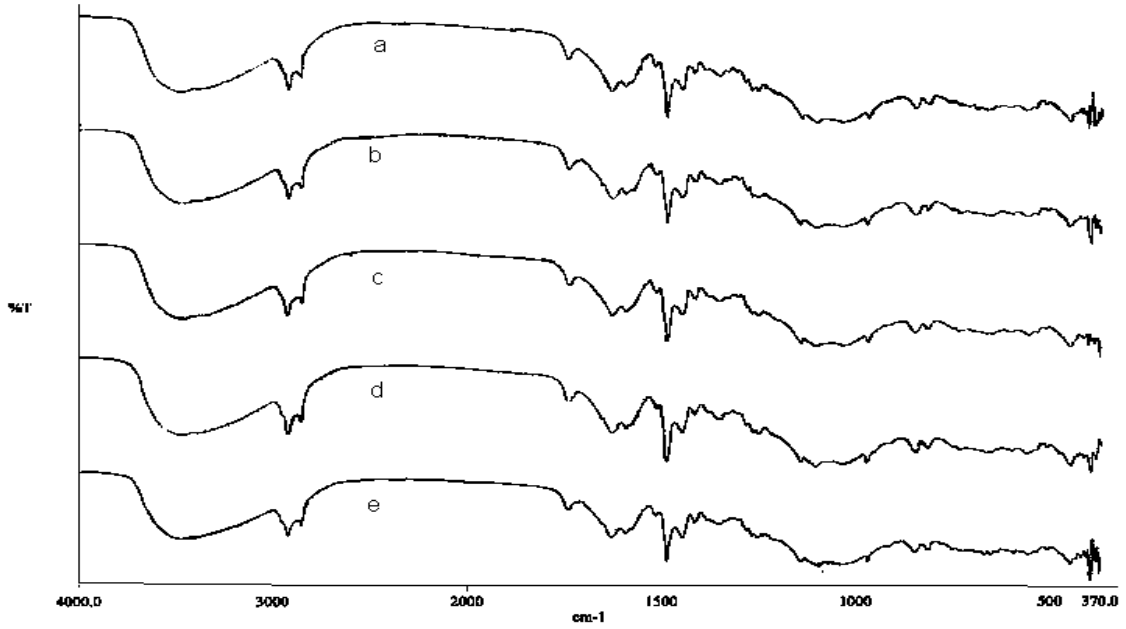

Figure 10.10 - Represents the FTIR for (a) ternary solid dispersion granules of 1:1:1.5 Dif/G/N initially and (b) at 25 ºC (c) at 30 ºC (d) at 35 ºC (e) at 40 ºC after one month.

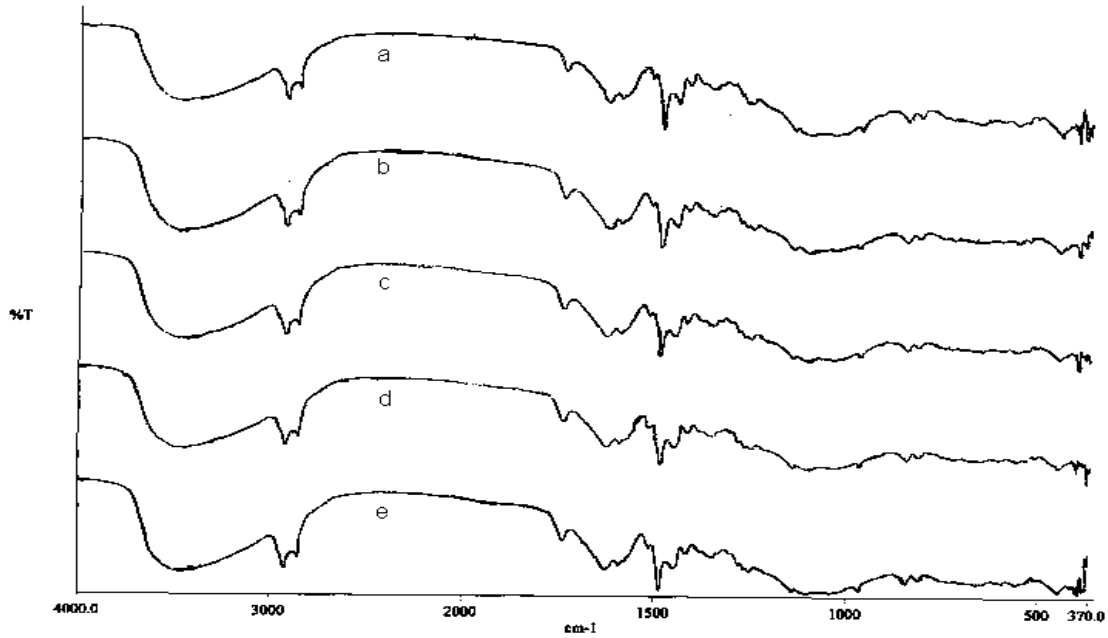

Figure 10.11 - Represents the FTIR for (a) ternary solid dispersion granules of 1:1:1.5 Dif/G/N initially and (b) at 22.5% RH (c) at 52.89% RH (d) at 75.29% RH (e) at 100% RH after one month.

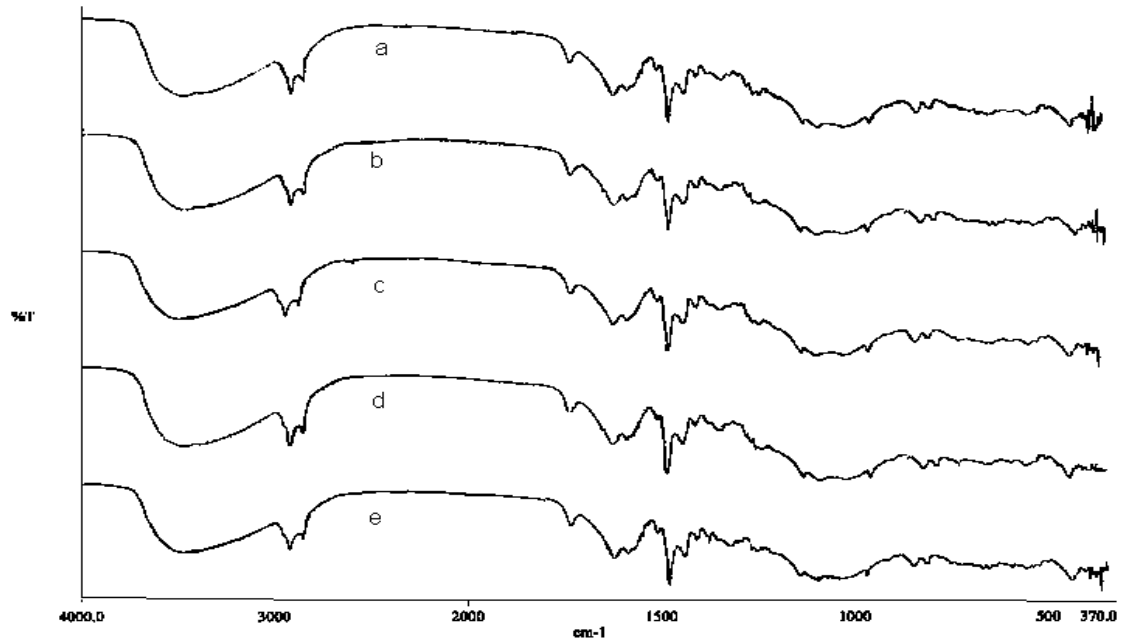

Figure 10.12 - Represents the FTIR for (a) ternary solid dispersion granules of 1:1:1.5 Dif/G/N initially and (b) at 25 ºC (c) at 30 ºC (d) at 35 ºC (e) at 40 ºC after two months.

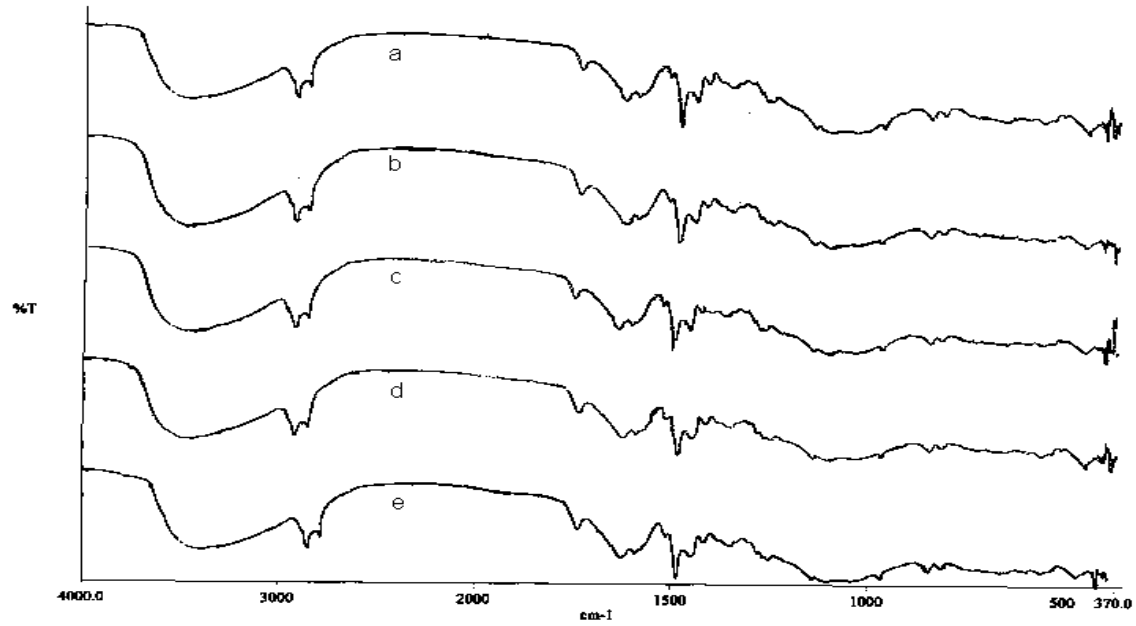

Figure 10.13 - Represents the FTIR for (a) ternary solid dispersion granules of 1:1:1.5 Dif/G/N initially and (b) at 22.5% RH (c) at 52.89% RH (d) at 75.29% RH (e) at 100% RH after two months.

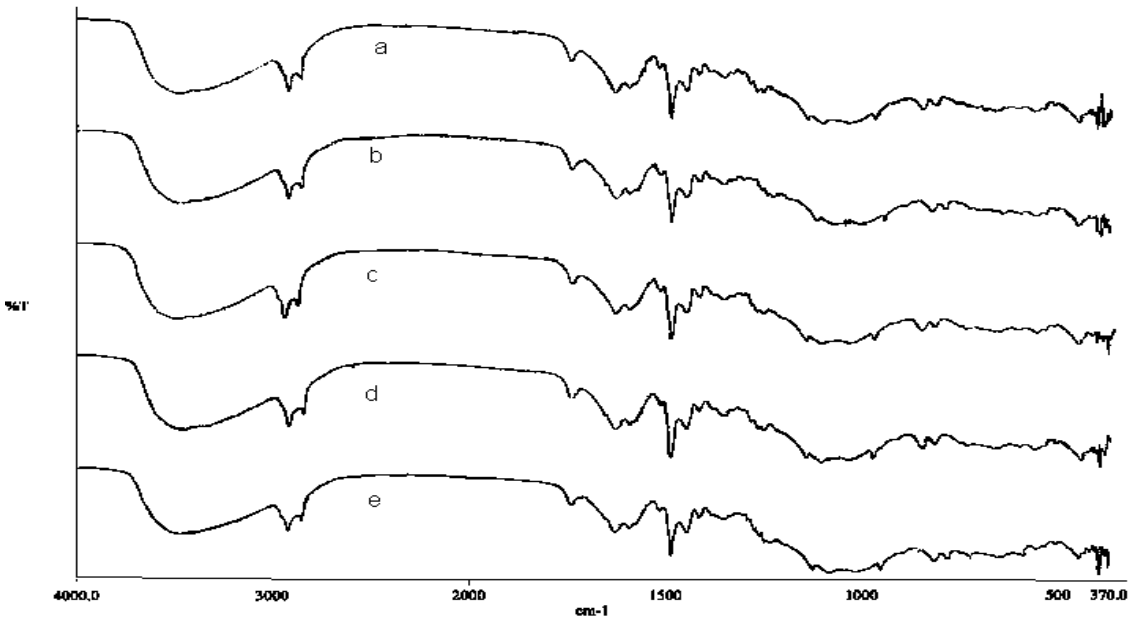

Figure 10.14 - Represents the FTIR for (a) ternary solid dispersion granules of 1:1:1.5 Dif/G/N initially and (b) at 25 ºC (c) at 30 ºC (d) at 35 ºC (e) at 40 ºC after three months.

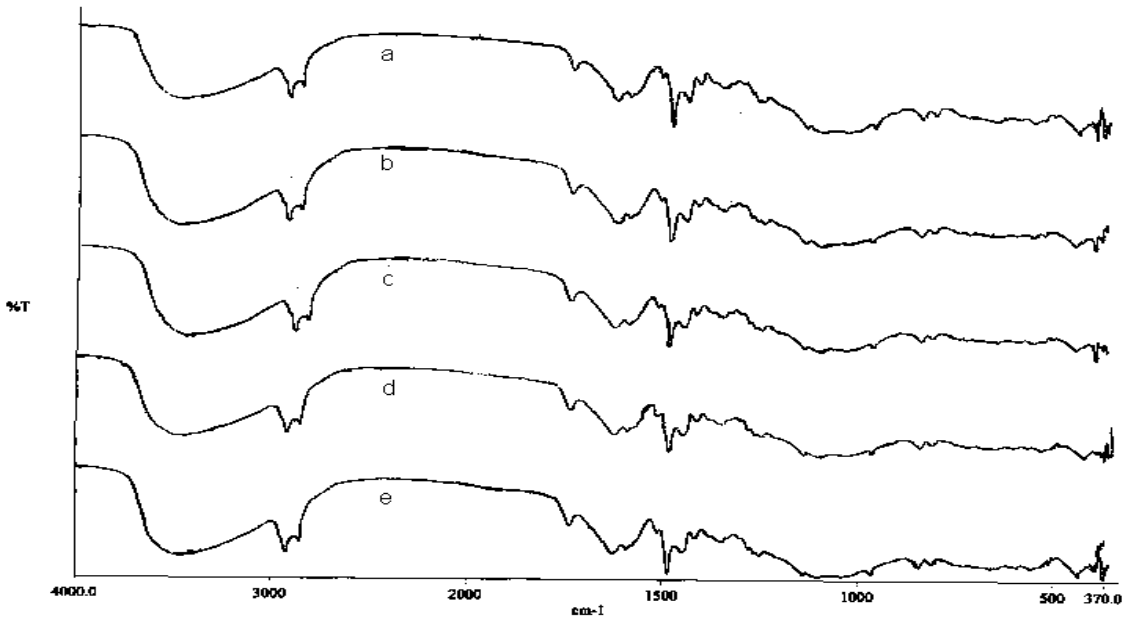

Figure 10.15 - Represents the FTIR for (a) Ternary solid dispersion granules of 1:1:1.5 Dif/G/N initially and (b) at 22.5% RH (c) at 52.89% RH (d) at 75.29% RH (e) at 100% RH after three months.

10.1.4 SEM study

The SEM study was performed to observe the characteristics (such as crystallinity, amorphous structures, porosity, and more) of the pure Diflunisal, Gelucire 50/13® (G), Neusilin US2® (N) and the ternary solid dispersion granules (Dif/G/N). SEM pictures for the pure Diflunisal, Gelucire 50/13® (G), Neusilin US2® (N) and ternary solid dispersion granules (Dif/G/N) are seen in Figure 10.16. From the SEM picture for the ternary solid dispersion granules (Dif/G/N), the reduction in particle size and conversion of the highly crystalline drug to its amorphous form in the solid dispersion phase is observed. The morphology of the ternary solid dispersion granules (Dif/G/N) resembled that of Gelucire 50/13® which is indicative of the drug (Diflunisal) is being dispersed into the Gelucire 50/13®.

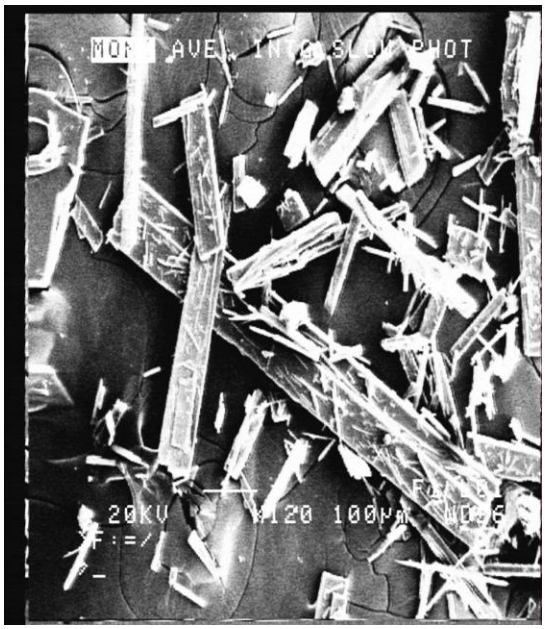

(a)

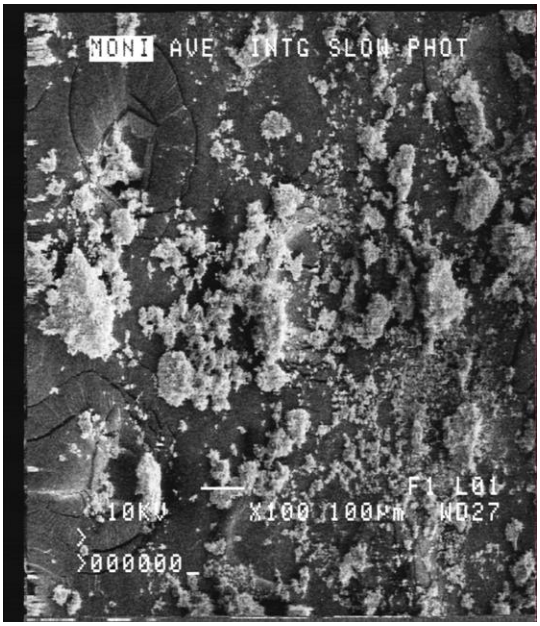

(b)

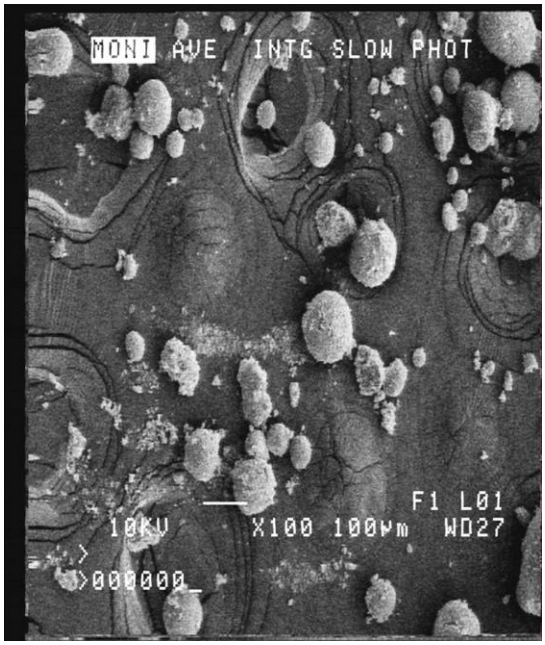

(c)

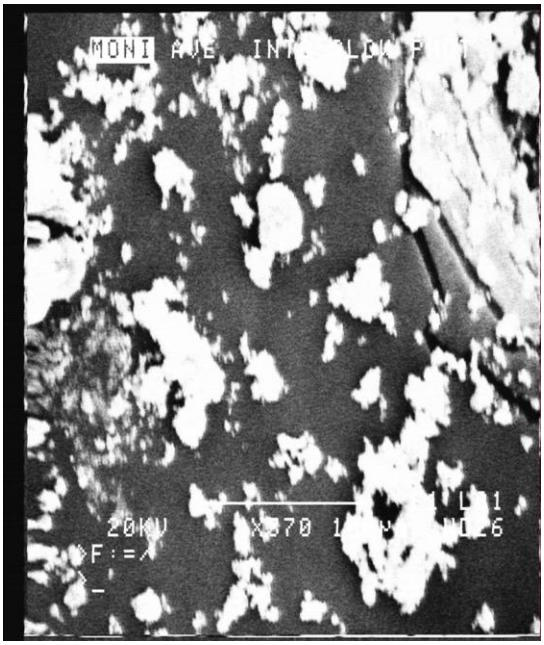

(d)

Figure 10.16 – Represents SEM pictures for (a) Diflunisal (b) Gelucire 50/13® (c) Neusilin US2® and (d) the 1:1:1.5 Dif/G/N Ternary solid dispersion granules.

The SEM pictures for the drug Diflunisal reveals the crystalline nature of the drug. The SEM picture for Gelucire 50/13® indicates that it is waxy solid material in nature. The SEM picture for Neusilin US2® indicates that it is spherical and porous in nature. The SEM picture for the solid dispersion granules of the drug (Diflunisal) indicates that the highly crystalline drug is converted to the amorphous form by formation of solid dispersion.

10.1.5 Dissolution study

10.1.5.1 Calibration curve for Diflunisal

In order to aid the process of dissolution analysis, the preparation of a calibration curve for the drug (diflunisal) was necessary. In this drug release study, the drug content analysis was performed in water as well as in a buffer solution of pH 7.2. Therefore, the calibration curve for diflunisal was prepared in both water and a pH 7.2 buffer solution. The absorbance and concentration values used to plot the calibration curve (Beer's curve) for diflunisal in water and buffer solution are given in Tables 10.1 and 10.2, respectively. Figures 10.17 and 10.18 represent the standard calibration curve for diflunisal in water and buffer solution, respectively. The linear regression equations thus obtained were used in analysis of the drug release studies and drug content analysis.

Table 10.1 – Data used to obtain the calibration curve for diflunisal in water

Concentration (mcg/mL)	Mean Absorbance at 254 nm	Standard Deviation
4	0.224	0.019
8	0.447	0.058
12	0.668	0.052
16	0.856	0.031
20	1.029	0.042

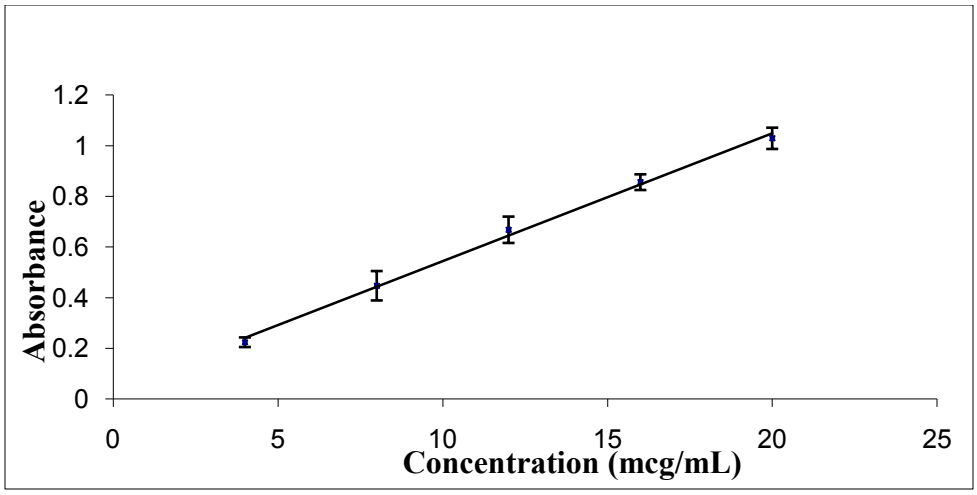

Figure 10.17 – Calibration curve for Diflunisal in water where slope = 0.0505 with an intercept of 0.0391 and an R^2 value of 0.9968.

`

Table 10.2– Data used to obtain the calibration curve for diflunisal in a pH 7.2 buffer solution .

Concentration (mcg/mL)	Mean Absorbance at 254 nm	Standard Deviation
5	0.117	0.025
10	0.401	0.020
15	0.593	0.036
20	0.821	0.045
25	1.001	0.057

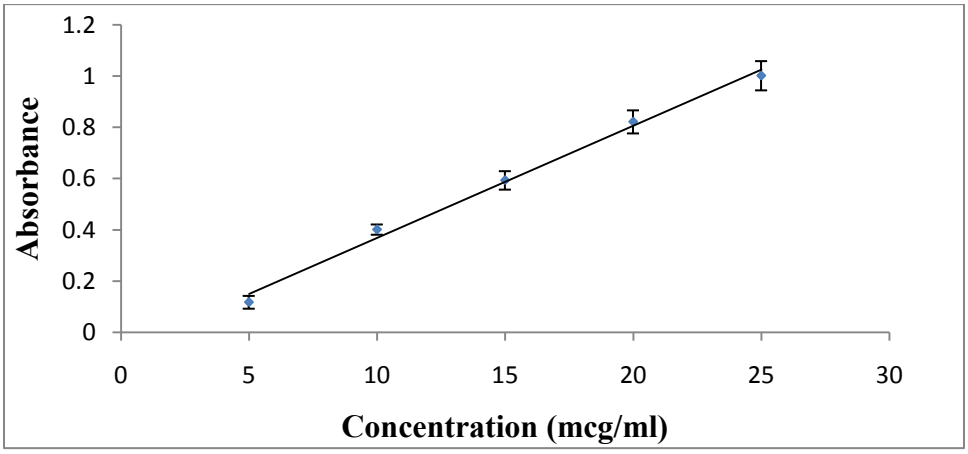

Figure 10.18 – Calibration curve for Diflunisal in a pH 7.2 buffer solution where the slope = 0.0438 with an intercept of 0.0694 and an R^2 value of 0.9939.

10.1.5.2 Diflunisal solid dispersion dissolution study

The dissolution test was performed in order to compare the amount of drug released from the ternary solid dispersion granules with the amount of drug released from the pure drug. The dissolution test for the solid dispersion granules of diflunisal granules and pure diflunisal was carried out in 900 ml of water as well as 900 ml of pH 7.2 buffer solution. Samples containing 50 mg of pure diflunisal and solid dispersion equivalent to 50 mg of drug (Diflunisal) were weighed and added to the dissolution medium. All the experiments were performed in triplicate. The drug release data for pure diflunisal and diflunisal solid dispersion granules in water and pH 7.2 buffer solution are seen in Figures 10.19 and 10.20, respectively. Tables 10.3 and 10.4 compares the amount of drug released after 20 min and 40 min from both the pure diflunisal and diflunisal solid dispersion granules in water and pH 7.2 buffer solution, respectively.

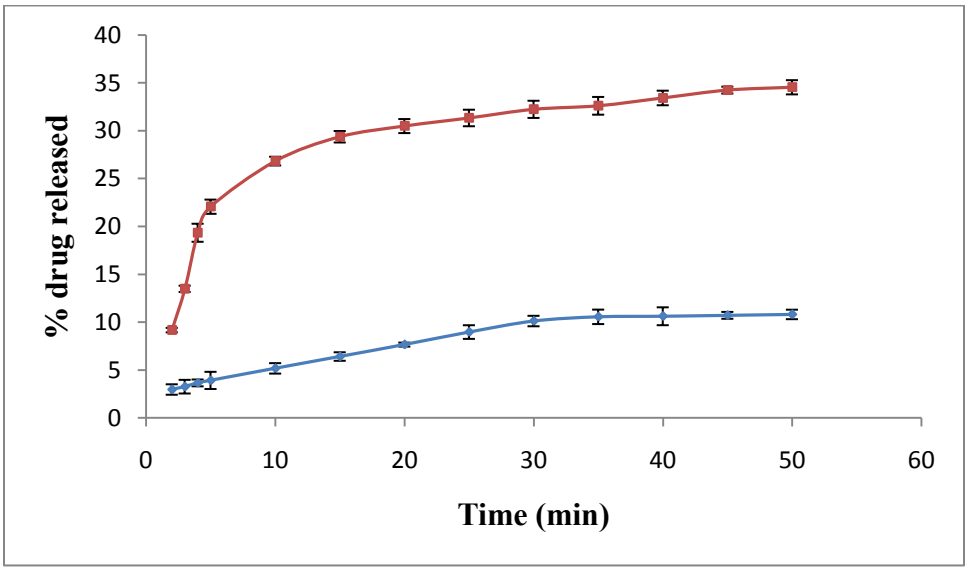

Figure 10.19 – Dissolution profile for diflunisal (bottom) and diflunisal solid dispersion (top) in water.

Table 10.3 – Comparison of the amount of drug released after 20 min and 40 min from pure diflunisal and diflunisal solid dispersion granules in water

Percentage drug released (in water) (± standard deviation)		
Batch name	After 20 min	After 40 min
Pure Diflunisal	7.67 ± 0.2057 %	10.63 ± 0.4956 %
Dif/G/N solid dispersion granules	30.49 ± 0.7326 %	34.54 ± 0.7419 %

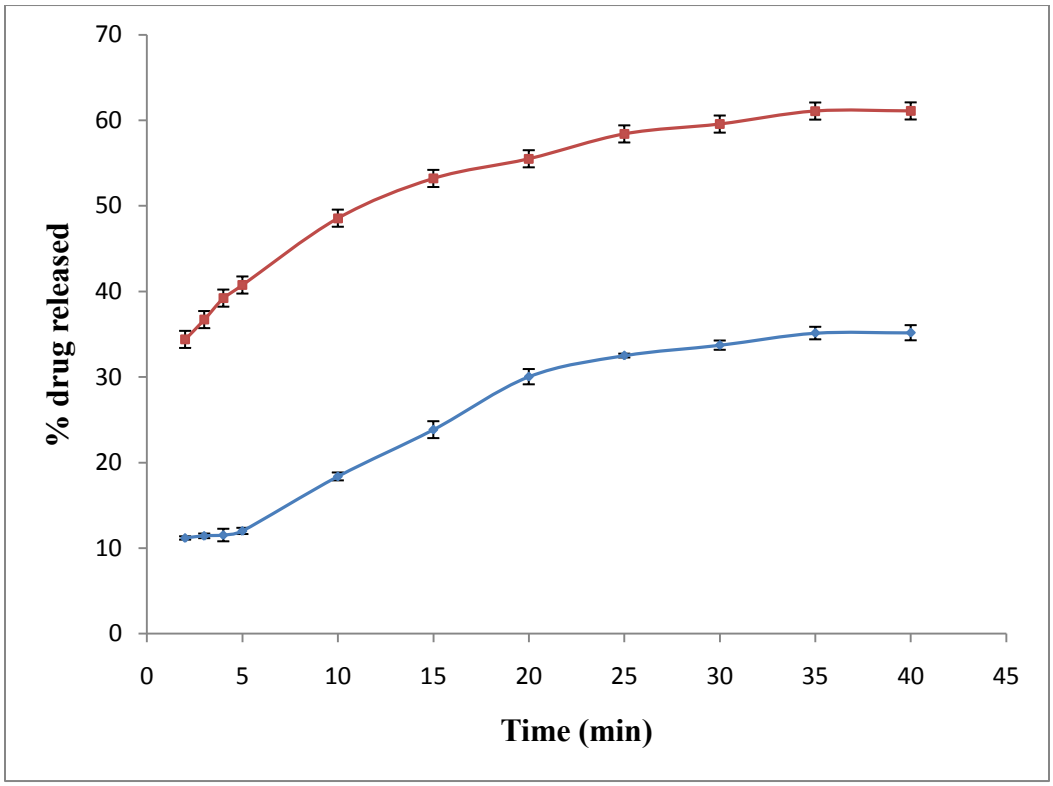

Figure 10.20 – Dissolution profile for diflunisal (bottom) and diflunisal solid dispersion (top) in pH 7.2 buffer solution.

Table 10.4 – Comparison of the amount of drug released after 20 min and 40 min from pure diflunisal and diflunisal solid dispersion granules in pH 7.2 buffer solution.

Percentage drug released (in buffer solution at pH 7.2) (± standard deviation)		
Batch name	After 20 min	After 40 min
Pure Diflunisal	30.03 ± 0.8926%	35.167 ± 0.8856 %
Dif/G/N solid dispersion granules	55.49 ± 0.8219 %	61.084 ± 0.8634 %

From the Figures 10.19 and 10.20 it was clear that the dissolution rate for the diflunisal solid dispersion granules was greater than the pure diflunisal in both the water and pH 7.2 buffer solution. From the table above it was clear that the bioavailability of drug at 20 min and 40 min was greater for the Diflunisal solid dispersion granules as compared to the pure Diflunisal in both water and pH 7.2 buffer solution. Increased solubility should lead to increased bioavailability.

The dissolution study in both water and pH 7.2 buffer solution was performed on the diflunisal solid dispersion granules after the first, second and third month to observe any change in dissolution profile for the ternary phase solid dispersion (Dif/G/N) when subjected to different temperatures and relative humidity conditions. After the first, second and third month, the dissolution study for the ternary solid dispersion granules (Dif/G/N) which were exposed to different temperatures (25ºC, 30ºC, 35ºC and 40ºC) and relative humidity conditions (22.5% RH, 52.89% RH, 75.29% RH and 100% RH),

showed no significant change with respect to the dissolution study for the ternary solid dispersion granules at the initial stage.

Tables 10.5 and 10.6 compares the amount of drug released after 20 min from diflunisal solid dispersion granules in water initially and after storage for 3 months at different temperatures (25ºC, 30ºC, 35ºC and 40ºC) and relative humidity conditions (22.5% RH, 52.89% RH, 75.29% RH and 100% RH), respectively. Tables 10.7 and 10.8 compares the amount of drug released after 20 min from diflunisal solid dispersion granules in pH 7.2 buffer solution initially and after storage for 3 months at different temperatures (25ºC, 30ºC, 35ºC and 40ºC) and relative humidity conditions (22.5% RH, 52.89% RH, 75.29% RH and 100% RH), respectively.

Table 10.5 – Comparison of the amount of drug released after 20 min from diflunisal solid dispersion granules in water, initially and after storage for 3 months at different temperature (25ºC, 30ºC, 35ºC and 40ºC).

Percentage drug dissolved (in water) after 20 minutes (±standard deviation)					
Batch Name	**Initial**	**1st month/ 25 ºC**	**1st month/ 30 ºC**	**1st month/ 35 ºC**	**1st month/ 40 ºC**
Dif/G/N Solid dispersion granules	30.49 ± 0.7326 %	30.26 ± 0.4405 %	30.85 ± 0.1145 %	30.10 ± 0.7419 %	31.03 ± 0.9939 %
		2nd month/ 25 ºC	**2nd month/ 30 ºC**	**2nd month/ 35 ºC**	**2nd month/ 40 ºC**
		31.37 ± 0.6931 %	29.83 ± 0.6673 %	30.31 ± 0.2394 %	31.02 ± 0.9782 %
		3rd month/ 25 ºC	**3rd month/ 30 ºC**	**3rd month/ 35 ºC**	**3rd month/ 40 ºC**
		29.84 ± 0.7012 %	31.22 ± 0.7721 %	29.68 ± 0.1921 %	30.58 ± 0.8519 %

Table 10.6 – Comparison of the amount of drug released after 20 min from diflunisal solid dispersion granules in water, initially and after storage for 3 months at different relative humidity conditions (22.5% RH, 52.89% RH, 75.29% RH and 100% RH).

Percentage drug dissolved (in water) after 20 minutes (±standard deviation)					
Batch Name	**Initial**	**1st month/ 22.5 %RH**	**1st month/ 52.89 %RH**	**1st month/ 75.29 %RH**	**1st month/ 100 %RH**
Dif/G/N Solid dispersion granules	30.49 ± 0.7326 %	31.13 ± 0.4405 %	30.05 ± 0.2519 %	31.24 ± 0.9631 %	30.99 ± 0.8970 %
		2nd month/ 22.5 %RH	**2nd month/ 52.89 %RH**	**2nd month/ 75.29 %RH**	**2nd month/ 100 %RH**
		29.33 ± 0.6439 %	31.47 ± 0.9326 %	30.59 ± 0.4651 %	30.14 ± 0.7419 %
		3rd month/ 22.5 %RH	**3rd month/ 52.89 %RH**	**3rd month/ 75.29 %RH**	**3rd month/ 100 %RH**
		29.75 ± 0.8920 %	31.33 ± 0.7315 %	30.76 ± 0.6686 %	29.99 ± 0.7239 %

Table 10.7 – Comparison of the amount of drug released after 20 min from diflunisal solid dispersion granules in pH 7.2 buffer solution, initially and after storage for 3 months at different temperature (25ºC, 30ºC, 35ºC and 40ºC).

Percentage drug dissolved (in buffer solution at pH 7.2) after 20 minutes (±standard deviation)					
Batch Name	**Initial**	**1st month/ 25 ºC**	**1st month/ 30 ºC**	**1st month/ 35 ºC**	**1st month/ 40 ºC**
Dif/G/N Solid dispersion granules	55.49 ± 0.8219 %	54.97 ± 0.3422 %	55.01 ± 0. 8923 %	54.24 ± 0.4432 %	55.55 ± 0.7336 %
		2nd month/ 25 ºC	**2nd month/ 30 ºC**	**2nd month/ 35 ºC**	**2nd month/ 40 ºC**
		56.12 ± 0.9069 %	54.64 ± 0.4078 %	55.38 ± 0.1069 %	54.88 ± 1.0675 %
		3rd month/ 25 ºC	**3rd month/ 30 ºC**	**3rd month/ 35 ºC**	**3rd month/ 40 ºC**
		55.17 ± 0.1031 %	56.21 ± 1.0693 %	54.93 ± 0.2946 %	54.81 ± 0.3117 %

Table 10.8 – Comparison of the amount of drug released after 20 min from diflunisal solid dispersion granules in pH 7.2 buffer solution, initially and after storage for 3 months at different relative humidity conditions (22.5% RH, 52.89% RH, 75.29% RH and 100% RH).

Percentage drug dissolved (in buffer solution at pH 7.2) after 20 minutes (±standard deviation)					
Batch Name	**Initial**	**1st month/ 22.5 %RH**	**1st month/ 52.89 %RH**	**1st month/ 75.29 %RH**	**1st month/ 100 %RH**
Dif/G/N Solid dispersion granules	55.49 ± 0.8219 %	55.50 ± 0.6783 %	54.96 ± 0.8736 %	55.90 ± 0.8219 %	54.63 ± 0.5535 %
		2nd month/ 22.5 %RH	**2nd month/ 52.89 %RH**	**2nd month/ 75.29 %RH**	**2nd month/ 100 %RH**
		54.48 ± 0.4946 %	55.96 ± 0.6983 %	56.32 ± 0.7351 %	56.11 ± 0.7638 %
		3rd month/ 22.5 %RH	**3rd month/ 52.89 %RH**	**3rd month/ 75.29 %RH**	**3rd month/ 100 %RH**
		55.09 ± 0.4613 %	56.32 ± 0.1189 %	55.30 ± 0.3436 %	54.99 ± 0.9428 %

A student's independent t-test was performed at an α-value of 0.05. No significant difference was observed between the dissolution data for the diflunisal solid dispersion granules in water and pH 7.2 buffer solution at the initial stage and after each successive storage.

10.2 Mefenamic acid solid dispersion granules

The ternary solid dispersion granules for Mefenamic acid were prepared by the hot melt granulation technique using Gelucire 50/13® as the dispersion carrier and Neusilin US2® as the adsorbent. Different ratios of the drug (Mefenamic acid), dispersion carrier (Gelucire 50/13®) and adsorbent (Neusilin US2®) were tried to obtain ternary solid

dispersion granules. The ratio for 1:1:1.5 of Mefenamic acid, Gelucire 50/13® and Neusilin US2® provided the best solid dispersion granules. Therefore, the solid dispersion granules thus obtained were further characterized using DSC, XRPD, FTIR, SEM and dissolution studies. The stability study was performed on the solid dispersion granules by subjecting it to different temperature conditions (25ºC, 30ºC, 35ºC and 40ºC) and different humidity condition (22.5% RH, 52.89% RH, 75.29% RH and 100% RH) for a period of three months. The solid dispersion granules under stability study were characterized by performing XRPD, FTIR and dissolution studies after the first, second and third month.

10.2.1 DSC study

DSC studies were performed for the determination of the melting point, to observe changes in crystallinity and to detect any possible interaction between the drug (mefenamic acid), dispersion carrier (Gelucire 50/13®) and adsorbent (Neusilin US2®). The DSC runs for pure Mefenamic acid, Gelucire 50/13®, Neusilin US2® and Ternary phase solid dispersion as seen in Figure 10.21.

The DSC curve for mefenamic acid showed a sharp melting peak at 229.69 ºC which corresponds to its melting point. This is indicative of the crystalline nature of the drug. The DSC curve for Neusilin US2® showed no peak which indicates the complete amorphous nature of Neusilin US2®. The DSC curve for Gelucire 50/13® showed a peak at 44.81 ºC which corresponds to its melting point. The DSC curve for the 1:1:1.5 Mef/G/N (ternary phase solid dispersion) showed a peak at 43.86 ºC but did not show any peak at 229.69 ºC. The disappearance of the endothermic peak at 229.69 ºC indicates that the drug is dispersed in the carrier Gelucire 50/13®. Thus the DSC studies indicate the

formation of solid dispersions for Mef/G/N in the ratio of 1:1:1.5 which is evident by the appearance of one peak in the DSC profile for the solid dispersions.

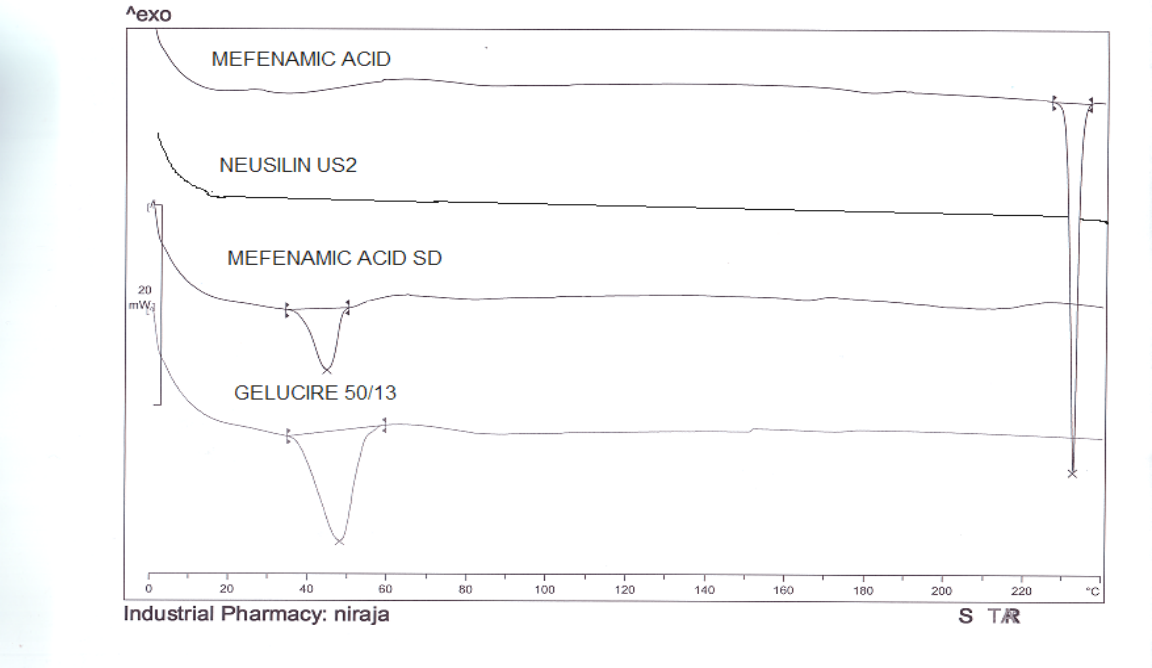

Figure 10.21 - Overlay of the DSC curves for Mefenamic acid, Neusilin US2®, 1:1:1.5 Mef/G/N Ternary phase Solid Dispersion and Gelucire 50/13®.

10.2.2 XRPD study

The X-ray powder diffraction studies were performed in order to study phase analysis and crystalline properties of the drug (mefenamic acid), dispersion carrier (Gelucire 50/13®) and adsorbent (Neusilin US2®). X-ray powder diffraction studies were performed to detect any changes in the crystallinity of the drug (mefenamic acid) in the ternary solid dispersion state. The x-ray diffraction pattern for pure mefenamic acid, Gelucire 50/13® (G), Neusilin US2® (N) and ternary phase solid dispersion (Mef/G/N) is shown in Figure 10.22. Pure drug (mefenamic acid) showed numerous peaks which

demonstrate the crystalline nature of the drug whereas Neusilin US2® showed diffused peak which is indicative of its amorphous nature. Gelucire 50/13® shows few peaks which is indicative of some crystalline characteristics. The ternary phase solid dispersion of Mef/G/N showed diffused peaks which is indicative of a significant conversion to the amorphous state when formulated into of solid dispersion granules.

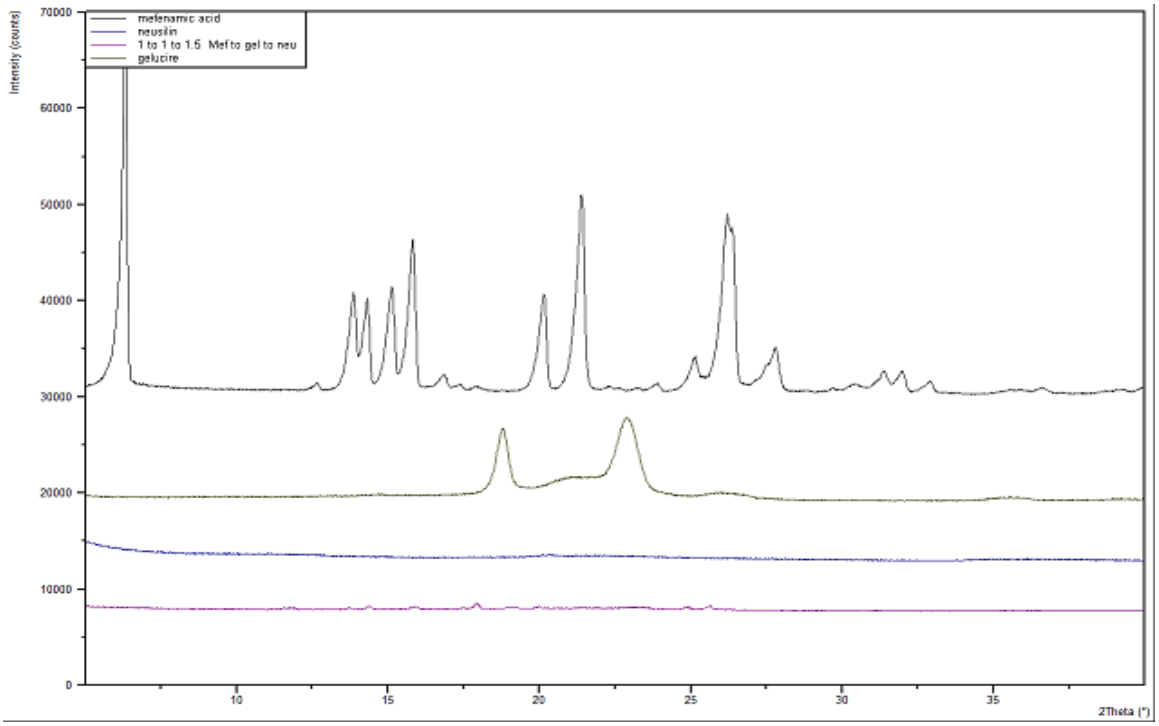

Figure 10.22 - Overlay of the XRPD patterns for mefenamic acid, Gelucire 50/13®, Neusilin US2® and 1:1:1.5 Mef:G:N solid dispersion displayed from top to bottom.

XRPD was performed on the solid dispersion granules after the first, second and third month to observe any change in the amorphous characteristic of the ternary phase solid dispersion (Mef/G/N) when subjected to different temperatures and relative humidity conditions. After the first, second and third month, the XRPD pattern for the ternary solid dispersion granules (Mef/G/N), which were exposed at different temperatures (25ºC, 30ºC, 35ºC and 40ºC) and relative humidity conditions (22.5% RH, 52.89% RH,

75.29% RH and 100% RH), showed no significant change with respect to the XRPD study of the ternary solid dispersion granules initially prepared.

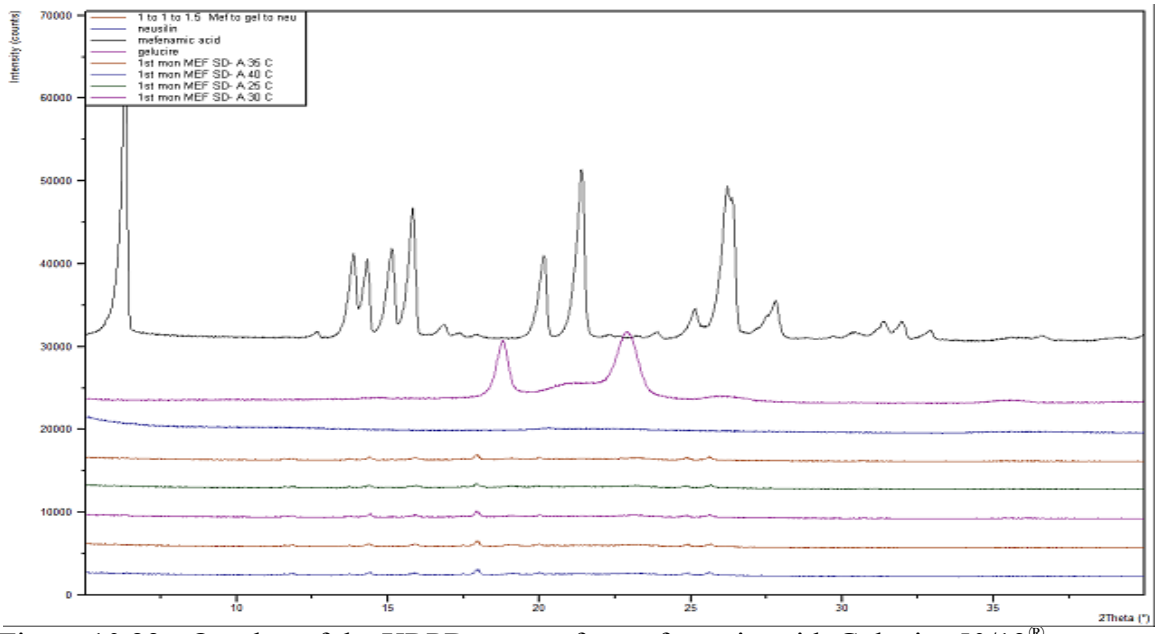

Figure 10.23 - Overlay of the XRPD pattern for mefenamic acid, Gelucire 50/13®, Neusilin US2®, 1:1:1.5 Mef:G:N solid dispersion granules initially, at 25ºC, 30ºC, 35ºC and 40ºC after one month, displayed from top to bottom.

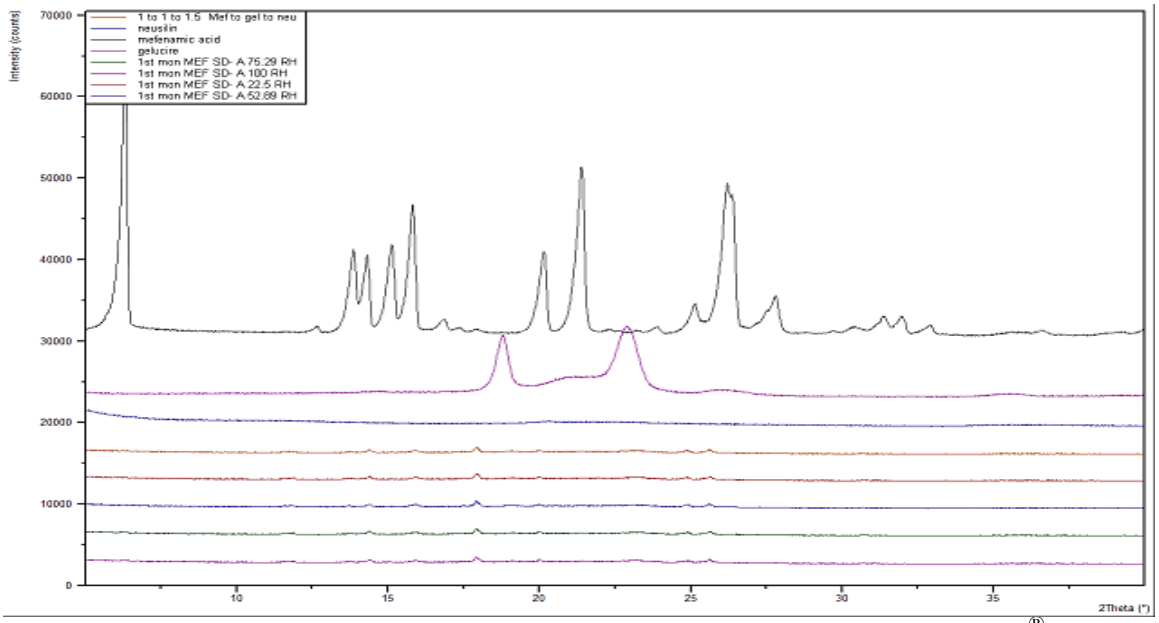

Figure 10.24 - Overlay of the XRPD pattern for mefenamic acid, Gelucire 50/13®, Neusilin US2®, 1:1:1.5 Mef:G:N solid dispersion granules initially, at 22.5% RH, 52.89% RH, 75.29% RH and 100% RH after one month, displayed from top to bottom.

Figures 10.23 and 10.24 represent the overlay of the XRPD profiles for mefenamic acid, Gelucire 50/13®, Neusilin US2®, solid dispersion granules of Mef/G/N initially and after one month storage at different temperatures (25ºC, 30ºC, 35ºC and 40ºC) and relative humidity conditions (22.5% RH, 52.89% RH, 75.29% RH and 100% RH) respectively.

Figures 10.25 and 10.26, represents the overlay of the XRPD profiles for mefenamic acid, Gelucire 50/13®, Neusilin US2®, solid dispersion granules of Mef/G/N initially and after two months storage at different temperatures (25ºC, 30ºC, 35ºC and 40ºC) and relative humidity conditions (22.5% RH, 52.89% RH, 75.29% RH and 100% RH), respectively. Figures 10.27 and 10.28 represents the overlay of the XRPD profiles for mefenamic acid, Gelucire 50/13®, Neusilin US2®, solid dispersion granules of Mef/G/N initially and after three months storage at different temperatures (25ºC, 30ºC, 35ºC and 40ºC) and relative humidity conditions (22.5% RH, 52.89% RH, 75.29% RH and 100% RH), respectively.

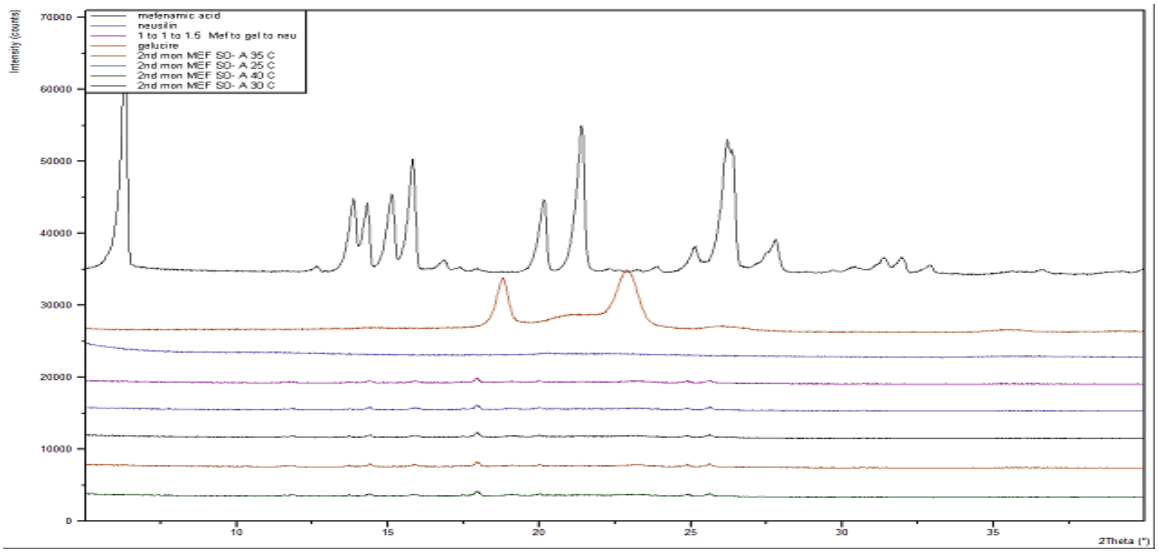

Figure 10.25 - Overlay of the XRPD pattern for mefenamic acid, Gelucire 50/13®, Neusilin US2®, 1:1:1.5 Mef:G:N solid dispersion granules initially, at 25ºC, 30ºC, 35ºC and 40ºC after two months, displayed from top to bottom.

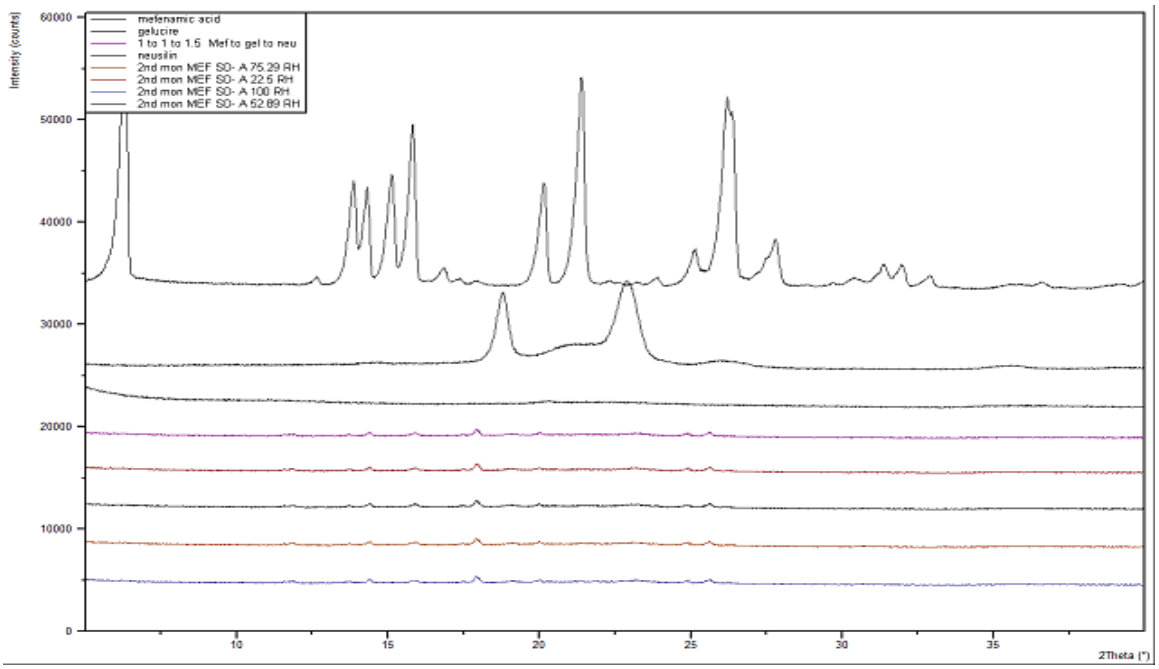

Figure 10.26 - Overlay of the XRPD pattern for mefenamic acid, Gelucire 50/13®, Neusilin US2®, 1:1:1.5 Mef:G:N solid dispersion granules initially, at 22.5% RH, 52.89% RH, 75.29% RH and 100% RH after two months displayed from top to bottom.

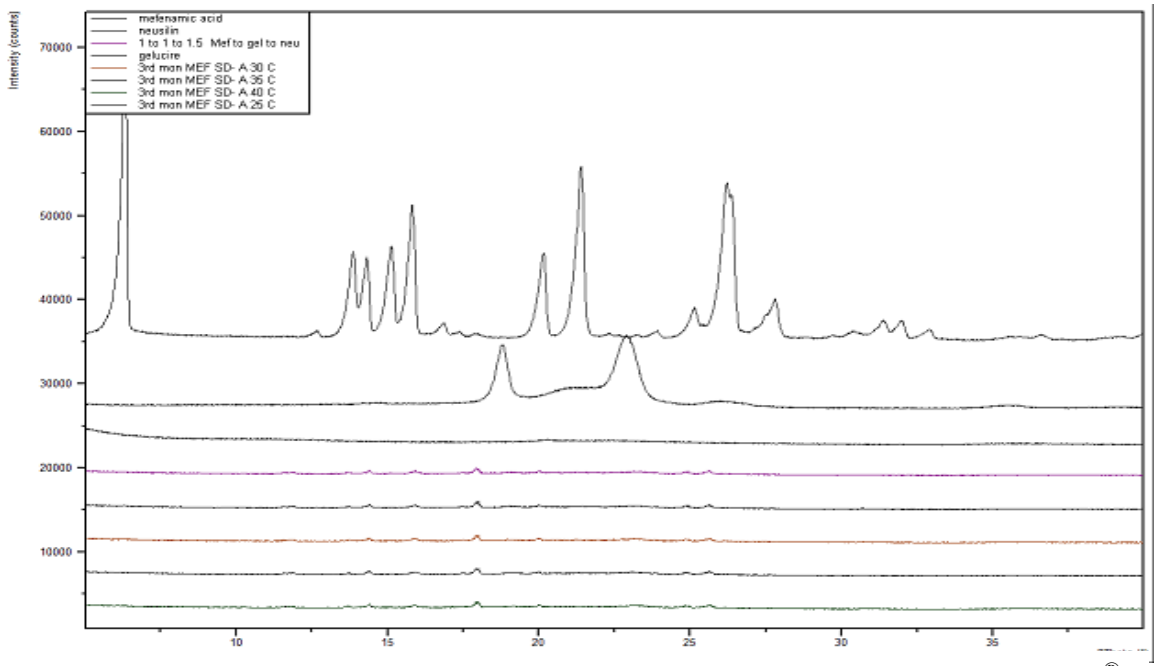

Figure 10.27 - Overlay of the XRPD pattern for mefenamic acid, Gelucire 50/13®, Neusilin US2®, 1:1:1.5 Mef:G:N solid dispersion granules initially, at 25ºC, 30ºC, 35ºC and 40ºC after three months, displayed from top to bottom.

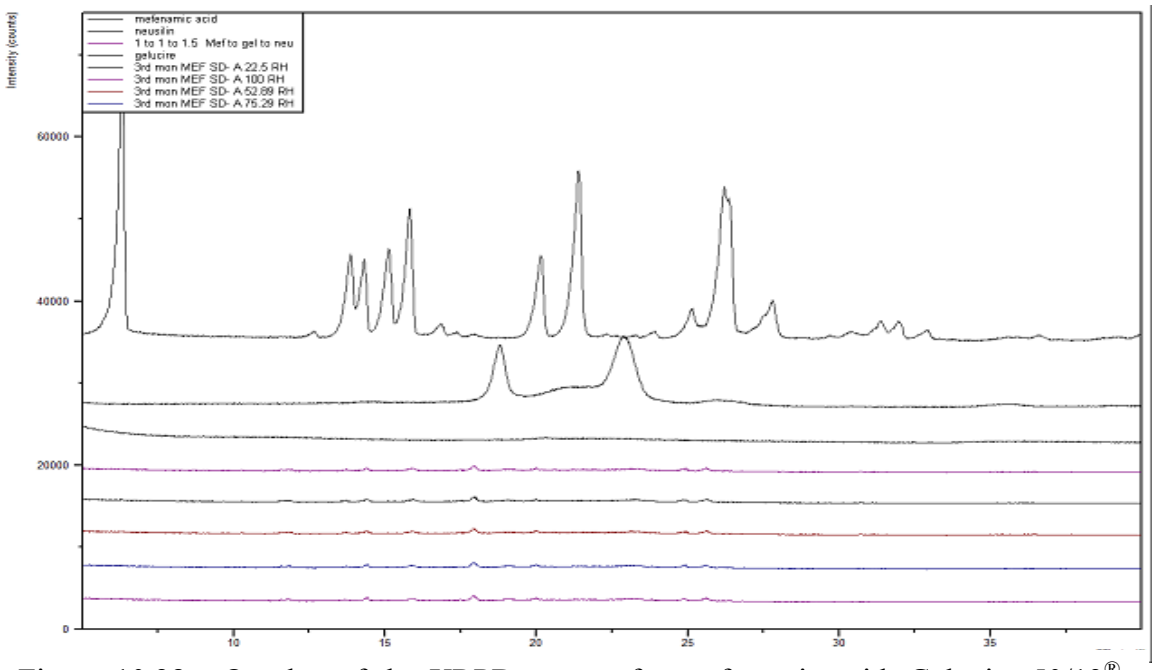

Figure 10.28 - Overlay of the XRPD pattern for mefenamic acid, Gelucire 50/13®, Neusilin US2®, 1:1:1.5 Mef:G:N solid dispersion granules initially, at 22.5% RH, 52.89% RH, 75.29% RH and 100% RH after three month displayed from top to bottom.

10.2.3 FTIR study

FTIR studies were performed in order to aid the evaluation of any possible chemical interaction between the drug (mefenamic acid), dispersion carrier (Gelucire 50/13®) and adsorbent (Neusilin US2®). Moreover, molecular level characterization of solid dispersions can also be obtained by performing FTIR studies. The FTIR for pure mefenamic acid, Gelucire 50/13® (G), Neusilin US2® (N) and Ternary phase solid dispersion (Mef/G/N) are shown in Figure 10.29.

The FTIR spectrum for mefenamic acid shows a weak peak at 3400 cm^{-1} due to the presence of a secondary amine[1,2]. The broad band in the range of 3200-2900 cm^{-1} is due to the presence of –OH[1,2]. The same also represents the intra- and intermolecular hydrogen bonding due to the –OH groups and also overlaps with the ($–CH_3$) group. The

peak at 1650- 1750 cm^{-1} is due to the presence of a C=O group. The presence of a peak at 1000 cm^{-1} indicates the presence of a phenyl group[1,2].

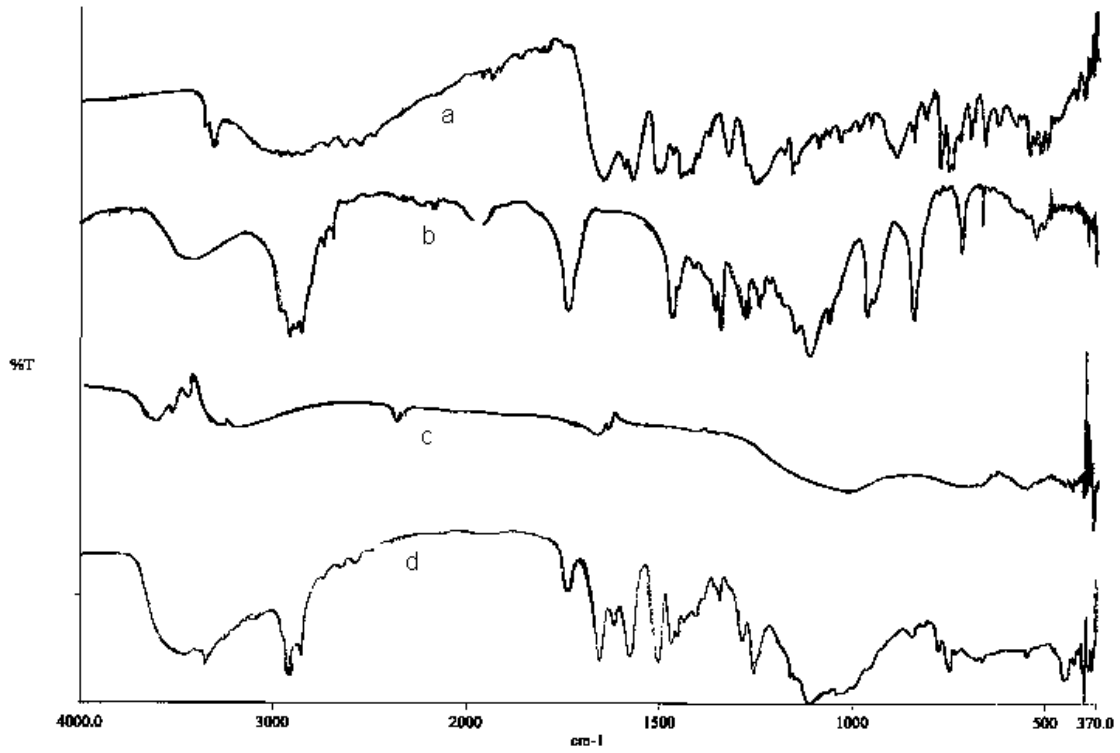

Figure 10.29 - Represents FTIR spectrum for (a) Mefenamic acid (b) Gelucire 50/13® (c) Neusilin US2® (d) Ternary phase solid dispersion of Mef/G/N.

The FTIR spectrum for Gelucire 50/13® shows a stretching band at 2800-3000 cm^{-1} due to the presence of (CH_3) groups. The peak at 1750 cm^{-1} is due to the presence of a C=O group[1,2].

The FTIR spectrum for Neusilin US2® shows a broad stretch band at 3400-3000 cm^{-1} which suggests the presence of a secondary amine[1,2].

The FTIR for the ternary phase solid dispersion of Mef/G/N shows the presence of strong bond at 3400-3000 cm^{-1} due to strong hydrogen bonding which is suggestive of the

formation of a solid dispersion. The peaks at 2900 cm $^{-1}$ are due to -CH_3 bonds. The peak at 1650-1750 cm^{-1} is due to the presence of a C=O group. The presence of a peak at 1000 cm $^{-1}$ indicates the presence of a phenyl group[1,2].

The FTIR was performed on the solid dispersion granules after the first, second and third month to observe any change in chemical interaction within the ternary phase solid dispersion (Dif/G/N) when subjected to different temperatures and relative humidity conditions. After the first, second and third month, the FTIR study for the ternary solid dispersion granules (Dif/G/N) which were exposed to different temperatures (25ºC, 30ºC, 35ºC and 40ºC) and relative humidity conditions (22.5% RH, 52.89% RH, 75.29% RH and 100% RH), showed no significant change with respect to the FTIR study performed on the ternary solid dispersion granules initially prepared.

Figures 10.30 and 10.31 represents the overlay of the FTIR profiles for the solid dispersion granules of Mef/G/N initially and after one month storage at different temperatures (25ºC, 30ºC, 35ºC and 40ºC) and relative humidity conditions (22.5% RH, 52.89% RH, 75.29% RH and 100% RH), respectively. Figures 10.32 and 10.33 represent the overlay of the FTIR profiles for the solid dispersion granules of Mef/G/N initially and after two months storage at different temperatures (25ºC, 30ºC, 35ºC and 40ºC) and relative humidity conditions (22.5% RH, 52.89% RH, 75.29% RH and 100% RH), respectively. Figures 10.34 and 10.35 represent the overlay of the FTIR profiles for the solid dispersion granules of Mef/G/N initially and after three months storage at different temperatures (25ºC, 30ºC, 35ºC and 40ºC) and relative humidity conditions (22.5% RH, 52.89% RH, 75.29% RH and 100% RH), respectively.

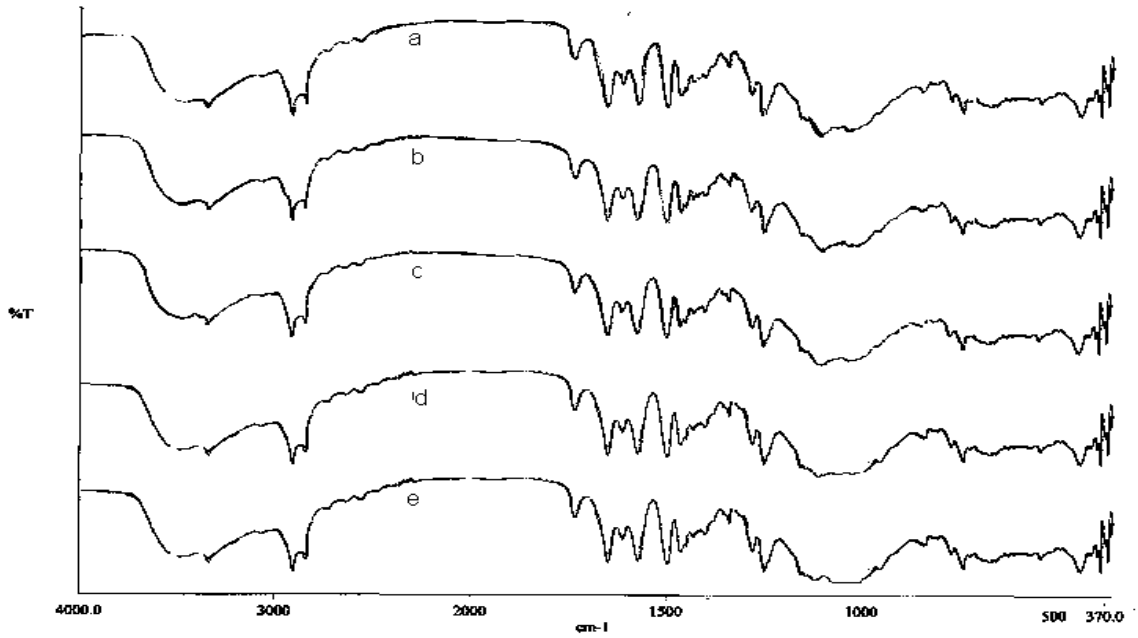

Figure 10.30 - Represents the FTIR profile for (a) ternary solid dispersion granules of 1:1:1.5 Mef/G/N initially and (b) at 25 ºC (c) at 30 ºC (d) at 35 ºC (e) at 40 ºC after one month.

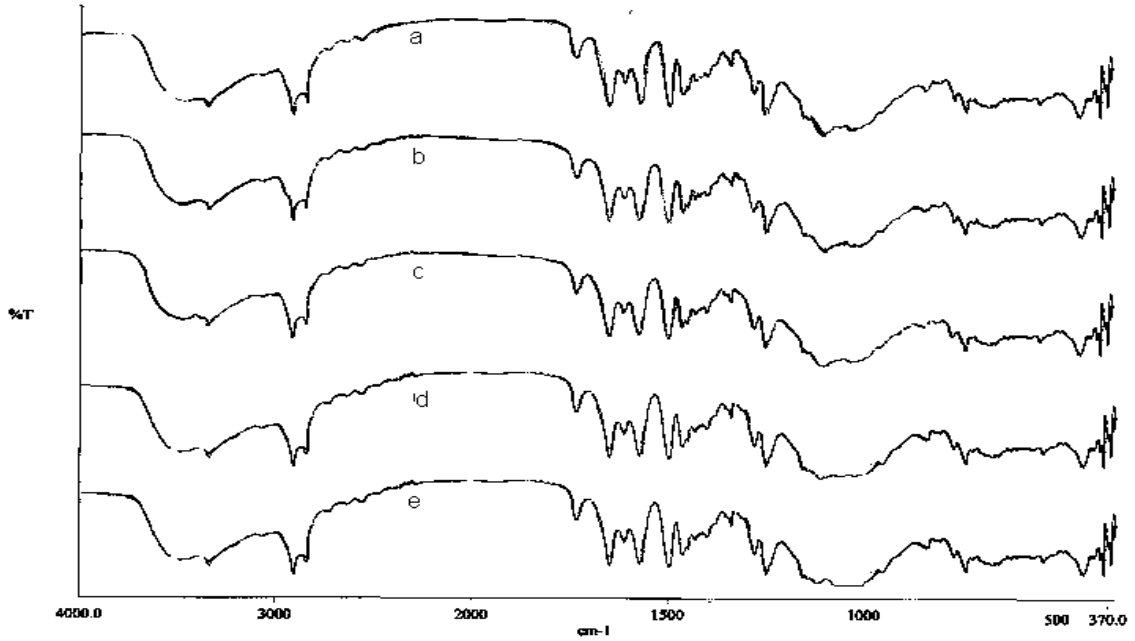

Figure 10.31 - Represents the FTIR profile for (a) ternary solid dispersion granules of 1:1:1.5 Mef/G/N initially and (b) at 22.5% RH (c) at 52.89% RH (d) at 75.29% RH (e) at 100% RH after one month.

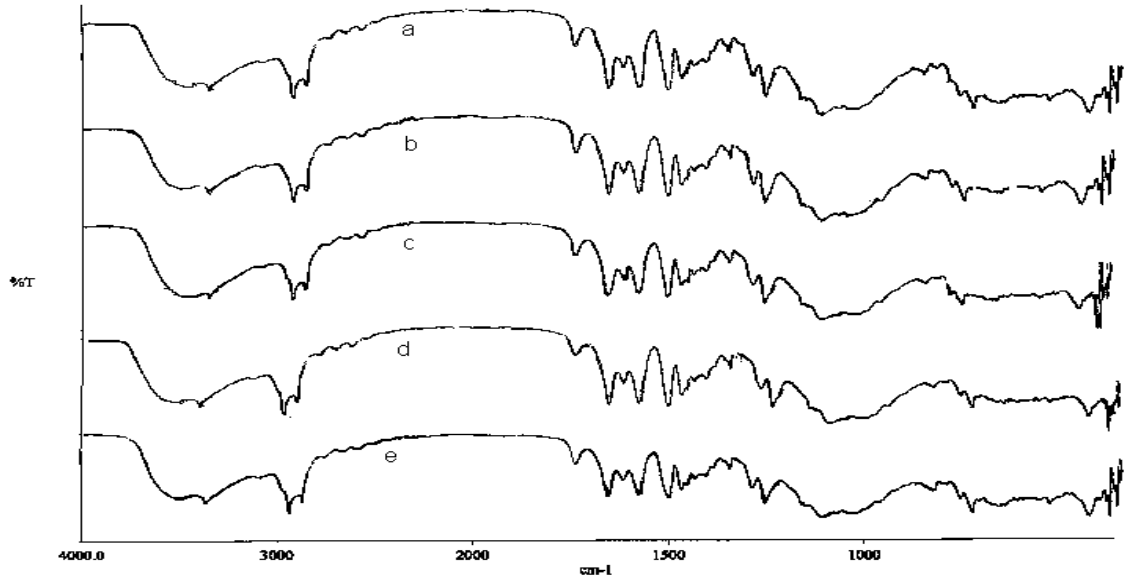

Figure 10.32 - Represents the FTIR profile for (a) ternary solid dispersion granules of 1:1:1.5 Mef/G/N initially and (b) at 25 ºC (c) at 30 ºC (d) at 35 ºC (e) at 40 ºC after two months.

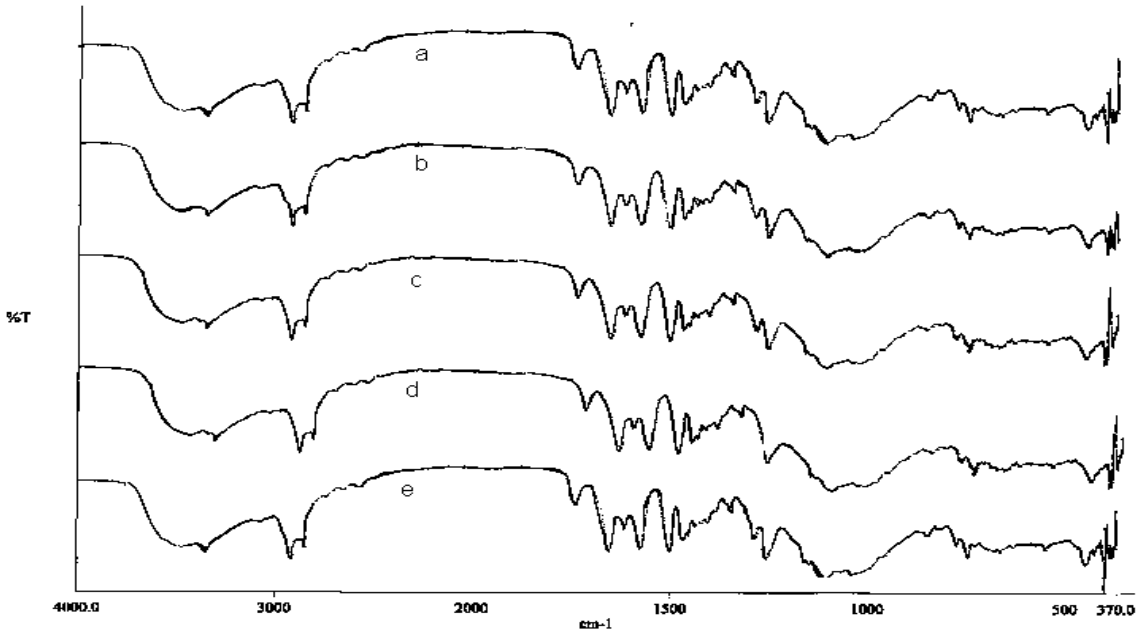

Figure 10.33 - Represents FTIR profile for (a) ternary solid dispersion granules of 1:1:1.5 Mef/G/N initially and (b) at 22.5% RH (c) at 52.89% RH (d) at 75.29% RH (e) at 100% RH after two months.

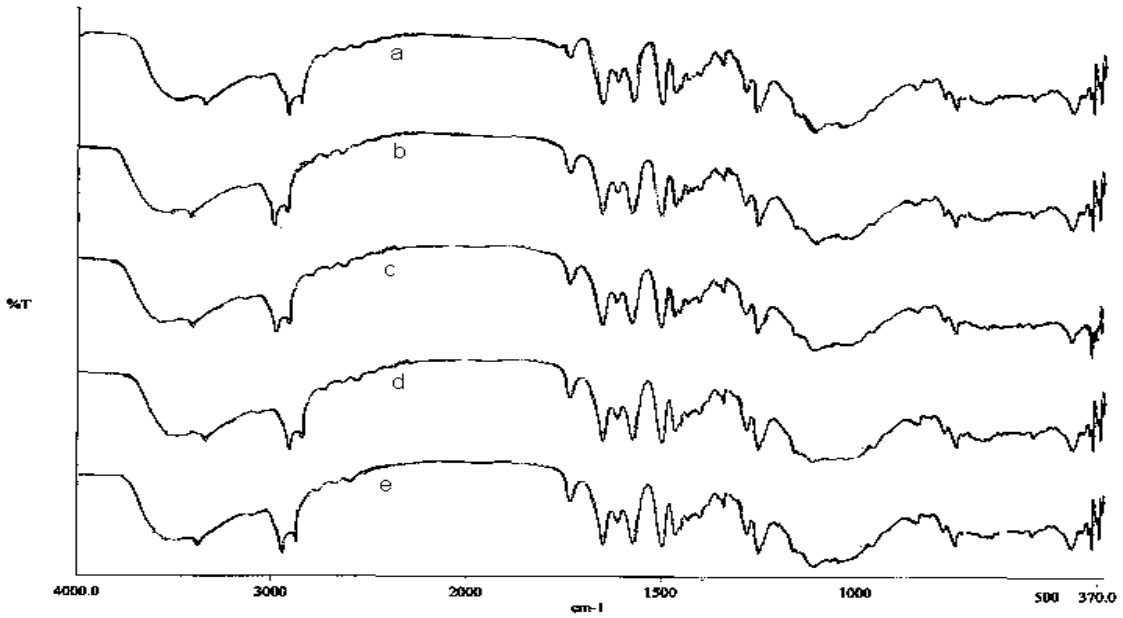

Figure 10.34 - Represents the FTIR profile for (a) ternary solid dispersion granules of 1:1:1.5 Mef/G/N initially and (b) at 25 ºC (c) at 30 ºC (d) at 35 ºC (e) at 40 ºC after three months.

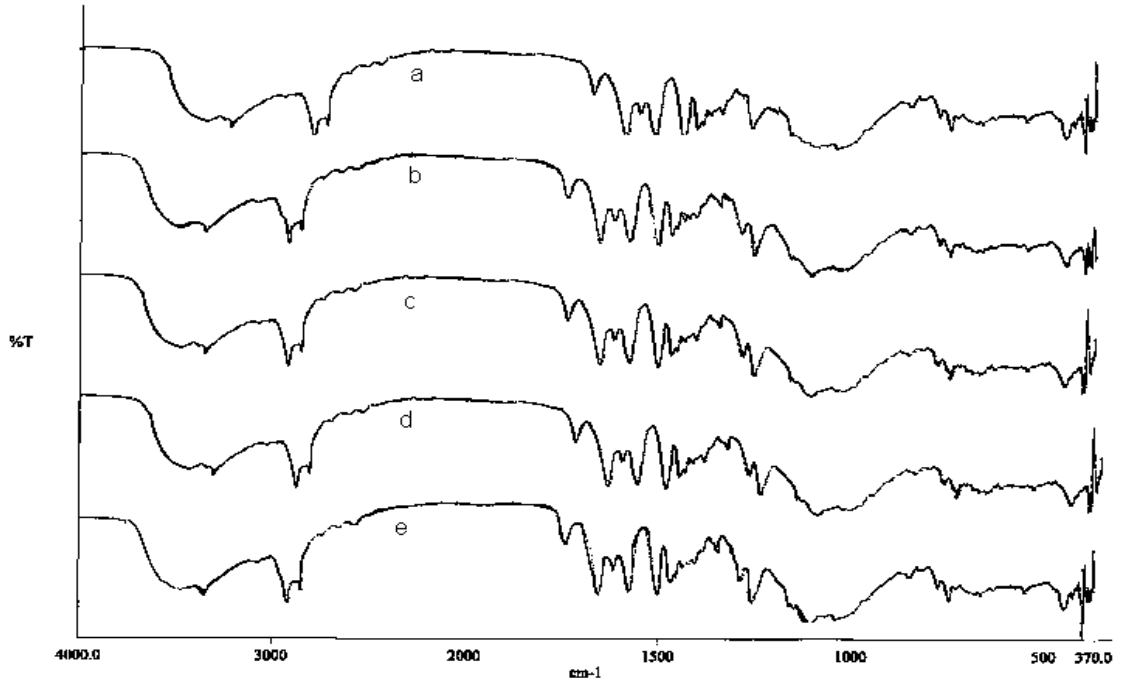

Figure 10.35 - Represents FTIR profile for (a) ternary solid dispersion granules of 1:1:1.5 Mef/G/N initially and (b) at 22.5% RH (c) at 52.89% RH (d) at 75.29% RH (e) at 100% RH after three months.

10.2.4 SEM study

The SEM study was performed to observe the characteristics (such as crystallinity, amorphous properties, porosity, etc) for the pure mefenamic acid, Gelucire 50/13® (G), Neusilin US2® (N) and ternary solid dispersion granules (Mef/G/N).

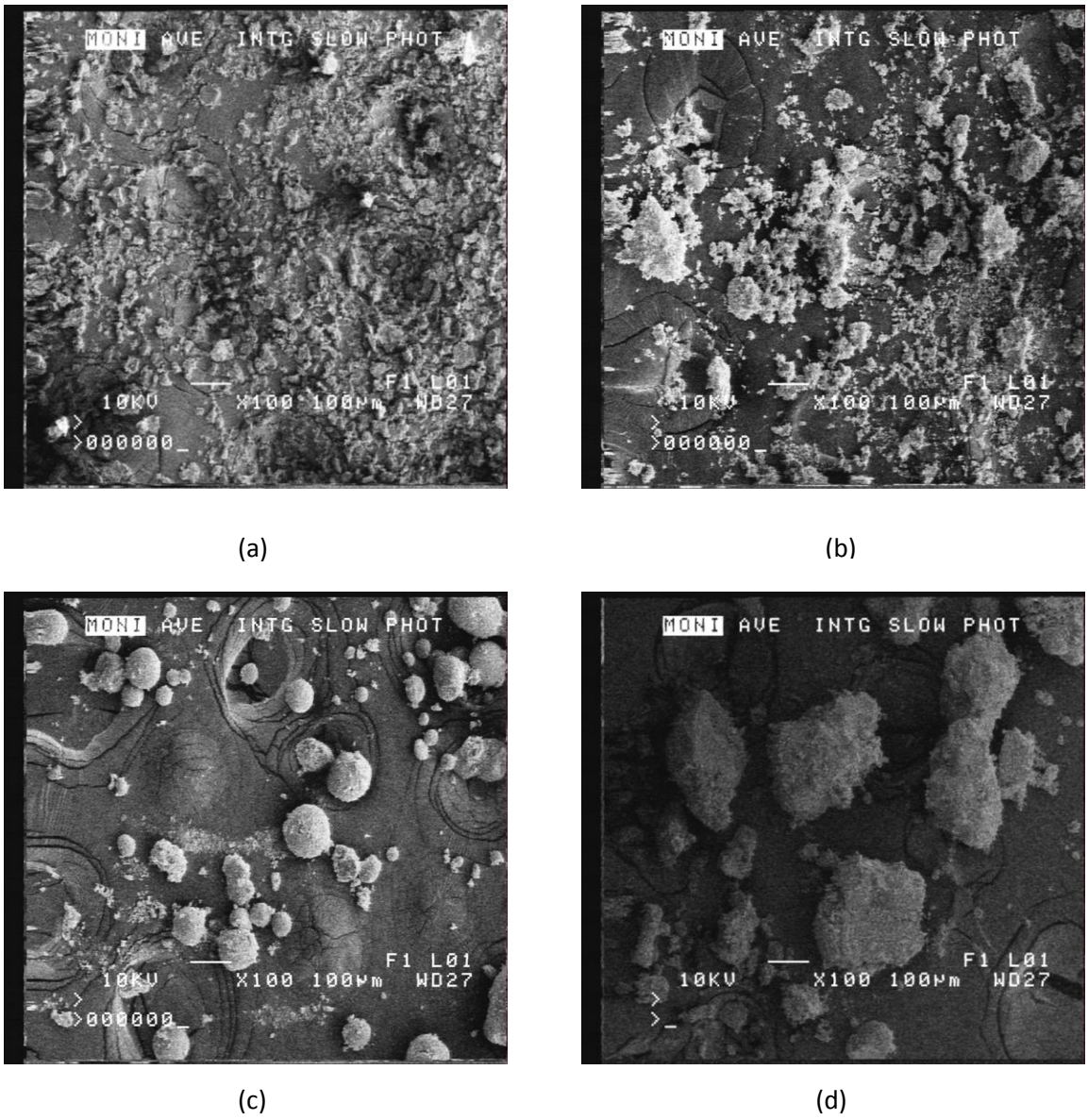

Figure 10.36 – Represents the SEM pictures for (a) mefenamic acid (b) Gelucire 50/13® (c) Neusilin US2® and (d) 1:1:1.5 Mef/G/N Ternary solid dispersion granules.

The SEM pictures for the pure mefenamic acid, Gelucire 50/13® (G), Neusilin US2® (N) and ternary solid dispersion granules (Mef/G/N) are seen in Figure 10.36. From the SEM picture of ternary solid dispersion granules (Mef/G/N), reduction in particle size and conversion of highly crystalline drug to amorphous form in solid dispersion phase is observed. The morphology of the ternary solid dispersion granules (Mef/G/N) resembled to that of Gelucire 50/13® which indicative of drug (Mefenamic acid) is being dispersed into the Gelucire 50/13®.

The SEM pictures for the drug (mefenamic acid) reveals the crystalline nature of the drug. The SEM picture for Gelucire 50/13® indicates that it is a waxy solid material in nature. The SEM picture for Neusilin US2® indicates that it is spherical and porous in nature. The SEM picture for the solid dispersion granules of drug (Mefenamic acid) indicates that this highly crystalline drug was converted to its amorphous form by the formation of the solid dispersion.

10.2.5 Dissolution study

10.2.5.1 Calibration curve for Mefenamic acid

In order to aid the process of dissolution analysis, the preparation of a calibration curve for the drug (mefenamic acid) was necessary. In this study, the drug release study and drug content analysis was performed in water as well as pH 9 buffer solution. Therefore a calibration curve for mefenamic acid was prepared in both water and pH 9 buffer solution. The absorbance and concentration values used to plot the calibration curve (Beer's curve) for mefenamic acid in both water and pH 9 buffer solution are given in Tables 10.9 and 10.10, respectively. Figures 10.37 and 10.38 represent the standard

calibration curve for diflunisal in water and pH 9 buffer solution, respectively. The linear regression equations thus obtained were used in the analysis of the drug release studies and drug content analysis.

Table 10.9 – Data used to obtain the calibration curve for mefenamic acid in water

Concentration (mcg/mL)	Mean Absorbance at 254 nm	Standard Deviation
10	0.135	0.003
20	0.313	0.010
30	0.424	0.028
40	0.588	0.055

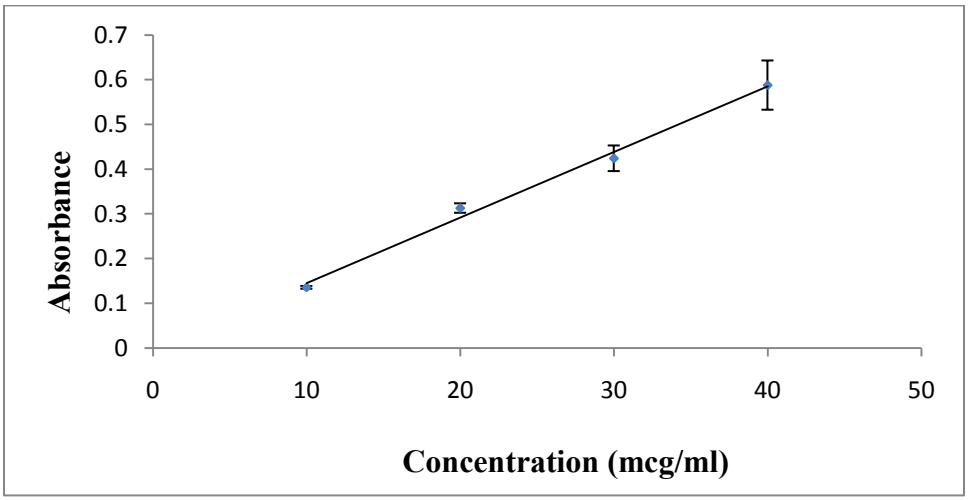

Figure 10.37 – Calibration curve for mefenamic acid in water where the slope = 0.0147 with an intercept of 0.0018 and an R^2 value of 0.9931.

Table 10.10 – Data used to obtain the calibration curve for mefenamic acid in pH 9 buffer solution

Concentration (mcg/mL)	Mean Absorbance at 254 nm	Standard Deviation
10	0.339	0.022
20	0.488	0.035
30	0.649	0.032
40	0.866	0.026
50	1.078	0.049

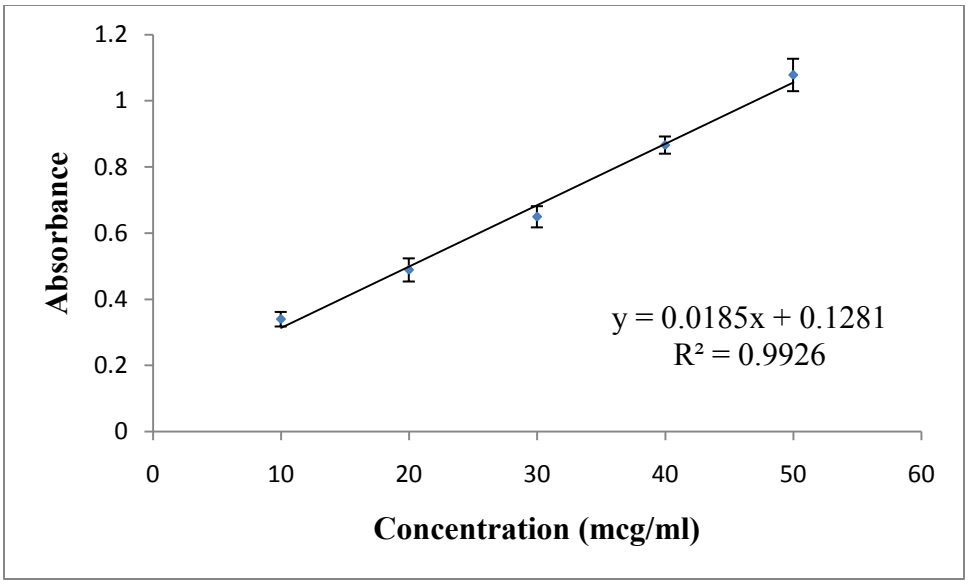

Figure 10.38 – Calibration curve for mefenamic acid in pH 9 buffer solution where the slope = 0.0185 with an intercept of 0.1281 and an R^2 value of 0.9926.

10.2.5.2 Mefenamic acid solid dispersion dissolution study

A dissolution test was performed to compare the amount of drug released from the ternary solid dispersion granules with the amount of drug released from the pure drug. The dissolution test for the solid dispersion granules of mefenamic acid and pure mefenamic acid was carried out in 900 ml of water as well as 900 ml of pH 9 buffer solution. Samples of 50 mg of pure mefenamic acid and solid dispersion equivalent to 50 mg of drug (mefenamic acid) were weighed and added to the dissolution medium. All the experiments were performed in triplicate. The drug release data for pure mefenamic acid and mefenamic acid solid dispersion granules in water and pH 9 buffer solution are seen in Figures 10.39 and 10.40, respectively. Tables 10.11 and 10.12 compare the amount of drug released after 20 min and 40 min from pure mefenamic acid and mefenamic acid solid dispersion granules in water and pH 9 buffer solution respectively.

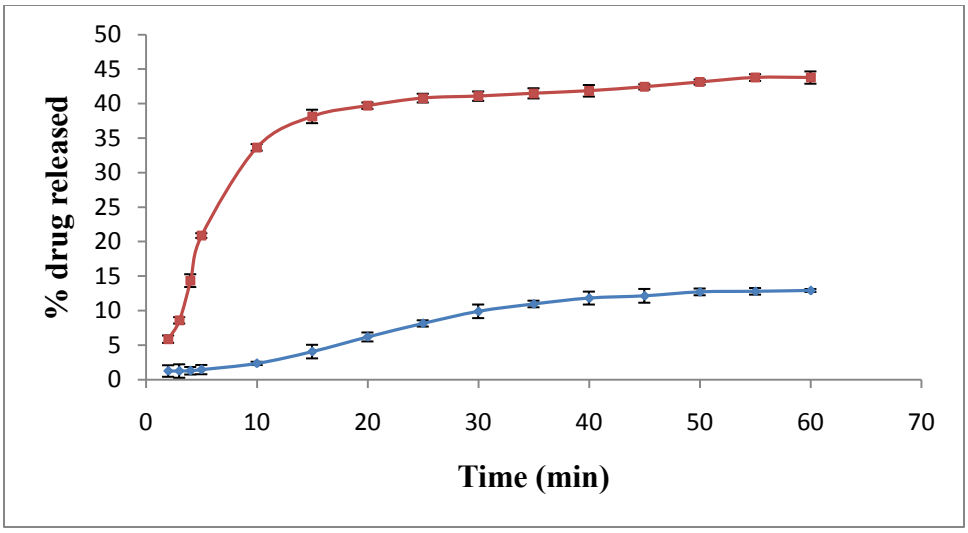

Figure 10.39 – Dissolution profile for mefenamic acid (bottom) and mefenamic acid solid dispersion (top) in water.

Table 10.11 – Comparison of the amount of drug released after 20 min and 40 min from pure mefenamic acid and mefenamic acid dispersion granules in water

Percentage drug released (in water) (± standard deviation)		
Batch name	After 20 min	After 40 min
Pure Mefenamic acid	6.17 ± 0.6474 %	11.81 ± 0.9374 %
Mef/G/N solid dispersion granules	39.68 ± 0.4673 %	41.85 ± 0.8373 %

Table 10.12 – Comparison of the amount of drug released after 20 min and 40 min from pure mefenamic acid and mefenamic acid solid dispersion granules in pH 9 buffer solution

Percentage drug released (in buffer solution at pH 9) (± standard deviation)		
Batch name	After 20 min	After 40 min
Pure Mefenamic acid	36.50 ± 0.3486 %	64.49 ± 0.4556 %
Mef/G/N solid dispersion granules	73.44 ± 0.5323 %	85.51 ± 0.8432 %

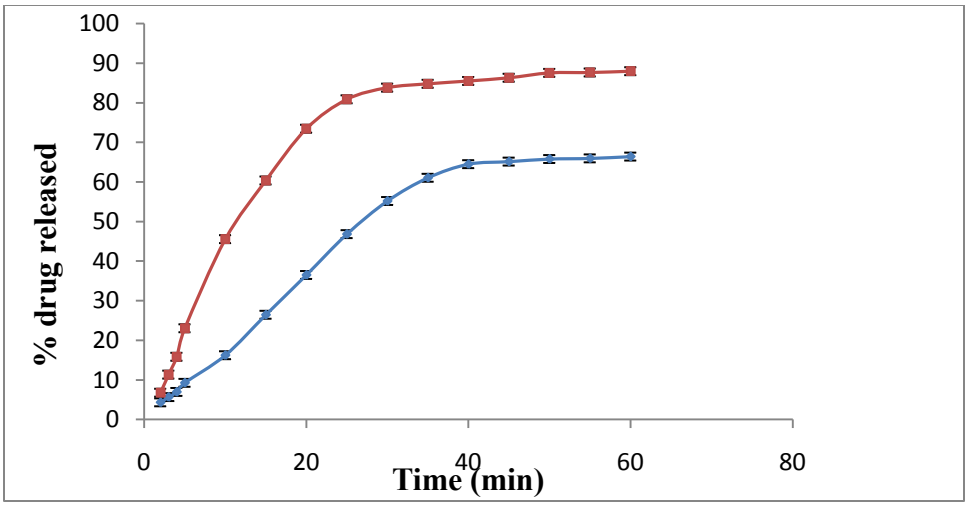

Figure 10.40 – Dissolution profile for mefenamic acid (bottom) and mefenamic acid solid dispersion (top) in pH 9 buffer solution.

From Figure 10.40 it was clear that the dissolution rate for mefenamic acid solid dispersion granules was greater than that for pure mefenamic acid in both water and pH 9 buffer solution. From the table above it was clear that the bioavailability for the drug at 20 min and 40 min was greater for mefenamic acid solid dispersion granules as compared to the pure mefenamic acid in both water and buffer solution (pH 9).

The dissolution study in water and pH 9 buffer solution was performed on the mefenamic acid solid dispersion granules after the first, second and third month to observe any change in dissolution profile for the ternary phase solid dispersion (Mef/G/N) when subjected to different temperatures and relative humidity conditions. After the first, second and third month, the dissolution study for the ternary solid dispersion granules (Mef/G/N), which were exposed at different temperatures (25ºC, 30ºC, 35ºC and 40ºC) and relative humidity conditions (22.5% RH, 52.89% RH, 75.29% RH and 100% RH),

showed no significant change with respect to the dissolution study for the ternary solid dispersion granules initially performed.

Tables 10.13 and 10.14 compare the amount of drug released after 20 min from mefenamic acid solid dispersion granules in water initially and after storage for 3 months at different temperatures (25ºC, 30ºC, 35ºC and 40ºC) and relative humidity conditions (22.5% RH, 52.89% RH, 75.29% RH and 100% RH), respectively. Tables 10.15 and 10.16 compares the amount of drug released after 20 min from mefenamic acid solid dispersion granules in pH 9 buffer solution initially and after storage for 3 months at different temperatures (25ºC, 30ºC, 35ºC and 40ºC) and relative humidity conditions (22.5% RH, 52.89% RH, 75.29% RH and 100% RH), respectively.

Table 10.13 – Comparison of the amount of drug released after 20 min from Mefenamic acid solid dispersion granules in water, initially and after storage for 3 months at different temperatures (25ºC, 30ºC, 35ºC and 40ºC).

Percentage drug dissolved (in water) after 20 minutes (±standard deviation)					
Batch Name	**Initial**	**1st month/ 25 ºC**	**1st month/ 30 ºC**	**1st month/ 35 ºC**	**1st month/ 40 ºC**
Mef/G/N Solid dispersion granules	39.68 ± 0.4673 %	38.55 ± 0.2548 %	39.97 ± 0.3337 %	38.37 ± 0.8988 %	39.43 ± 0.8704 %
		2nd month/ 25 ºC	**2nd month/ 30 ºC**	**2nd month/ 35 ºC**	**2nd month/ 40 ºC**
		40.14 ± 0.8321 %	39.09 ± 0.7031 %	38.83 ± 0.3373 %	39.42 ± 0.7955 %
		3rd month/ 25 ºC	**3rd month/ 30 ºC**	**3rd month/ 35 ºC**	**3rd month/ 40 ºC**
		39.26 ± 0.9016 %	40.37 ± 0.2085 %	39.98 ± 0.6654 %	40.01 ± 0.106931 %

Table 10.14 – Comparison of the amount of drug released after 20 min from mefenamic acid solid dispersion granules in water, initially and after storage for 3 months at different relative humidity conditions (22.5% RH, 52.89% RH, 75.29% RH and 100% RH).

Percentage drug dissolved (in water) after 20 minutes (±standard deviation)					
Batch Name	**Initial**	**1st month/ 22.5 %RH**	**1st month/ 52.89 %RH**	**1st month/ 75.29 %RH**	**1st month/ 100 %RH**
Mef/G/N Solid dispersion granules	39.68 ± 0.4673 %	40.06 ± 0.5489 %	39.19 ± 0.3239 %	38.78 ± 0.4898 %	40.25 ± 0.7419 %
		2nd month/ 22.5 %RH	**2nd month/ 52.89 %RH**	**2nd month/ 75.29 %RH**	**2nd month/ 100 %RH**
		39.95 ± 0.3466 %	38.76 ± 0.9245 %	40.11 ± 0.5539 %	39.24 ± 0.4086 %
		3rd month/ 22.5 %RH	**3rd month/ 52.89 %RH**	**3rd month/ 75.29 %RH**	**3rd month/ 100 %RH**
		39.83 ± 0.7371 %	40.46 ± 0.6367 %	39.12 ± 0.2734 %	39.81 ± 0.8172 %

Table 10.15 – Comparison of the amount of drug released after 20 min from mefenamic acid solid dispersion granules in pH 9 buffer solution, initially and after storage for 3 months at different temperatures (25ºC, 30ºC, 35ºC and 40ºC).

Percentage drug dissolved (in buffer solution at pH 9) after 20 minutes (±standard deviation)					
Batch Name	**Initial**	**1st month/ 25 ºC**	**1st month/ 30 ºC**	**1st month/ 35 ºC**	**1st month/ 40 ºC**
Mef/G/N Solid dispersion granules	73.44 ± 0.5323 %	73.02 ± 0.8624 %	74.59 ± 0.9986 %	72.88 ± 0.4578 %	73.78 ± 0.8926 %
		2nd month/ 25 ºC	**2nd month/ 30 ºC**	**2nd month/ 35 ºC**	**2nd month/ 40 ºC**
		73.89 ± 0.2764 %	73.26 ± 0.3133 %	74.28 ± 0.3196 %	73.79 ± 0.7964 %
		3rd month/ 25 ºC	**3rd month/ 30 ºC**	**3rd month/ 35 ºC**	**3rd month/ 40 ºC**
		72.63 ± 0.4482 %	74.15 ± 0.7634 %	73.69 ± 0.8378 %	72.86 ± 0.6159 %

Table 10.16 – Comparison of the amount of drug released after 20 min from mefenamic acid solid dispersion granules in pH 9 buffer solution, initially and after storage for 3 months at different relative humidity conditions (22.5% RH, 52.89% RH, 75.29% RH and 100% RH).

Percentage drug dissolved (in buffer solution at pH 9) after 20 minutes (±standard deviation)					
Batch Name	**Initial**	**1st month/ 22.5 %RH**	**1st month/ 52.89 %RH**	**1st month/ 75.29 %RH**	**1st month/ 100 %RH**
Mef/G/N Solid dispersion granules	73.44 ± 0.5323 %	73.99 ± 0.5984 %	74.29 ± 0.6849 %	74.001 ± .7962 %	74.58 ± 0.2025 %
		2nd month/ 22.5 %RH	**2nd month/ 52.89 %RH**	**2nd month/ 75.29 %RH**	**2nd month/ 100 %RH**
		74.09 ± 0.4146 %	72.99 ± 0.9882 %	74.22 ± 0.8472 %	73.75 ± 0.7498 %
		3rd month/ 22.5 %RH	**3rd month/ 52.89 %RH**	**3rd month/ 75.29 %RH**	**3rd month/ 100 %RH**
		73.81 ± 0.6733 %	72.63 ± 0.5981 %	73.37 ± 0.8377 %	73.69 ± 0.7419 %

Student's independent t-test was performed at an α-value of 0.05. No significant difference was observed between the dissolution data for mefenamic acid solid dispersion granules in water as well as pH 9 buffer solution initially and after storage.

Chapter Eleven

Conclusions and Recommendations

11.1 Conclusions from the study

The aim of this study was to prepare ternary solid dispersions granules of two poorly water-soluble drugs (diflunisal and mefenamic acid) in order to improve their solubility. The study also includes characterization of the ternary solid dispersion granules for their physicochemical properties initially and after storage for 3 months. Gelucire 50/13® was used as a dispersion carrier for the poorly water-soluble drugs (diflunisal and mefenamic acid). Neusilin US2® was used as an adsorbent. When the drugs tend to have proton donating or accepting groups, Neusilin® tends to form a hydrogen bond. In order to obtain a ternary solid dispersion, the melt prepared from the drug (diflunisal or mefenamic acid) and the dispersion carrier (Gelucire 50/13®) was added to the Neusilin US2® (preheated at 80 ˚C) in a dropwise manner and then subjected to liquid nitrogen for its quench cooling effect. The ternary solid dispersion thus obtained was further subjected to physicochemical characterization including Differential Scanning Calorimetry (DSC), X-Ray Powder Diffraction (XRPD), Fourier Transform Infrared Spectroscopy (FTIR), Scanning Electron Microscopy (SEM) and in vitro dissolution studies. The ternary solid dispersion was also subjected to stability studies for three months under different temperatures (25ºC, 30ºC, 35ºC and 40ºC) and relative humidity conditions (22.5% RH, 52.89% RH, 75.29% RH and 100% RH).

It is very important for the drug to disperse evenly into the dispersion carrier in order to produce a solid dispersion. A DSC study was undertaken to observe any type of

interaction which could occur between the components and to verify if the drug was evenly dispersed in the dispersion carrier. The DSC curve for the Ternary phase solid dispersion for both drugs (diflunisal and mefenamic acid) showed a single melting peak. The disappearance of the endothermic melting peak for the drug indicates that the drug is dispersed within the carrier Gelucire 50/13®. Thus, we can conclude that the outcome of formulation (mixture of drug, carrier and adsorbent) was a ternary solid dispersion granule and successful in improving drug dissolution.

The solid dispersion prepared by quench cooling in liquid nitrogen usually leads to a huge reduction in particle size. The XRPD study was performed to determine the crystallinity of each component and that of the ternary solid dispersion. Moreover, XRPD studies also reveal any kind of interaction between the components in the solid dispersion. The XRPD graph for the solid dispersion for both drugs (diflunisal and mefenamic acid) depicted the highly amorphous nature of the solid dispersion. Thus it can be concluded that the ternary phase solid dispersion prepared by the fusion method, followed by quench cooling, leads to significant conversion of the highly crystalline drug to its amorphous form.

FTIR studies were performed to aid in the evaluation of any possible chemical interaction between the drug, carrier and adsorbent in the solid dispersion. The solid dispersions for both drug (diflunisal and mefenamic acid) showed significant hydrogen bonding between drug and adsorbent. No other interactions were observed.

Various mechanisms which are responsible for enhanced dissolution include: increase in drug specific area, conversion of the drug to its amorphous state, solublization effect of

the carrier and improvement in wettability [1]. The SEM study confirmed the reduction in particle size, conversion of the drug to its amorphous state and increased surface area. The dissolution study was performed to study the rate of dissolution and bioavalability. A significant increase in dissolution rate for the solid dispersion for both drugs (diflunisal and mefenamic acid) was observed as compared to the dissolution rate for the pure drugs (diflunisal and mefenamic acid).

The stability study was performed on the solid dispersion for both drugs (diflunisal and mefenamic acid) by subjecting them to different temperatures (25ºC, 30ºC, 35ºC and 40ºC) and relative humidity conditions (22.5% RH, 52.89% RH, 75.29% RH and 100% RH) for three months. The stability study was undertaken to observe the effect of temperature and humidity on the solid dispersion. The solid dispersion for both drugs (diflunisal and mefenamic acid) remained unaffected by the temperature and humidity conditions under which they were exposed throughout the three months period.

11.2 Recommendation for future work

Tablets can be prepared from the ternary solid dispersions for the drugs (diflunisal and mefenamic acid) and evaluated for the onset and duration of action. Various combinations of different dispersion carriers and adsorbents should be tried with both drugs (diflunisal and mefenamic acid). The dissolution study should be carried out using simulated gastric fluid to determine the drug release profile. A long term stability study should be performed in order to study the stability of the prelimary dosage formulation.

Reference for Chapter One

1. www.pharmatimes.com/WorldNews/article.aspx?id=17655

2. "Solution for Poorly water-Soluble Drugs": Solid Dispersion by Fuji Chemical Industry's CSD Technology, Technical Newsletter, at www. Fujichemical.co.jp/English.

3. Peter L.D., Michael D.M. and Wildfong: Aqueous solubility enhancement through engineering of binary solid composites – Pharmaceutical applications, J. Pharm. Innov, 2009, 4, pp 36-49.

4. Suess, Wolfgang: Physicochemical and pharmacological aspects of the use of surface - active agents in medicinal technolog, Pharmazeutische Zentralhalle fuer Deutschland, (1967), 106(10), pp 669-681.

5. Lima, Adley A. N., Sobrinho, Jose L. S., Correa, Roberto A. C., Rolim Neto and Pedro J.: Alternative technologies to improve solubility of poorly water soluble drugs, Latin American Journal of Pharmacy, (2008), 27(5), pp 789-797.

6. Alexanian, C., Papademou, H., Vertzoni, M., Archontaki, H. and Valsami, G.: Effect of pH and water-soluble polymers on the aqueous solubility of nimesulide in the absence and presence of cyclodextrin derivatives, Journal of Pharmacy and Pharmacology, (2008), 60(11), pp 1433-1439.

7. Chiou, W.L, and Riegelman, S.: Pharmaceutical Applications of Solid Dispersion Systems, 1971, J. Pharm. Sci., 60(9), pp 1281-1302.

8. Modi, A., and Tayade, P.: Enhancement of Dissolution Profile by Solid Dispersion (Kneading) Technique. 2006, AAPS Pharm. Sci. Tech., 7(3) pp E1-E6.

9. Trivedi, Jay S. and Wells, Mickey L.: Solubilization using cosolvent approach : Water-Insoluble Drug Formulation (2000), pp 141-168.

10. Good, David J., and Rodriguez-Hornedo, Nair.: Solubility - advantage of Pharmaceutical Cocrystals. Crystal Growth & Design.

11. Habib M.J.: Pharmaceutical Solid Dispersion Technology, 2001, Lancaster, P.A.: Technomic Publishing company, Inc., pp 20-21.

12. Sheen, P.C., Kim, S.I., Petillo, J.J. and Serajuddin, A.T.: Bioavailability of a Poorly Water-Soluble Drug from Tablet and Solid Dispersion in Humans, J. Pharm. Sci., 1991, 80, pp 712–714.

13. Ford, J.L. The Current Status of Solid Dispersions. Pharm. Acta Helv. 1986, 61, pp 69–88.

14. Serajuddin, A.T.M. Solid Dispersions of Poorly Water-Soluble Drugs: Early Promises, Subsequent Problems, and Recent Breakthroughs. J. Pharm. Sci. 1999, 88, pp 1058–1066.

15. http://www.neusilin.com/product/index.php

16. http://www.neusilin.com/product/general_properties.php

Reference for Chapter Two

1. Younggil Kwon: Handbook of essential pharmacokinetics, pharmacodynamics, and drug metabolism for industrial scientists, Kluwer academics, Plenum publisher, New York, pp 35-38.
2. http://www.fda.gov/AboutFDA/CentersOffices/CDER/ucm128219.htm
3. Fincher J.H.: Particle size of drugs and its relationship to absorption and activity, J.Pharm. Sci., 1968, 57(11), pp 1825-1835.
4. Scheikh, M.A., Price, J.C. and Gerraughty, R.J.: Effect of ultrasound on particle size suspensions of polyethylene spheres, J.Pharm. Sci., 1966, 55, pp 1048-1050.
5. Kornblum, S.S. and Hirschorn. J. O.: Disolution of poorly water-slouble drugs, I. Some physical parameters related to method of micronization and tablet manufacture of a quinazolinone compound, J. Pharm. Sci., 1970, 59(5), pp 606-609.
6. Levy, G.: Effect of particle size on dissolution and gastrointestinal absorption rates of pharmaceuticals, Amer. J. Pharm., 1963, pp 78-92.
7. Jones A.: Pharmaceutical Eutectics: Formation, Evaluation and Relevance in preformulation studies using thermal analytical methods, Master Thesis, 2005.
8. Sekiguchi, K. and Obi, N.: "Studies on absorption of eutectic mixtures. I. A comparison of the behavior of eutectic mixture of sulfathiazole and that of ordinary sulfathiazole in man." Chem. Pharm. Bull., 1961, 9, pp 866-872.
9. Kanig J.L.: Properties of fused mannitol in compressed tablets, J. Pharm. Sci., 1964, 53, pp 188-192.

10. Chiou, W.L. and Niazi, S.: Differential thermal analysis and X-ray diffraction studies of griseofulvin-succinic acid eutectic mixture, J.Pharm Sci., 1973, 62(3), pp 498-501.
11. Chiou, W. L. and Riegelman, S.: "Pharmaceutical applications of solid dispersion systems." J.Pharm. Sci., 1971, 60(9), pp 1281-1302.
12. Simonelli, A.P., Mehta, S.C. and Higuchi, W.I.: "Dissolution rates of high energy polyvinylpyrrolidone (PVP)-sulfathiazole coprecipitates." J.Pharm. Sci., 1969, 58(5), pp 538-549.
13. Habib M.J.: Pharmaceutical Solid Dispersion Technology, 2001, Lancaster, P.A.: Technomic Publishing company, Inc., pp 16-19.
14. Habib, M.J.: Pharmaceutical Solid Dispersion Technology, 2001, Lancaster, P.A.: Technomic Publishing company, Inc., pp 51.
15. Leuner, C. and Dressman, J.: Improving drug solubility for oral delivery using solid dispersions, European J. Pharm. and Biopharm., 2000, 50, pp 47-60.
16. Goldberg A., Gibaldi M. and Kanig L.: Increasing dissolution rates and gastrointestinal absorption of drugs via solid solutions and eutectic mixtures II experimental evaluation of a eutectic mixture: urea-acetaminophen system, J. Pharm. Sci. 1966, 55, pp 482-487.
17. Martin, A.N., Swarbrick, J., and Cammarata, A. 1969. "Physical Pharmacy," 2nd ed., Philadelphia PA: Lea and Febiger, pp 313.
18. Kaplun-Frischoff, Yael; Touitou, Elka. Testosterone Skin Permeation Enhancement by Menthol through Formation of Eutectic with Drug and

Interaction with Skin Lipids. Journal of Pharmaceutical Sciences (1997), 86(12), pp 1394-1399.

19. Guillory, J.K., Hwang, S.C. and Lach, J.L., J.Pharm.Sci., 1969, 58, pp 301-308.
20. Levy, G.: Effect of dosage form on drug absorption – A frequent variable in clinical pharmacology, Arch.Int.Pharmacodyn.Ther., 1964, 1(152), pp 59-68.
21. http://www.pharmainfo.net/reviews/solid-dispersions
22. Lo, W.Y. and Law, S.L.: "Dissolution behavior of griseofulvin solid dispersions using polyethylene glycol, talc, and their combination as dispersion carriers." Drug Dev. In. Pharm. 22: pp 231-236.
23. http://www.substech.com/dokuwiki/lib/exe/fetch.php?w=&h=&cache=cache&mediainterstitialsolution.png.
24. Chiou W.L., Riegelman S.: Preparation and dissolution characteristics of several fast-release solid dispersions of griseofulvin, J. Pharm. Sci.,1969; pp 1505-1510.
25. Jones, G.O. : "Glass", 1958, New York, Wiley, pp 1-9.
26. Sopade P.A., Lee S.B., White E.T. and Halley P.J.: Glass transition phenomena in molasses, LWT, 2007, 40, pp 1117-1122.
27. Alfred Martin, Physical Pharmacy, 5th edition.
28. Moriyama, M., Inoue, A., Isoya, M. Tanaka, M. and Hanano, M.: Dissolution properties and gastrointestinal absorption of chloramphenicol from hydrophilic high molecular weight compound coprecipitates. 1978, 98(8), pp 1012-1018.
29. Sekikawa, H., Nakano, M. and Aritra, T.: Dissolution mechanisms of drug-polyvinylpyrrolidone co-precipitates in aqueous solution, 1979, Chem. Pharm. Bull., (Tokyo), 27(5), pp 1223-1230.

30. Habib M.J.: Pharmaceutical Solid Dispersion Technology, 2001, Lancaster, P.A.: Technomic Publishing company, Inc., pp 20-21.
31. H.M El-Banna, N.A Daabis, L.M Mortada and S. Abd-Elfattah: Physicochemical study of drug-binary systems. Part 3: tolbutamide-urea and tolbutamide-mannitol systems, Pharmazie, (1975), 30(12), pp 788-792.
32. S.E.Walker, J.A. Ganley, K.Bedford and T.Eaves: The filling of molten and thixotropic formulations into hard gelatin capsules, Journal of Pharmacy and Pharmacology, (1980), 32(6), pp 389-393.
33. James L. Ford and Michael H. Rubinstein: Formulation and ageing of tablets prepared from indomethacin-polyethylene glycol 6000 solid dispersions, Pharmaceutica Acta Helvetiae, (1980), 55(1), pp 1-7.
34. James L. Ford and Michael H. Rubinstein: Preparation, properties and ageing of tablets prepared from the chlorpropamide-urea solid dispersion, International Journal of Pharmaceutics, (1981), 8(4), pp 311-322.
35. Chiou, W.L.: Pharmaceutical applications of solid dispersion system - X-ray diffraction and aqueous solubility studies on griseofulvin-poly(ethylene glycol) 6000 system, J.Pharm Sci., 1977, 66(3), pp 989-991.
36. James L. Ford, F. Stewart and Michael H. Rubinstein: The assay and stability of chlorpropammide in solid dispersion with urea, J. Pharm. Pharmac. 31, 1979, pp 726-729.
37. Carcano E.C. and Gana I.M.: Eutectic mixtures and solid solutions of acetylsalicylic acid and urea – Stability of acetylsalicylic acid, An. R. Acad. Farm. 40, 1974, pp 487-493.

38. Habib M.J.: Pharmaceutical Solid Dispersion Technology, 2001, Lancaster, P.A.: Technomic Publishing company, Inc., pp 22-23.
39. Theodore R Bates: Dissolution characteristics of reserpine-polyvinylpyrrolidone coprecipitates, Journal of Pharmacy and Pharmacology, (1969), 21(10), pp 710-712.
40. Sekikawa, H., Fukuda, N., Takada, M., Ohtani, K., Aritra, T. and Nakano, M. Dissolution behavior and gastrointestinal absorption of disumarol-polyvinylpyrrolidone and dicumarol-β-cyclodextrin, Chemical and Pharmaceutical Bulletin, (1983), 31(4), pp 1350-1356.
41. Usui F., Maeda K., Kusai A., Ikeda M., Nishimura K. and Yamamoto K. : Dissolution improvement of RS-8359 by solid dispersion prepared by solvent method, Int. J. Pharm., 1998, 170, pp 247-256.
42. Habib M.J.: Pharmaceutical Solid Dispersion Technology, 2001, Lancaster, P.A.: Technomic Publishing company, Inc., pp 67-70.
43. Stevens L.A. and Padfield J.M.: Co precipitated system of salicylsalicylic acid (SSA) with PVP – physical and bioavailability studies, Expo. Congr. Int. Technol. Pharm., 1977, 5, pp 135-141.

Reference for Chapter Three

1. Brittain H.: Physical characterization of Pharmaceutical Solids, M. Dekker, New York (1995), pp 13-18.
2. Crompton, T.R.: Analysis of Polymer, Pergamon, New York, 1989, pp 208.
3. Lever, T.J., Hardy, M.J. and Barnes, A.F.: A review of the application of thermal methods in the pharmaceutical industry, J.Therm.Anal., 1993, (4), pp 499.
4. Skoog, D.A. and Leary, J.J.: Principles of instrumental analysis; Saunder's College Publishing, 4th Edition, 1971, USA.
5. Groenewoud, W.M.: Characterization of Polymers by Thermal Analysis, First edition, 2001, Netherland.
6. Brittain H.: Physical characterization of Pharmaceutical Solids, M. Dekker, New York (1995), pp 234-245.
7. Pungor, E.: A practical guide to instrumental analysis, 1995 by CRC Press, Inc., pp 181.
8. Townsend, I.: Basic strategy for the thermal stability assessment of pharmaceutical synthetic intermediates and products, J.Therm.Anal., 1991 (37), pp 2031.
9. Timmins, P. and Ford, J.L.: Pharmaceutical Thermal Analysis – Techniques and Applications, New York, 1989, pp 10-12.
10. Bhadeshia, H.K.D.H.: "Differential Scanning Calorimetry" University of Cambridge, Materials Science & Metallurgy.

11. Haines, P.J.: Thermal methods of analysis – Principles, Applications and Problems, First edition, 1995, Blackie academic and professional, New Zealand, pp 65-69.
12. http://www.anasys.co.uk/library/dsc3.htm
13. Wunderlich, B.J., Jin, Y. and Boller, A., B.J.Therm.Anal., 1994, (42), pp 307-330.
14. Sichina, W.J. and Haake S.: Tips for obtaining the best possible DSC data, Application note An-9, 2008, pp 2.
15. Sichina, W.J. and Haake S.: Tips for obtaining the best possible DSC data, Application note An-9, 2008, pp 3.
16. Sichina, W.J. and Haake S.: Tips for obtaining the best possible DSC data, Application note An-9, 2008, pp 1.
17. Alan T Riga, Shouvik Roy, Kenneth S. Alexander : A statistical approach for the evaluation of parameters affecting preformulation studies of pharmaceuticals by Differential scanning Calorimetry, American Pharmaceutical Review, 2002, pp 64-72.
18. United States Pharmacopoeia 23, General test <891>, 1995, pp 1837-1838.
19. Magri, A.L. Marini, D., Sacchini, A., Magri A.D. and Balestrieri F.: Application of Differential Scanning Calorimetry to the study of drug-execipient compatibility, Ther.Acta., 1996 (285), pp 337-345.
20. Alvarez J., Fazio G., Fini A., garuti, M. and Holgado M.A.: Diclofenac salts. I. Fractal and Thermal analysis of sodium and potassium diclofenac salts, J. pharm. Sci., 2001, 90(12), pp 2049-2057.
21. Gehenot, A., Rao, R.C. and Maire, G., Int. J. Pharm., 1988, (45), pp 13-17.

Reference for Chapter Four

1. Brittain H.: Physical characterization of Pharmaceutical Solids, M. Dekker, New York, (1995), pp 188-195.
2. Skoog, D. A., Donald M. West: Principles of Instrumental Analysis, California (1971), pp 358.
3. Skoog, D.A., Holler, F.J., and Nieman, T.A. 1998: Principles of Instrumental analysis, 5th edition USA: Thomson Learning Inc., pp 295.
4. Cullity B.: Elements of X-Ray Diffraction, Addison-Wesley, Reading, Mass (1978).
5. William Bragg: An introduction to crystal analysis, G. Bell and Sons, London, 1993, pp 12-21.
6. Klug H., Alexander L.: X-Ray Diffraction Procedure for Polycrystalline and Amorphous Materials, Wiley, New York (1974).
7. http://www.nightlase.com.au/education/optics/diffraction.htm
8. Shechtman D.: Quasiperiodic Crystals – Experimental Evidence, Journal de Physique, july (1986), pp 1.
9. Brittain H.: Physical characterization of pharmaceutical solids, M.Dekker, New York (1995), pp 1-8.
10. Bragg, W. L.: The diffraction of short electromagnetic waves by a crystal, Proc. Cambridge Phil. Soc., 1913, 17, pp 43-57.
11. Pungor, E.: A practical guide to instrumental analysis, 1995 by CRC Press, Inc., pp 151.

12. Bragg, W. L.: The structure of some crystals as indicated by their diffraction of x-rays, Proc. Roy. Soc. London, 1913, 89: pp 248-277.
13. http://neon.otago.ac.nz/chemlect/chem203/symmetrylectures/3dimensions.pdf
14. Brittain H.: X-ray diffraction III: Pharmaceutical applications of x-ray powder diffraction; Spectroscopy; 16(7);(2001); pp14-18.
15. Parrish, W. and Robert, B.W. : "Crystals Monochromator Technique", In International tablets for X – Ray Crystallography, Vol.III, Kynoch Press, England, 1962, pp 73-78.
16. Pungor, E.: A practical guide to instrumental analysis, 1995 by CRC Press, Inc., pp 152-154.
17. Schrenier, W.N., Dismore, P.F. and JenkinsR.: XRD instrument sensitivity results from a round robin study, Adv. X-ray Anal., 1992, 35, pp 333-340.
18. Snyder, R.L., Jenkin, R.: Introduction to X-ray Powder Diffractometry, John Wiley and Sons, New York, 1996, pp 97-120.
19. Fawcet, T.G., Smith, D.K., Jenkin, R., Visser, J.W., Frevel, L.K., and Morris, M.C.: Sample preparation methods in X-ray powder diffraction, InJCPDS-ICDD, Methods and Practice in X-ray Powder Diffraction, Sect. 5.2.1., International Center for Diffraction Data, Newtown Square, P.A., 1988.
20. Brittain H.: Physical characterization of Pharmaceutical Solids, M. Dekker, New York (1995), pp 1-8.
21. Bunge, H.J.: Texture Analysis in aterial Science, Butterworth, London, 1982.
22. Snyder, R.L., Jenkin, R.: Introduction to X-ray Powder Diffractometry, John Wiley and Sons, New York, 1996, pp 248-261.

23. Bystrom-Asklund, A.M. 1966. Am. Mineral., 51:1233.

24. http://pubs.usgs.gov/info/diffraction/html

25. Skoog, D. A., Donald M. West: Principles of Instrumental Analysis, California (1971), pp 360.

26. Pungor, E.: A practical guide to instrumental analysis, 1995 by CRC Press, Inc., pp 157.

27. Lavigueur, C., Foster, E.J., Williams, V.E. : A simple and inexpensive capillary furnace for variable - temperature X - ray diffraction, Journal of Applied Crystallography (2008).

28. USP30/NF 25 2007 pp 187-188 <941>

29. Yonemochi, E., Hoshino, T., Yoshihashi, Y., Terada, K. : Evaluation of the physical stability and local crystallization of amorphous terfenadine using XRD -DSC and micro-TA, Thermochimica Acta (2005), 432(1), pp70-75.

Reference for Chapter Five

1. Vij, D. R. and Neena Jaggi: Hand Book of Applied Solid State Spectroscopy, Springer US, 2006, pp 411-446.
2. www.ericweisstein.com
3. Joseph B. Lambert, Herbert E. Shurvell, David A. Lightner and Graham Cooks: Organic structural spectroscopy, Prentice Hall, 1998, pp 152-174.
4. Brittain, H.: Physical Characterization of pharmaceutical solids, M. Dekker, New York, (1995), pp 1-8.
5. Alben, J.O. and Fiamingo, F.G.: Fourier transform infrared spectroscopy, in Optical Techniques in Biological Research, (1984), Academic, New York, pp 133–179.
6. Ernest Orlando Lawrence Berkeley National Laboratory Document on FTIR; pp 1.
7. Barbara H. Stuart: Infrared spectroscopy - Fundamentals and applications, John Wiley & Sons Ltd, pp 18-20.
8. Green, D.W. & Reedy, G.T.: Fourier Transform Infrared Spectroscopy - Applications to Chemical Systems, Vol. 1, Ferraro, J.R. & Basile; L.J., New York, Academic Press, (1978), pp 18–38.
9. Skoog D.A., Leary J.J.: Principles of Instrumental analysis; Saunders College Publishing; 4th Edition; 1971; U.S.A pp. 256.
10. Thackeray, P.P.C., Miller, R.G.J., Stace, B.C.: Laboratory Methods in Infrared Spectroscopy, London, Heyden and Son Ltd., (1972), pp 8.

11. Kember, D., Chenery, D.H., Sheppard, N. & Fell, J. Spectrochimica Acta. (1979), pp 455-459.
12. Markham, J.R., Best, P.E. & Solomon, P.R. (1994) Appl. Spectrosc. 48, pp 265-270.
13. R. Silverstein and F.Webster: Spectroscopic identification of Organic compounds, 6th Edn, John Wiley and sons, Inc, New York, pp 71-78.

Reference for Chapter Six

1. Zhou, Weilie and Wang, Zhong Lin: Scanning Microscopy for Nanotechnology : Techniques and Applications, Springer New York, 2007, pp 1.
2. http://serc.carleton.edu/research_education/geochemsheets/techniques/SEM.html
3. Argast, Anne and Tennis, Clarence F., III: A web resource for the study of alkali feldspars and perthitic textures using light microscopy, scanning electron microscopy and energy dispersive X-ray spectroscopy, Journal of Geoscience Education 52, no. 3, 2004, pp 213-217.
4. Goldstein, J.: Scanning electron microscopy and x-ray microanalysis, Kluwer Adacemic, Plenum Pulbishers, (2003), pp 689-702.
5. Egerton, R.F. : Physical principles of electron microscopy : An introduction to TEM, SEM, and AEM; Springer, (2005), pp 202.
6. Goldstein, J., Newbury, D., David C. Joy, Patrick Echlin, Charles E. Lyman and Eric Lifshin: Scanning electron microscopy and x-ray microanalysis, Springer, third edition, pp 29 – 41.
7. http://serc.carleton.edu/research_education/geochemsheets/techniques/SEM.html
8. Isaacson, M.: Electron gun using a Field Emission Source, Rev. Sci. Instr>, (1968), 39, pp 576-584.
9. Paszowski, B.: Electron Optics, Iliffe ltd., London, (1968), pp 305.
10. Goldstein, J., Newbury, D., David C. Joy, Patrick Echlin, Charles E. Lyman and Eric Lifshin: Scanning electron microscopy and x-ray microanalysis, Springer, third edition, pp 42 – 66, 125-132.

11. Moody, M.F.: Image Analysis of Electron Micrograph, Academic press, New York, (1990), pp 145-287.
12. Reimer, L.: Scanning Electron Microscopy: Physics of image formation and microanalysis. Springer, (1998), pp 527.
13. Mills, A.A.: Silver as a removable conductive coating for Scanning Electron Microscopy, (1988), 2, pp 1265-1271.
14. Hart, R.K.: Scanning Electron Spectroscopic Microscopy – In principles and techniques of scanning electron microscopy, New York, 4, (1975), pp 174-223.
15. http://serc.carleton.edu/research_education/geochemsheets/techniques/SEM.html
16. Murphey, J.A.: Scanning Electron Microscope, SEM Inc., AMF O'Hare, Illinois, (1978), 2, pp 209.

Reference for Chapter Seven

1. Skoog, et. al.: Principles of Instrumental Analysis. 6th ed. Thomson Brooks/Cole. 2007, pp 169-173.
2. http://www.chemistry.adelaide.edu.au/external/soc-rel/content/uv-vis.htm
3. http://www.cem.msu.edu/~reusch/VirtualText/Spectrpy/UV-Vis/spectrum.htm
4. Murrel,J.N.: The Theory of Electronic Spectra of Organic Molecules, Methuen and Co., London, 1963.
5. Jaffe, H.H. and Orchin, M.: Theory and Application of Ultraviolet Spectroscopy,John Wiley and Sons, New York, 1962.
6. Ingle D. James, Crouch R. Stanley: Spectrochemical Analysis, Prentice Hall, New Jersey, 1988.
7. Skoog A. Douglas, West M. Donalds: Principles of Instrumental Analysis,1971, pp 31-37.
8. W.R.Brode: Chemical Spectroscopy, John Wiley and Sons.New York, 1950.
9. Skoog, et. al.: Principles of Instrumental Analysis. 6th ed. Thomson Brooks/Cole. 2007, pp 349-350.
10. Skoog, et. al.: Principles of Instrumental Analysis. 6th ed. Thomson Brooks/Cole. 2007, pp 351.
11. Skoog A. Douglas, West M. Donalds: Principles of Instrumental Analysis,1971, pp 84-85.
12. Skoog A. Douglas, West M. Donalds: Principles of Instrumental Analysis,1971, pp 85-86.

Reference for Chapter Eight

1. Hansen, W.: Handbook of Dissolution Testing, Pharmaceutical technology publications, 1982, pp 1-2, 28-31.
2. Hansen, W.: Handbook of Dissolution Testing, Aster Publishing Corporation, 2nd edition, (1991), pp 1-2.
3. Leeson L. and Cartensen J.: Dissolution technology, 1974, Washington D.C., Academy of Pharmaceutical sciences.
4. Wurster, D.E., Taylor, P.W.: Dissolution rates, J.Pharm. Sci., 1965, (54), pp 169
5. http://dictionary.reference.com/browse/dissolution.
6. Banakar, Umesh V.: Pharmaceutical Dissolution Testing; Drugs and the Pharmaceutical Sciences, pp 1-2.
7. Alfred Martin, Physical Pharmacy, 1995, Waverly International, Maryland, pp 330-326.
8. Noyes, A. and Whitney W.R.: The rate of solution of solid substances in their own solutions, J. Am. Chem. Soc. 1897, (19), pp 930-934.
9. USP XXX/NF XXV, Vol. I, MD, 2008, pp 277-281.
10. BP, Vol. II, London, 1988.
11. Krowczynski, L.: Extended released dosage forms, 1987, Boca Raton, Fla: CRC Press.

Reference for Chapter Nine

1. Remington's Pharmaceutical Sciences, 17th Edition, 1985, Mack Publishing Company, Easton, Pennesylvania, pp – 1119.
2. http://www.drugbank.ca/drugs/DB00784
3. Ahad Bavili Tabrizi.Bull: Determination of Mefenamic Acid in Human Urine by Means of Two Spectroscopic Methods by Using Cloud Point Extraction Methodologyas a Tool for Treatment of Samples. Department of Medicinal Chemistry, Faculty of Pharmacy & Biotechnology Research Center, Tabriz University of Medical Sciences, Tabriz, Iran. E-mail:a.bavili@tbzmed.ac.irReceived May 21, 2006, . Korean Chem. Soc. 2006, Vol. 27, No. 11.
4. JB Sharma, J Aruna, Praveen Kumar, Kallol Kumar Roy, Neena Malhotra, Sunesh Kumar :Comparison of efficacy of oral drotaverine plus mefenamic acid with paracervical block and with intravenous sedation for pain relief during hysteroscopy and endometrial biopsy. Department of Obstetrics and Gynecology, All India Institute of Medical Sciences, New Delhi, India 2009, Vol 63, No. 6 , pp 244-252.
5. Essentials of Medical Pharmacology, 5th Edition, JAYPEE BROTHERS, MEDICAL PUBLISHERS(P) LTD, New Delhi, pp 177.
6. Kakuta H, Zheng X, Oda H, *et al*: Cyclooxygenase-1-selective inhibitors are attractive candidates for analgesics that do not cause gastric damage. design and in vitro/in vivo evaluation of a benzamide-type cyclooxygenase-1 selective inhibitor. *J. Med. Chem.* **51** (8), pp 2400–11.

7. http://www.drugs.com/mtm/mefenamic-acid.html
8. Dockeray, C.J., Sheppard, B.L., Bonnar, J.: Comparison between mefenamic acid and danazol in the treatment of established menorrhagia. Blackwell Publishers Ltd., British Journal of Obstetrics and Gynecology, Subject: Health, ISSN: 0306-5456, 1989.
9. Essentials of Medical Pharmacology, 5th Edition, JAYPEE BROTHERS, MEDICAL PUBLISHERS(P) LTD, New Delhi, pp – 177.
10. Remington's Pharmaceutical Sciences, 17th Edition, 1985, Mack Publishing Company, Easton, Pennesylvania, pp – 1116.
11. http://www.drugs.com/pro/diflunisal.html
12. Holguín JA.: Ionophoretic and inhibitory action of the analgesic, diflunisal, on sarcoplasmic reticulum. Departamento de Bioquímica, Instituto Nacional de Cardiología, México, D.F. México. Biochem Pharmacol. 1988 Nov 1;37(21), pp 4035-40.
13. Stone,C.A.; Van Arman, C.G.; Lotti, V.J.; Minsker, D.H.; Risley, E.A.; Bagdon, W.J.; Bokelman, D.L.; Jensen, R.D.; Mendlowski,B.; Tate,C.L.; Peck,H.M.; Zwickey,R.E. and Mckinney,S.E.: Pharmacology and Toxicology of Diflunisal. British journal of Clinical Pharmacology 4(Suppl. 1):19(1977).
14. www.merck.com/mmpe/lexicomp/diflunisal.html
15. Keet, J.G.M.: A comparative clinical trial of Diflunisal and Ibuprofen in the control of pain in osteoarthritis. Journal of international Medical Research 7: pp 272 (1979).

16. Petersen, J.K.: Diflunisal, a new analgesic, in the treatment of postoperative pain following removal of impacted mandibular third molar. International Journal of Oral Surgery 8, pp 102-113 (1979b).
17. Talbot, R. and Rees, H.: Perforated duodenal ulcer on Diflunisal (Dolobid). British Medical Journal 2: 1229 (1978).
18. Steelman, S.L.; Tempero,K.F. and Cirilli V.J.: The chemistry, pharmacology, toxicology and clinical pharmacology of Diflunisal. Clinical Therapeutics 1(Suppl. A) (1978b).
19. Torchiana, M.L.; Wiese, S.R. and Westrick, B.L.: Comparison of the effects of Diflunisal and other salicylates on the intragastric potential. Journal of Pharmacy and Pharmacology 31: 112 (1979).
20. http://www.drugs.com/ingredient/diflunisal.html
21. http://www.gattefossecanada.ca/en/products/pharmaceutical/gattefosse_oral.shtml #gel50
22. Company datasheet Gattefosse, NJ Gelucire 50/13.
23. http://www.neusilin.com/product/index.php
24. http://www.neusilin.com/product/general_properties.php
25. http://www.fujichemical.co.jp/english/newsletter/images/0902/Fuji_Email_Blast_ Neusilin_JAN21.pdf pg 3
26. http://www.fujichemical.co.jp/english/bulk/neusilin_pro.html
27. http://www.neusilin.com/product/pharmaceutical_application.php
28. Remington's Pharmaceutical Sciences, 17th Edition, 1985, Mack Publishing Company, Easton, Pennesylvania, pp – 947.

29. F.E.M. O'brien : The Control of humidity by saturated salt solutions; British electrical and Allied industries research association, London (1947).
30. Remington's Pharmaceutical Sciences, 17th Edition, 1985, Mack Publishing Company, Easton, Pennesylvania, pp – 715.
31. Remington's Pharmaceutical Sciences, 17th Edition, 1985, Mack Publishing Company, Easton, Pennesylvania, pp – 919.

Reference for Chapter Ten

1. Silverstein R. M., Webster F. X. and Kiemle D. J.: Spectrometric identification of organic compounds, State university of New York, John Wiley & Sons Inc., pp 86-87.
2. http://wwwchem.csustan.edu/Tutorials/infrared.htm

Reference for Chapter Eleven

1. Ford, James L.: The current status o solid dispersion, Pharmaceutica Acta Helvetiae, 1986, 61, pp 69-87.